主論文

Final Fate of Generic Gravitational Collapse
– Is Shell-Focusing Naked Singularity Realized ? –

Tomohiro Harada[1]
Department of Physics, Kyoto University,
Kyoto 606-8502, Japan

Ph.D. thesis submitted to Department of Physics, Kyoto University
January, 1999

[1]Electronic address: harada@tap.scphys.kyoto-u.ac.jp

Abstract

I summarize my and our works on the final fate of generic gravitational collapse. It is known that the spherically symmetric dust collapse results in the shell-focusing naked singularity from generic smooth initial data. Then we concentrate on the effect of tangential pressure, counterrotation, pressure and break of spherical symmetry on the final fate of collapse, in particular, the central naked singularity formation. The results are the following. In the presence of generic counterrotation the shell-focusing naked singularity formation is prevented. Pressure with a sufficiently soft, γ-law equation of state cannot prevent the central naked singularity formation. At the central naked singularity, linear perturbations of the Riemann tensor diverge for the odd-parity mode. However, the naked shell-focusing singularity is not a strong source of odd-parity gravitational radiation. In summary, the occurrence of the naked shell-focusing singularity is not generic in the collapse of gas of collisionless particles and is not a serious counterexample to the cosmic censorship hypothesis.

Contents

Chapter 1

Introduction

We follow the sign conventions of the textbook by Misner, Thorne and Wheeler (1973) about the metric, Riemann and Einstein tensors. We use the units with $c = G = 1$ all over this thesis unless otherwise stated. The Greek indices denote the components with respect to the coordinate basis, while we follow the abstract index notation of Wald (1984) as for the Latin indices $a, b, c, \ldots$

1.1 Introduction

Gravitational collapse is one of the most intriguing phenomena in gravitational physics and astrophysics. Considering the final fate of complete gravitational collapse we cannot help mentioning a *black hole*.

The possibility of an object from which light cannot escape due to its strong gravity was already noted by Laplace (1795) who considered Newton gravity and Newton's corpuscular theory of light. Einstein (1915) proposed a field equation for gravitational field which is now called *Einstein's field equation* and completed *general relativity* which took the place of Newton gravity. He first brought the concept of curved space-time to physics. Schwarzschild (1916) found the exact solution of Einstein equation which describes the external gravitational field of a spherical mass. This solution turned out to have *singularity*. Chandrasekhar (1931) discovered the existence of an upper limit to the mass of completely degenerate fermion gas. Landau (1932) gave more intuitive derivation of this upper limit. From these arguments, it was suggested that a massive stellar core above this upper limit which exhausted its fuel ends to continued gravitational collapse. Oppenheimer and Snyder

(1939) solved the collapse of a homogeneous dust ball and showed that a black hole forms and that the dust ball becomes cut off from all communication with the outer region. Kerr (1963) discovered a family of exact vacuum solutions to Einstein equation. The Kerr solution which describes a rotating black hole turned out to be a unique stationary vacuum solution with a regular event horizon of Einstein equation. Wheeler (1968) named "black hole". Discovery of quasars, pulsars and compact X-ray sources in 1960's strongly encouraged researches on gravitational collapse and black holes.

The Schwarzschild and the Kerr solutions contain singularity inside an *event horizon*. Another typical example of singularities is the *big bang* singularity which appears in the Friedmann-Lemaître-Robertson-Walker (FLRW) space-time. At these singularities, curvature invariants of the space-time diverge. General relativity and all other known physics do not apply there because singularities cannot be a part of the space-time manifold. Some people felt that the singularity is only due to the presence of singular matter-source and that it could be avoided if we considered non-singular matter-source only. Others felt that the occurrence of singularity is an artifact of the high symmetry of the metric which we had to assume in order to obtain exact solutions. For example, in Newton gravity, a cloud of collisionless particles from velocity dispersion free and spherical initial data collapses to singularity while there appears no singularity from generic initial data (Pfaffelmoser (1993)).

In fact, it was proved that the occurrence of singularity is generic in gravitational collapse. This theorem is called the *singularity theorem*. It proves the existence of singularity under the null energy condition for matter content, generic condition and causality. The theorem also strongly suggests the existence of the big bang singularity or the initial singularity in our universe. For a proof, see Hawking and Ellis (1973). From this theorem, the singularity formation was proved to be a generic property of gravitational collapse. However, the singularity theorem only proves the causally geodesic incompleteness of the space-time and does not mention the properties of the singularity. Is the singularity observable ? Do curvature invariants blow up at the singularity ? Is an object which goes toward the singularity crushed by the tidal force ? The singularity theorem does not answer to such problems.

As for observable singularities, there is a serious problem. If the singularity is observable, then what occurs ? What does the singularity emit ? What boundary conditions does the ordinary well-known physical field, such as the electromagnetic field, follow ? So far, we have no answer to these problems.

If the curvature blows up at the singularity, the space-time curvature becomes beyond the order of $l_{\rm p}^{-2}$, where $l_{\rm p} \equiv (\hbar G/c^3)^{1/2} \approx 1.6 \times 10^{-33}$cm is the Planck length. Some people expect that classical general relativity breaks down at the stage characterized by the Planck length, in which quantum effects will play a dominant role and it will save the situation. The full description of such mechanism will need quantum gravity which is expected to describe the Planck-scale physics. Some people think that classical theory has some mechanism which makes itself self-contained at least in an observational sense. In other words, Nature hides singularities from observations in gravitational collapse. This idea was proposed explicitly by Penrose (1969, 1979) and is called a *cosmic censorship hypothesis* (CCH). The hypothesis has weak and strong versions. If the hypothesis holds, we can completely discuss the time evolution from complete initial data in the framework of classical general relativity, not knowing quantum gravity. Various useful theorems on gravitational collapse and black holes are proved under the assumption of this hypothesis (Hawking and Ellis (1973)). In spite of its attraction and fruitage, all attempts to prove the hypothesis have not yet succeeded. The difficulty mainly comes from the fact that there exist space-times which contain observable singularities. Such singularities are referred to as *naked singularities.*

As Penrose (1969) noted already when he first proposed the hypothesis, the key idea of the hypothesis is the "*physical reasonableness*". In fact, we can easily construct a naked-singular space-time which is a solution of Einstein equation. This can be done by taking any naked-singular space-time and assuming matter content which is a source term of this metric through Einstein equation. Since the physical reasonableness is somewhat an ambiguous concept, we would rather say what is physically unrealistic. We can recognize, for example, high symmetry of space-time, negative energy, superluminal energy flows and special choice of initial data as physically unrealistic.

Thorne (1972) proposed apparently similar but different conjecture on the formation of black holes. See also box 32.3 of Misner, Throne and Wheeler (1973). He conjectured that black holes with horizons form when and only when a mass M gets compactified into a region whose circumference in every direction $C \lesssim 4\pi M$. This is called the *hoop conjecture.* A version of the "when" half of the hoop conjecture can be proved by the Schoen and Yau (1983)'s theorem if we assume the weak cosmic censorship. However there is no proof which does not assume the cosmic censorship. Nevertheless, there has not been discovered any counterexample to this conjecture and many

evidences for validity of this conjecture have been accumulating.

In recent years, there are some important advances in studies on the gravitational collapse and the cosmic censorship. We will briefly explain them after the precise formulation of singularities, CCH and curvature strength.

1.2 Singularity

1.2.1 Definition of Singularity

The definition of singularity in general relativity is not a trivial task. There has been a succession of changes of meaning. Since general relativity has invariance to a general coordinate transformation, the definition of singularity should not depend on the coordinate system. We will sketch the definition of singularity, following Clarke (1993).

The space-time manifold is denoted by M with the metric g_{ab}. We begin with definitions about a curve in M. The *generalized affine parameter length* $l_{\rm E}(\gamma)$ of a curve $\gamma : [0, a) \to M$ with respect to a frame

$$\mathbf{E}^a = (E^a_{(i)} : i = 0, 1, 2, 3) \tag{1.1}$$

is given by

$$l_{\rm E}(\gamma) \equiv \int_0^a ds \left(\sum_{i=0}^{3} \left(g_{ab} \dot{\gamma}^a E^b_{(i)}(s) \right)^2 \right)^{1/2}, \tag{1.2}$$

where $\dot{\gamma}^a \equiv (\partial/\partial s)^a$ denotes the tangent vector and $\mathbf{E}^a(s)$ is defined by parallel propagation along the curve, starting with an initial value $\mathbf{E}^a(0)$: that is, we impose

$$\dot{\gamma}^a \nabla_a \mathbf{E}^b(s) = 0, \tag{1.3}$$

$$\mathbf{E}^a(0) = \mathbf{E}^a. \tag{1.4}$$

γ is said to be *incomplete* if $l_{\rm E}(\gamma)$ is finite with respect to some $\mathbf{E}^a$. This definition turns out to be independent of the choice of the reference frame. $\gamma : [0, a) \to M$ is said to be *inextendible* if there is no curve $\gamma' : [0, b) \to M$ with $b > a$ such that $\gamma'|[0, a) = \gamma$. This is equivalent to saying that γ has no endpoint in M.

Then we proceed definitions about a space-time. A space-time is said to be *incomplete* if it contains an incomplete inextendible curve. An *extension* of a space-time (M, g_{ab}) is an isometric embedding $\theta : M \to M'$, where (M', g'_{ab}) is a space-time and θ is onto a proper subset of M'. A space-time

is termed *extendible* if it has an extension. The following proposition holds: if M has an extension $\theta : M \to M'$, then there is an incomplete timelike geodesic γ in M such that $\theta \circ \gamma$ is extendible. A space-time M is said to be *singular* if it contains an incomplete curve γ such that there is no extension $\theta : M \to M'$ for which $\theta \circ \gamma$ is extendible.

Space-time itself consists entirely of regular points at which g_{ab} is well behaved, while singularities belong to ∂M, the boundary of M, which is a set of "ideal points" added on M. We define appropriately the topology of $M \cup \partial M$, the closure of M. The construction of the boundary of the space-time can be carried out in various ways, for example, b-boundary, g-boundary and causal boundary. Suppose we are given a singular space-time M. Then a *singularity* in ∂M is defined as a point which is an endpoint of an incomplete inextendible curve γ, where γ is such that there is no extension θ of M for which $\theta \circ \gamma$ is extendible.

A singularity may be classified to three types: (i) a scalar constructed polynomially from the Riemann tensor and its covariant derivatives blows up along the geodesic ("scalar curvature singularity"), (ii) no such scalar blows up but a component of the Riemann tensor and its covariant derivatives in a parallely propagated frame blows up along the geodesic ("parallely propagated curvature singularity") and (iii) no such curvature scalar or component blows up ("non-curvature singularity"). Examples of (i) are the singularities in the Schwarzschild and the FLRW space-times. An example of (ii) is the singularity in the plane gravitational wave solution. An example of (iii) is the conical singularity which appears in the wedge-removed Minkowski space-time. It should be noted that there exist singular space-times which are geodesically complete.

1.2.2 Singularity Theorem

Hawking and Penrose (1970) proved the following singularity theorem. See Hawking and Ellis (1973) for a proof.

Theorem 1.2.1 (Singularity Theorem) *Suppose a space-time (M, g_{ab}) satisfies the following four conditions:*

(1) $R_{ab}v^a v^b \geq 0$ for all timelike and null v^a.

(2) Every non-spacelike geodesic possesses at least a point where

$$k_{[e}R_{a]bc[d}k_{f]}k^b k^c \neq 0,$$

where k^a is the tangent vector of the geodesic.

(3) No closed timelike curve exists.

(4) At least one of the following three conditions holds:

- *(a) M possesses a compact achronal set without edge.*
- *(b) M possesses a trapped surface.*
- *(c) There is a point p in M such that the expansion of the null geodesics emanating from p becomes negative.*

Then M must contain at least an incomplete causal geodesic.

Condition (1) is satisfied for all plausible non-quantum matter. Condition (2) is a generic condition serving only to rule out certain high symmetry. Condition (3) has no direct support but it seems to be reasonable to assume it. Condition (4a) is satisfied if the universe is compact. It is believed that condition (4b) is quite likely to be satisfied in gravitational collapse in our universe. And it is also believed that condition (4c) is satisfied for any past-directed null cone in our universe from the fact that the expanding FLRW model is a very good approximation of our universe at least after the epoch of decoupling. Then the theorem strongly suggests the existence of singularity in our universe and in generic continued gravitational collapse.

1.3 Cosmic Censorship

1.3.1 Cosmic Censorship Hypothesis

Though the singularity theorem strongly suggests the existence of singularities in generic gravitational collapse, it does not answer where it is. If an observer can see singularity, which is called *naked singularity*, we cannot say anything about the causal future of it unless we know appropriate boundary conditions at the singularity. Since we do not find any plausible boundary conditions at the singularity, the predictability within the framework of classical physics is broken and we are at lost in the presence of naked singularities. According to these discussions, it has been conjectured that general relativity might have a remarkable feature that no naked singularity would be formed in realistic gravitational collapse. This conjecture is called CCH. The CCH, which prohibits the formation of naked singularities, has two versions, weak and strong ones. Both were formulated by Penrose (1969, 1979).

The weak cosmic censorship hypothesis (WCCH) was first formulated by Penrose (1969). It states that all singularities in generic gravitational collapse are hidden within black holes. More precisely, we restrict attention to weakly asymptotically simple space-times having a partial Cauchy surface S such that all past-directed generators of future null infinity enter and remain in the boundary of the future domain of dependence of S. We will also suppose that S is $\mathbf{R}^3$ with some map $\mathbf{R}^3 \to S$ so that data on S can be pulled back to data on $\mathbf{R}^3$. Then we call a set of such things *generic* if the corresponding collection of such data sets on $\mathbf{R}^3$ is open and dense in some suitable topology.

Hypothesis 1.3.1 (Weak Cosmic Censorship) *For a generic set of space-times and partial Cauchy surfaces as above, the whole of null infinity lies in the boundary of the future domain of dependence of S, i.e., the space-time is future strongly asymptotically predictable.*

A singularity which is censored by WCCH is termed a *globally naked singularity*. The WCCH proves the existence of black hole together with the singularity theorem. The WCCH is often assumed in theorems on general properties of a black hole, such as that it cannot bifurcate, that apparent horizon must be contained in it and that area of it cannot decrease.

Progress towards proving this hypothesis has been much limited. The difficulty comes from the fact that we are concerned with a global existence proof for the nonlinear hyperbolic equations of general relativity and that such global proofs are notoriously hard to come by. As a result, it has been understood that the strong hypothesis described below would be more tractable to prove.

The strong cosmic censorship hypothesis (SCCH) was first formulated by Penrose (1979). It states that no singularity except for initial singularities is visible to any observer. More precisely,

Hypothesis 1.3.2 (Strong Cosmic Censorship) *Every generic inextendible space-time containing physically reasonable matter is globally hyperbolic.*

A singularity which is censored by SCCH but not by WCCH is termed a *locally naked singularity*. It should be noted that the violation of either WCCH or SCCH does not necessarily mean the existence of naked singularity. It should be also noted that, although SCCH is intuitively stronger than WCCH, the violation of WCCH does not necessarily mean the violation of SCCH. This is because, if a singularity is formed from asymptotically

flat initial data and it propagates out to null infinity destroying asymptotic flatness while preserving global hyperbolicity, this would violate WCCH but not SCCH.

Let S be a closed achronal set. We define the *future Cauchy horizon* of S, denoted by $H^+(S)$ by

$$H^+(S) = \overline{D^+(S)} - I^-[D^+(S)], \tag{1.5}$$

where $D^+(A)$ and $I^-(A)$ denote the future domain of dependence and the chronological past of A, respectively, and $\overline{A}$ denotes the closure of A. Similarly we can define the *past Cauchy horizon* of S, i.e., $H^-(S)$. The *Cauchy horizon* of a closed achronal set S is defined by

$$H(S) = H^+(S) \cup H^-(S). \tag{1.6}$$

It can be shown easily that $H(S) = \partial D(S)$, where ∂A denotes the boundary of A. Moreover, if M is connected, then a nonempty closed achronal set, Σ, is a Cauchy surface for (M, g_{ab}) and therefore (M, g_{ab}) is globally hyperbolic with a Cauchy surface Σ if and only if $H(\Sigma) = \emptyset$ is satisfied.

1.3.2 Curvature Strength of Singularity

In attempts to prove CCH, the curvature strength was defined. By introducing this, it was hoped that all real singularities were strong singularities and that strong singularities were always covered by horizons. In spite of the hope, there has been no satisfactory definition of curvature strength. Here we first present the definition of *strong curvature condition* (SCC) by Tipler (1977). It refers to a timelike (resp. null) geodesic $\gamma : [0, s_0) \to M$, the singularity being approached as the affine parameter s tends to s_0, and is conveniently expressed in terms of Jacobi fields that vanish at a point on γ. We define $J_{s_1}(\gamma)$ for $s_1 \in [0, s_0)$ to be a set of maps $Z : [0, s_0) \to TM$ (TM means the tangent bundle) such that

$$Z^a(s) \in T_{\gamma(s)}M, \tag{1.7}$$

$$Z^a(s_1) = 0, \tag{1.8}$$

$$\dot{\gamma}^a \nabla_a (\dot{\gamma}^b \nabla_b Z^c) = -R_{abd}{}^c Z^b \dot{\gamma}^a \dot{\gamma}^d, \tag{1.9}$$

$$\dot{\gamma}^a \dot{\gamma}^b \nabla_b Z_a \Big|_{s_1} = 0, \tag{1.10}$$

where $\dot{\gamma}^a$ is the tangent vector of γ. For a timelike (resp. null) geodesic we use three (resp. two) such fields independent of each other. Their exterior

product defines a spacelike volume (resp. area) element, whose magnitude at the affine parameter value s we denote $V(s)$.

Definition 1.3.1 (Strong Curvature Condition) *For all $s_1 \in [0, s_0)$ and all three (resp. two) linearly independent fields $Z_1, Z_2, Z_3 \in J_{s_1}$ (resp. $Z_1, Z_2 \in J_{s_1}$), we have*

$$\liminf_{s \to s_0} V(s) = 0.$$

This definition intuitively says that any object that hits a strong singularity is crushed to zero volume (resp. area).

Królak (1983, 1987) proved a theorem which roughly says that, if all physically realistic singularities are strong, then WCCH holds but with rather strong additional assumptions. Królak (1987) realized that weaker condition for the strength of singularity is sufficient for the proof. We will refer to the condition as the *limiting focusing condition* (LFC).

Definition 1.3.2 (Limiting Focusing Condition) *For all $s_1 \in [0, s_0)$ and all three (resp. two) linearly independent fields $Z_1, Z_2, Z_3 \in J_{s_1}$ (resp. $Z_1, Z_2 \in J_{s_1}$), there exists $s \in [s_1, s_0)$ with*

$$\frac{dV}{ds}(s) < 0.$$

Clarke and Królak (1985) found necessary conditions and sufficient conditions for SCC and LFC that are very useful in determining the curvature strength of singularity. See Clarke and Królak (1985) and Clarke (1993) for proofs.

For a timelike geodesic $\gamma : [0, s_0) \to M$, we prepare a parallely propagated frame $E_i^a : (i = 1, 2, 3, 4)$ with $E^a_{(1)} E_{(1)a} = E^a_{(2)} E_{(2)a} = E^a_{(3)} E_{(3)a} = -E^a_{(4)} E_{(4)a} = 1$, all other products vanish and $E^a_{(4)} = \dot{\gamma}^a$. For a null geodesic $\gamma : [0, s_0) \to M$, we prepare a parallely propagated frame $E_i^a : (i = 1, 2, 3, 4)$ with $E^a_{(1)} E_{(1)a} = E^a_{(2)} E_{(2)a} = -E^a_{(3)} E_{(4)a} = -E^a_{(4)} E_{(3)a} = 1$, all other products vanish and $E^a_{(4)} = \dot{\gamma}^a$. Necessary conditions for SCC are:

Proposition 1.3.1 *For both the timelike and the null cases, if SCC is satisfied, then for some component $R^{(i)}{}_{(4)(j)(4)}$ of the Riemann tensor in a parallely propagated frame the integral*

$$I^{(i)}{}_{(j)}(s) \equiv \int_0^s ds' \int_0^{s'} ds'' |R^{(i)}{}_{(4)(j)(4)}(s'')| \tag{1.11}$$

does not converge as $s \to s_0$, where $i, j = 1, 2, 3$ ($i, j = 1, 2$ in the null case).

In the null case, it is possible to consider the Ricci and Weyl tensors separately. The Weyl tensor $C_{\mu\nu\sigma\lambda}$ is defined as

$$C_{\mu\nu\sigma\lambda} \equiv R_{\mu\nu\sigma\lambda} + (g_{\mu[\lambda}R_{\sigma]\nu} + g_{\nu[\sigma}R_{\lambda]\mu}) + \frac{1}{3}Rg_{\mu[\sigma}g_{\lambda]\nu}. \tag{1.12}$$

Proposition 1.3.2 *Let $\gamma(s)$ be a null geodesic. Let $R_{(4)(4)}$ and $C^{(m)}{}_{(4)(n)(4)}$ is the components of the Ricci tensor and Weyl tensor, respectively. If SCC is satisfied, then either the integral*

$$K(s) \equiv \int_0^s ds' \int_0^{s'} ds'' R_{(4)(4)}(s'') \tag{1.13}$$

or the integral

$$L^{(m)}{}_{(n)}(s) \equiv \int_0^s ds' \int_0^{s'} ds'' \left(\int_0^{s''} ds''' |C^{(m)}{}_{(4)(n)(4)}(s''')| \right)^2 \tag{1.14}$$

for some $m, n = 1, 2$ does not converge as $s \to s_0$.

A sufficient condition is as follows:

Proposition 1.3.3 *For both the timelike and the null geodesics, if the integral $K(s)$ diverges and has a positive integrand, then SCC is satisfied.*

Similar conditions for LFC hold but with one less integral in all cases:

Proposition 1.3.4 *For both the timelike and the null cases, if LFC is satisfied, then for some component $R^{(i)}{}_{(4)(j)(4)}$ of the Riemann tensor in a parallely propagated frame the integral*

$$J^{(i)}{}_{(j)}(s) \equiv \int_0^s ds' |R^{(i)}{}_{(4)(j)(4)}(s')| \tag{1.15}$$

does not converge as $s \to s_0$, where $i, j = 1, 2, 3$ ($i, j = 1, 2$ in the null case).

Proposition 1.3.5 *Let $\gamma(s)$ be a null geodesic. Let $R_{(4)(4)}$ and $C^{(m)}{}_{(4)(n)(4)}$ is the components of the Ricci tensor and Weyl tensor, respectively. If LFC is satisfied, then either the integral*

$$M(s) \equiv \int_0^s ds' R_{(4)(4)}(s') \tag{1.16}$$

or the integral

$$N^{(m)}{}_{(n)}(s) \equiv \int_0^s ds' \left(\int_0^{s'} ds'' |C^{(m)}{}_{(4)(n)(4)}(s'')| \right)^2 \tag{1.17}$$

for some $m, n = 1, 2$ does not converge as $s \to s_0$.

Proposition 1.3.6 *For both the timelike and the null geodesics, if the integral $M(s)$ diverges and has a positive integrand, then LFC is satisfied.*

1.3.3 Examples of Non-Globally Hyperbolic Space-Time

In spite of all attempts, neither WCCH nor SCCH has been proved. In fact, there have been found a number of solutions of Einstein equation that are not globally hyperbolic with matter content which satisfies the dominant energy condition. Important examples are summarized in Table 1.1.

Yodzis, Seifert and Müller zum Hagen (1973) showed that "shell-crossing" singularities occur in a generic spherically symmetric collapse of a dust ball. Moreover, Müller zum Hagen, Yodzis and Seifert (1974) extended the analysis to a perfect fluid with bounded pressure.

Another type of naked singularities in the spherically symmetric collapse of a fluid was discovered. Eardley and Smarr (1979) indicated that the central "shell-focusing" singularity is naked in the collapse of a spherical dust ball. Christodoulou (1984) mathematically proved the appearance of central shell-focusing singularity in the collapse of a spherical dust ball from a generic set of smooth initial data.

The smooth initial data mean initial data in which the center is not singularity and physical quantities, such as energy density and specific energy, are C^∞ functions. The regular initial data mean initial data the center is not singularity.

Newman (1986) showed that, for the first null ray from the singularity, neither SCC nor LFC is satisfied for the shell-crossing singularity in the spherically symmetric dust collapse from generic smooth initial data. He showed also that not SCC but only LFC is satisfied for the shell-focusing singularity in the spherically symmetric dust collapse from generic smooth initial data.

Apart form spherical symmetry, Szekeres (1975) discovered a class of exact solutions which describes the irrotational dust collapse with no Killing vector. This model is often said to be "quasi-spherical". He found that shell-crossing singularities that occur in these space-times can be naked. Joshi and Królak (1996) found shell-focusing naked singularities that satisfy not SCC but only LFC can occur from regular initial data.

Returning to spherical symmetry, Singh and Joshi (1996) discovered another type of shell-focusing singularities in the collapse of a spherical dust ball. The initial data from which this type of singularity develops is only

regular but neither smooth nor generic. They showed that this type of naked singularity satisfies both SCC and LFC for the first null ray from the singularity.

We should mention the collapse of imploding null dust (directed radiation) described by the Vaidya space-time (Vaidya 1943, 1951a, 1951b). Joshi and Dwivedi (1992a) found that there appears naked singularity which satisfies both SCC and LFC if the implosion rate is sufficiently small.

Ori and Piran (1987, 1988, 1990) discovered an important example of naked singularity in the system in which pressure is not negligible. They considered the spherically symmetric self-similar collapse of a perfect fluid with barotropic equation of state. The assumptions restrict an equation of state to the form $P = (\gamma - 1)\epsilon$. They showed the naked singularity formation in the pure collapse for $\gamma \lesssim 1.0105$. They showed also that there are naked-singular solutions with oscillations in the velocity field for $1 < \gamma < 1.4$. Lake (1988) showed that SCC is satisfied for the first null ray from the singularity. Furthermore, Waugh and Lake (1989) showed that central naked singularity in a self-similar space-time with the Cauchy horizon generated by the homothetic Killing vector satisfies SCC for the first null geodesic.

On the other hand, some people think that, since the fluid description is only phenomenological, the formulation of CCH should be done by "elementary fields" which obey some quasi-linear hyperbolic equation (Wald 1984). In this context, Christodoulou (1994) proved analytically that, in the spherically symmetric collapse of a scalar field, naked singularities may arise from regular initial data on a low differentiability class ("collapsed cone singularity") and that those solutions are not generic.

Choptuik (1993) discovered numerically the "black-hole critical behavior" which is analogous to the critical behavior in solid state physics. He showed the appearance of a "zero-mass black hole" (which may be recognized as naked singularity) in the critical collapse of a spherically symmetric scalar field. This phenomenon turned out to be universal for the collapse of several matter fields, such as, axisymmetric gravitational waves (Abrahams and Evans (1993)) and a spherically symmetric radiation fluid (Evans and Coleman (1994)). It is noted that the zero-mass black hole formation is unstable phenomenon.

In gravitational astrophysics, a system of collisionless particles is often studied since it models a stellar system such as an elliptical galaxy and a globular cluster. Shapiro and Teukolsky (1991, 1992) showed numerically the divergence of curvature invariant without apparent horizon in the collapse of a (slowly rotating) prolate spheroid with sufficiently elongated

initial configuration of collisionless particles. After the shape it is called "spindle singularity". Their numerical simulation was done in the maximal time slicing. Since the occurrence of singularity without detection of apparent horizon does not necessarily mean the naked singularity formation (cf. Chap. 5), whether or not this simulation is the naked singularity formation is rather controversial.

There have also been discovered examples of locally naked singularity. The most famous example would be a timelike singularity in the Kerr and the Reissner-Nordström black holes (RNBH). It is known that there is a similar type of locally naked singularities in the Reissner-Nordström-de Sitter black holes (RNdSBH). On the other hand, there are other types of non-globally hyperbolic space-times, such as the Taub-NUT space-time which is a spatially homogeneous vacuum solution with violation of strong causality.

We have to consider if such a space-time is physically realizable or not. It was proved that the Cauchy horizon inside the event horizon is unstable due to the infinite blueshift effect in the case of the RNBH (Chandrasekhar and Hartle (1982), Poisson and Israel (1990)), the RNdSBH (Brady and Poisson (1992), Brady, Moss and Myers (1998)) and the Kerr black hole (Ori (1998)). Since the Cauchy horizon will be transformed to null, scalar curvature singularity through nonlinear evolution (Brady and Smith (1995), Burko (1997)), global hyperbolicity of the space-time will be recovered.

In the Taub-NUT case, it is believed that, if one slightly perturbes the initial data in a suitable way, one would convert the Cauchy horizon to singularity due to the violation of strong causality. Hence, it is believed that no generic violation of global hyperbolicity exists since small perturbations may destroy the extendibility of the maximal Cauchy development because of the appearance of singularity on the Cauchy horizon (Wald 1984).

On the other hand, it has not yet clearly shown that some examples of the formation of naked singularities in a space-time with divergence of the matter density enumerated above cannot be counterexamples to CCH. The main difficulty is the choice of matter model for revealing the essential properties of gravity. A bad choice of matter model will lead us to the matter-generated singularities, which we could define as a singularity formed in the situation in which the dynamics of the matter leads, independent of the presence of gravitation, to the blow-up of the stress-energy tensor and it causes the space-time geometry become singular through Einstein equation (see, for example, Rendal (1992)). Thus it is important to choose physically reasonable matter.

Table 1.1: Examples of non-globally hyperbolic space-time.

Example	Matter	Symmetry	Notes
shell-crossing[1]	dust	spherical	weak
shell-crossing[2]	perfect fluid $\lvert P\rvert < \infty$	spherical	weak
shell-focusing[3]	dust	spherical	LFC
shell-focusing[4]	dust	(quasi-spherical)	LFC
shell-focusing[5]	dust	spherical	SCC, not generic not smooth initial data
central[6]	null dust	spherical	SCC
central, in pure collapse[7]	perfect fluid $P = (\gamma - 1)\epsilon$	spherical self similar	SCC $\gamma \lesssim 1.0105$
collapsed cone[8]	scalar field	spherical	not generic not smooth initial data
zero-mass BH[9]	scalar field	spherical	unstable
zero-mass BH[10]	GW	axisymmetric	unstable
zero-mass BH[11]	radiation fluid	spherical	unstable
RNBH[12]	EM	static, spherical	unstable
RNdSBH[13]	EM+Λ	static, spherical	unstable
Kerr BH[14]	vacuum	stationary axisymmetric	unstable
Taub-NUT[15]	vacuum	spatially homogeneous	strong causality violation believed to be unstable
spindle[16]	collisionless particles	axisymmetric	numerical simulation controversial

[1] Yodzis, Seifert and Müller zum Hagen (1973)
[2] Müller zum Hagen, Yodzis and Seifert (1974)
[3] Eardley and Smarr (1979), Christodoulou (1984), Newman (1986)
[4] Szekeres (1975), Joshi and Królak (1996)
[5] Singh and Joshi (1996)
[6] Vaidya (1943, 1951a 1951b), Joshi and Dwivedi (1992)
[7] Ori and Piran (1987, 1988, 1990), Lake (1988)
[8] Christodoulou (1994)
[9] Choptuik (1993)
[10] Evans and Coleman (1993)
[11] Abrahams and Evans (1994)
[12] Chandrasekhar and Hartle (1982), Poisson and Israel (1990)
[13] Brady and Poisson (1992), Brady, Moss and Myers (1998)
[14] Ori (1998)
[15] Hawking and Ellis (1973), Wald (1984)
[16] Shapiro and Teukolsky (1991, 1992)

Chapter 2

Spherically Symmetric Dust Collapse

It is difficult to obtain a general solution of the Einstein equation even with the assumption of spherical symmetry. The simplest model of spherical collapse of a star is that with uniform density and zero pressure. The pressureless fluid is called a "dust". The dust can be regarded as a cloud of collisionless particles which obey collisionless Boltzmann (Vlasov) equation with vanishing velocity dispersion. Therefore, in this sense, we can say that dust matter is zero-temperature gas. This model was first solved and analyzed by Oppenheimer and Snyder (1939) and is called the Oppenheimer-Snyder solution. This model first presents a clear vision on the black hole formation as a final fate of complete gravitational collapse. This model can be generalized by introducing inhomogeneities. The solution was given by Tolman (1934) and Bondi (1947) and is often called the Lemaître-Tolman-Bondi (LTB) solution. These models of spherically symmetric dust collapse give us a deep insight into the final fate of collapse and CCH. It was proved that shell-crossing and shell-focusing naked singularities emerge from generic regular or smooth initial data (Yodzis, Seifert and Müller zum Hagen (1973), Eardley and Smarr (1979), Christodoulou (1984), Joshi and Dwivedi (1993a), Singh and Joshi (1996), Jhingan, Joshi and Singh (1996)).

2.1 Spherically Symmetric Space-Time

Before restricting to dust matter, we present the Einstein equation for a general spherically symmetric space-time. In the spherically symmetric space-

time, without loss of generality, the line element is written in the diagonal form as

$$ds^2 = -e^{2\nu(t,r)}dt^2 + e^{2\lambda(t,r)}dr^2 + R^2(t,r)(d\theta^2 + \sin^2\theta d\phi^2). \tag{2.1}$$

Here we adopt the comoving coordinates as a time slicing condition. In these coordinates, the stress-energy tensor $T^{\mu}_{\ \nu}$ which is a source of the spherically symmetric gravitational field must be of the following form:

$$T^{\mu}_{\ \nu} = \begin{pmatrix} -\epsilon & 0 & 0 & 0 \\ 0 & \Sigma & 0 & 0 \\ 0 & 0 & \Pi & 0 \\ 0 & 0 & 0 & \Pi \end{pmatrix}, \tag{2.2}$$

where $\epsilon(t,r)$, $\Sigma(t,r)$ and $\Pi(t,r)$ are the energy density, the radial pressure and the tangential pressure, respectively. If we consider a perfect fluid, which is given as

$$T^{\mu\nu} = (\epsilon + P)u^{\mu}u^{\nu} + Pg^{\mu\nu}, \tag{2.3}$$

then the pressure must be isotropic, i.e.,

$$\Sigma = \Pi = P. \tag{2.4}$$

From the Einstein equation and the equation of motion for the matter, we obtain

$$m' = 4\pi\epsilon R^2 R', \tag{2.5}$$

$$\dot{m} = -4\pi\Sigma R^2 \dot{R}, \tag{2.6}$$

$$\dot{R}' = \dot{R}\nu' + R'\dot{\lambda}, \tag{2.7}$$

$$\Sigma' = -(\epsilon + \Sigma)\nu' - 2(\Sigma - \Pi)\frac{R'}{R}, \tag{2.8}$$

$$m = \frac{R}{2}\left(1 - R'^2 e^{-2\lambda} + \dot{R}^2 e^{-2\nu}\right), \tag{2.9}$$

where $m = m(t,r)$ is the Misner-Sharp mass (Misner and Sharp (1964)) and the prime and overdot denote the partial derivatives with respect to t and r, respectively.

Here we locate apparent horizon, which is defined as the outer boundary of a connected component of the trapped region. The remarkable feature of the apparent horizon is that, if the space-time is strongly asymptotically predictable, i.e., WCCH holds, and the null convergence condition holds,

the presence of the apparent horizon implies the existence of event horizon outside or coinciding with it. If the connected component of the trapped surface has the structure of a manifold with boundary, then the apparent horizon is an outer marginally trapped surface with vanishing expansion (Hawking and Ellis (1973)). Along a future-directed outgoing null geodesic,

$$\frac{dR}{dt} = \dot{R} + R'\frac{dr}{dt} = e^{\nu}\left(\pm\sqrt{-1+\frac{2m}{R}+R'^2e^{-2\lambda}}+R'e^{-\lambda}\right) \tag{2.10}$$

is satisfied, where the upper and lower signs correspond to the expanding and collapsing phases, respectively, and we assume $R' > 0$. Therefore, in the expanding phase, there is no apparent horizon. In the collapsing phase, $R = 2m$ is apparent horizon, $0 \leq R < 2m$ is a trapped region, and $2m < R$ is an untrapped region.

Here we should mention about singularities which may occur in the spherically symmetric collapse. The shell-crossing singularity is the one characterized by $R' = 0$ and $R > 0$, while the shell-focusing singularity is the one characterized by $R = 0$. It is believed that the space-time can be extended beyond the shell-crossing singularities because they satisfy neither SCC nor LFC (for example, Clarke (1993)). The central singularity is the one characterized by $r = 0$, while the non-central singularity is the one characterized by $r > 0$, where $r = 0$ is set to be the symmetric center. It is noted that, since

$$R = 8\pi(\epsilon - \Pi - 2\Pi) \tag{2.11}$$

$$R^{ab}R_{ab} = 64\pi^2(\epsilon^2 + \Sigma^2 + 2\Pi^2) \tag{2.12}$$

are satisfied, the divergence of the energy density directly implies the scalar curvature singularity.

2.2 Spherically Symmetric Dust Collapse

We restrict the matter content to dust, which is defined as a pressureless fluid, i.e.,

$$\Sigma = 0, \tag{2.13}$$

$$\Pi = 0. \tag{2.14}$$

Then, Eqs. (2.5)-(2.9) become

$$m' = 4\pi\epsilon R^2 R', \tag{2.15}$$

$$\dot{m} = 0, \tag{2.16}$$
$$\dot{R}' = \dot{R}\nu' + R'\dot{\lambda}, \tag{2.17}$$
$$\nu' = 0, \tag{2.18}$$
$$m = \frac{R}{2}\left(1 - R'^2 e^{-2\lambda} + \dot{R}^2 e^{-2\nu}\right). \tag{2.19}$$

The above equations are integrable as

$$m = F(r), \tag{2.20}$$
$$\epsilon = \frac{F'}{4\pi R^2 R'}, \tag{2.21}$$
$$e^{2\lambda} = \frac{R'^2}{1+f}, \tag{2.22}$$
$$\nu = 0, \tag{2.23}$$
$$\dot{R}^2 = f + \frac{2F}{R}, \tag{2.24}$$

where arbitrary functions $F = F(r)$ and $1 + f = 1 + f(r) > 0$ are the conserved Misner-Sharp mass and the specific energy, respectively. In Eq. (2.23), using the rescaling freedom of the time coordinate, we have set $\nu(t, r) = 0$. This means that the synchronous comoving coordinates exist in this system. Eq. (2.24) is integrable, as

$$t = \pm\left[\frac{R^{3/2}}{\sqrt{2F}} G\left(-\frac{fR}{2F}\right)\right]_{R^0}^{R}, \tag{2.25}$$

where $R^0(r)$, $G(y)$ and $[Q(R)]_{R^0}^{R}$ are defined as

$$R^0(r) \equiv R(0, r), \tag{2.26}$$
$$G(y) \equiv \begin{cases} \dfrac{\mathrm{Arcsin}\sqrt{y}}{y^{3/2}} - \dfrac{\sqrt{1-y}}{y}, & \text{for } 0 < y \leq 1 \\ \dfrac{2}{3}, & \text{for } y = 0 \\ \dfrac{-\mathrm{Arcsinh}\sqrt{-y}}{(-y)^{3/2}} - \dfrac{\sqrt{1-y}}{y}, & \text{for } y < 0, \end{cases} \tag{2.27}$$
$$[Q(R)]_{R^0}^{R} \equiv Q(R) - Q(R^0), \tag{2.28}$$

and the upper and lower signs in Eq. (2.25) correspond to expanding and collapsing phases, respectively. Hereafter our main concern is turned on the collapsing phase.

Assuming that R is initially a monotonically increasing function of r and rescaling the radial coordinate r, we identify r with the circumferential radius R on the initial spacelike hypersurface $t = 0$. Hereafter we take this radial coordinate r. Then, regularity of the center requires

$$f(0) = 0, \tag{2.29}$$

$$R(t,0) = 0, \tag{2.30}$$

$$\frac{F(r)}{r^3} < \infty \quad \text{at} \quad r \to 0. \tag{2.31}$$

The solution can be matched with the Schwarzschild space-time at an arbitrary radius $r = r_b$ if we identify the Schwarzschild mass parameter with $F(r_b)$.

2.3 Occurrence of Naked Singularity

We concentrate on shell-focusing singularity. The nonextendibility beyond the shell-focusing singularity by the spherically symmetric space-time with dust was shown by Eardley and Smarr (1979). Eq. (2.24) implies that every mass shell labeled by r which is initially collapsing inevitably results in shell-focusing singularity.

It is easily found that the time of the occurrence of shell-focusing singularity $t_s(r)$ and that of apparent horizon $t_{AH}(r)$ is given by

$$t_s(r) = \frac{r^{3/2}}{\sqrt{2F}} G\left(-\frac{fr}{2F}\right), \tag{2.32}$$

$$t_{AH}(r) = t_s(r) - 2FG(-f). \tag{2.33}$$

Therefore, the shell-focusing singularity which occurs at $r > 0$ is in the future of the apparent horizon.

The non-central shell-focusing singularity is not naked. Indeed, suppose a light ray emanates from the shell-focusing singularity at some $r_1 > 0$, which is given by $t = t(r)$. Then by continuity there must exist an $\epsilon > 0$ such that for $r_1 < r < r_1 + \epsilon$ the light ray with positive expansion is later than the apparent horizon and earlier the shell-focusing singularities since the apparent horizon is everywhere but at the center earlier than the shell-focusing singularities. This means $0 < R(t(r), r) < 2F(r)$ and $dR/dt(t(r), r) > 0$. By Eq. (2.10) they lead to a contradiction. Thus the shell-focusing singularities possibly except for the central shell-focusing singularity are not visible to

an observer. Therefore it is sufficient to consider central shell-focusing singularity in order to examine whether or not strong naked singularity exists. By the above argument such a light ray must lie to the past of the apparent horizon.

Here we show that the LTB solution from generic smooth initial data results in shell-focusing naked singularity at the center $r = 0$. In order to investigate the existence of naked singularity, we investigate the geodesic equation for a future-directed outgoing null geodesic which emanates from the singularity. In the coordinates (2.1), we derive thereby the root equation which probes the naked singularity as follows (Joshi and Dwivedi (1993a)). A future-directed outgoing null geodesic is given as

$$\frac{dr}{dt} = e^{\nu-\lambda}. \tag{2.34}$$

Here we define

$$x \equiv \frac{R}{r^\alpha}, \tag{2.35}$$

where $\alpha > 1$ is determined by requiring that x has a positive finite limit x_0. Note that the regular center correspond to $\alpha = 1$. Then, from l'Hospital rule, we obtain

$$\begin{aligned} x_0 &= \lim_{r\to 0} \frac{R}{r^\alpha} \\ &= \lim_{r\to 0} \frac{1}{\alpha r^{\alpha-1}} \frac{dR}{dr}\bigg|_{R=x_0 r^\alpha} \\ &= \lim_{r\to 0} \frac{1}{\alpha r^{\alpha-1}} \left(R' + e^{\lambda-\nu}\dot{R}\right)\bigg|_{R=x_0 r^\alpha}. \end{aligned} \tag{2.36}$$

Substituting the LTB solution obtained in the previous subsection, we obtain

$$x_0 = \lim_{r\to 0} \frac{R'}{\alpha r^{\alpha-1}} \left(1 - \frac{\sqrt{f + \frac{2F}{R}}}{\sqrt{1+f}}\right)\bigg|_{R=x_0 r^\alpha}. \tag{2.37}$$

In order to obtain the root equation for the LTB solution, we must have the explicit expression for R'. By differentiating both sides of Eq. (2.25) with respect to r, we obtain the expression R' after a straightforward but rather lengthy calculation as,

$$R' = N(x, r) r^{\alpha-1}, \tag{2.38}$$

where $N(x,r)$ is given by

$$N(x,r) \equiv (\eta-\beta)x + \left[\Theta - \left(\eta - \frac{3}{2}\beta\right) x^{3/2} G(-Px)\right] \sqrt{P + \frac{1}{x}}. \tag{2.39}$$

Therefore, the desired root equation is

$$x_0 = \frac{N(x_0,0)}{\alpha} \lim_{r\to 0} \left(1 - \frac{\sqrt{f + \frac{\Lambda}{x_0}}}{\sqrt{1+f}}\right) \tag{2.40}$$

with

$$\eta(r) \equiv \frac{rF'}{F}, \tag{2.41}$$

$$\beta(r) \equiv \begin{cases} \dfrac{rf'}{f}, & \text{for } f \neq 0 \\ 0, & \text{for } f = 0 \end{cases} \tag{2.42}$$

$$p(r) \equiv \frac{rf}{2F}, \tag{2.43}$$

$$P(r) \equiv pr^{\alpha-1}, \tag{2.44}$$

$$\Lambda(r) \equiv \frac{2F}{r^\alpha}, \tag{2.45}$$

$$\Theta(r) \equiv \frac{1+\beta-\eta}{(1+p)^{1/2} r^{3(\alpha-1)/2}} + \frac{\left(\eta - \frac{3}{2}\beta\right) G(-p)}{r^{3(\alpha-1)/2}}. \tag{2.46}$$

Note that α is determined uniquely by the requirement that $\Theta(r)$ has a finite limit as $r \to 0$.

For simplicity we assume that $F(r)$ and $f(r)$ are

$$F(r) = F_3 r^3 + F_5 r^5 + F_7 r^7 + \cdots, \tag{2.47}$$

$$f(r) = f_2 r^2 + f_4 r^4 + f_6 r^6 + \cdots. \tag{2.48}$$

This implies that the density field and specific energy field are initially not only regular but also smooth at the symmetric center. That is, the initial density and specific energy profiles are C^∞ functions on the entire real space r if extended to the negative r as even functions. Hereafter we assume $F_3 > 0$, which ensures the positivity of the central energy density at $t = 0$. For marginally bound collapse, which is defined by $f = 0$, the positive finite root of Eq. (2.40) is obtained for $F_5 < 0$ as

$$x_0 = \left(-\frac{F_5}{2F_3}\right)^{2/3} \tag{2.49}$$

with $\alpha = 7/3$. $F_5 < 0$ means $\epsilon''(0,0) < 0$. Therefore, there exists naked singularity in the marginally bound collapse with $\epsilon''(0,0) < 0$ initially. This was first proved by Christodoulou (1984).

On the other hand, for $F_5 = 0$, it is easily found that the root equation (2.40) has no positive finite root for any $\alpha > 1$. Therefore, in this case, the singularity is spacelike. For a homogeneous case, which is given by the marginally bound Oppenheimer-Snyder solution, the singularity is covered because of $F_5 = 0$.

For non-marginally bound case $f_2 \neq 0$, Singh and Joshi (1996) found the following criterion for the occurrence of naked singularity. We define the quantity Q_2 as

$$Q_2 \equiv \left(1 - \frac{f_2}{4F_3}\right)\left[2G\left(-\frac{f_2}{2F_3}\right)\left(\frac{F_5}{F_3} - \frac{3f_4}{2f_2}\right)\left(1 + \frac{f_2}{4F_3}\right) + \frac{2f_4}{f_2} - \frac{F_5}{F_3}\right]. \tag{2.50}$$

If Q_2 is positive, then the singularity is naked, and the positive finite root of Eq. (2.40) is given as

$$x_0 = \left(\frac{3Q_2}{4}\right)^{2/3} \tag{2.51}$$

with $\alpha = 7/3$.

Singh and Joshi (1996) and Jhingan, Joshi and Singh (1996) also investigated more general class in which $F(r)$ and $f(r)$ are of the form

$$F(r) = F_3 r^3 + F_4 r^4 + F_5 r^5 + F_6 r^6 + F_7 r^7 + \cdots, \tag{2.52}$$

$$f(r) = f_2 r^2 + f_3 r^3 + f_4 r^4 + f_5 r^5 + f_6 r^6 + \cdots. \tag{2.53}$$

This choice corresponds to the initial density and specific energy distributions which are not C^∞ on the entire real space r if extended to negative r as even functions. They found that a naked singularity also occurs from generic initial data in this extended space of data. They also showed that, for $F_3 > 0$, $F_4 = F_5 = 0$ and $F_6 < -(26\sqrt{2} + 15\sqrt{6})F_3^{5/2}$ for marginally bound collapse, Eq. (2.40) has a finite positive root x_0 with $\alpha = 3$ and hence the singularity is naked. x_0 is given by the root of some quartic equation. In this thesis, we mainly restrict our attention to smooth initial data.

With respect to the globality of the naked singularity, we can give a simple answer. If the expansion of $F(r)$ and $f(r)$ around the center is the one in which a naked singularity occurs, we can immediately construct a space-time with a globally or locally naked singularity, taking the sufficiently small or large dust ball. This can be done because the LTB solution can be

matched with the Schwarzschild space-time at an arbitrary comoving radius $r = r_b$.

2.4 Curvature Strength of Naked Singularity

Here we investigate the curvature strength of the naked singularity. We restrict our attention to the marginally bound collapse. It is noted that an analysis is very similar for non-marginally bound collapse. For marginally bound collapse, from Eqs. (2.22), (2.25)-(2.28), we obtain

$$e^{\lambda} = R', \tag{2.54}$$

$$R = r\left(1 - \frac{t}{t_{\rm s}}\right)^{2/3}, \tag{2.55}$$

where $t_{\rm s}$ is given by

$$t_{\rm s}(r) = \frac{\sqrt{2}}{3\sqrt{F}} r^{3/2}. \tag{2.56}$$

At $t = t_{\rm s}(r)$, shell-focusing singularity occurs at a mass shell labeled by r.

We consider a future-directed outgoing radial null geodesic which emanates from the singularity. We prepare the tetrad basis $E^a_{(i)}$ $(i = 1, 2, 3, 4)$ with $E^a_{(1)}E_{(1)a} = E^a_{(2)}E_{(2)a} = -E^a_{(3)}E_{(4)a} = -E^a_{(4)}E_{(3)a} = 1$, all other products vanish and $E^a_{(4)}$ is the tangent vector of the geodesic. Define

$$R_{(4)(4)} \equiv R_{ab}k^a k^b, \tag{2.57}$$

where k^a is the tangent vector of the null geodesic. Using Eqs. (2.21), (2.34), (2.54) and the Einstein equation, we obtain

$$\lambda^2 R_{(4)(4)} = 2\frac{F'R'}{R^2}\left(\frac{\lambda}{r}\frac{dr}{d\lambda}\right)^2, \tag{2.58}$$

where λ is the affine parameter such that $\lambda \to +0$ corresponds to approach to the singularity. From Eq. (2.35), (2.38), (2.47) and

$$N(x_0, 0) = \frac{7}{3}x_0, \tag{2.59}$$

we obtain

$$\lambda^2 R_{(4)(4)} \approx 14p^2\frac{F_3 r^{2/3}}{x_0}, \tag{2.60}$$

where p is given by

$$p \equiv \lim_{r \to 0} \frac{d \ln r}{d \ln \lambda}, \tag{2.61}$$

and $\approx$ means the equality up to the lowest order. In order to obtain the value of p, we write the geodesic equation for the radial null geodesic

$$\frac{d}{d\lambda}\left(R'^2 k^r\right) - R' R'' k^{r2} = 0. \tag{2.62}$$

Using the following rule of partial derivatives:

$$\begin{aligned} \left(\frac{\partial}{\partial r}\right)_t &= \left(\frac{\partial}{\partial r}\right)_x + \left(\frac{\partial x}{\partial r}\right)_t \left(\frac{\partial}{\partial x}\right)_r \\ &= \left(\frac{\partial}{\partial r}\right)_x + \frac{N - \alpha x}{r}\left(\frac{\partial}{\partial x}\right)_r, \end{aligned} \tag{2.63}$$

we obtain R'' along the null geodesic as

$$R'' = \frac{28}{9} x_0 r^{1/3}. \tag{2.64}$$

Using this, the null geodesic equation is reduced to the following form:

$$\frac{d^2 r}{d\lambda^2} = -\frac{4}{3}\frac{1}{r}\left(\frac{dr}{d\lambda}\right)^2. \tag{2.65}$$

The solution of the above equation is

$$r = (C\lambda + D)^{3/7}, \tag{2.66}$$

where C and D are constants of integration. We should set $D = 0$. Therefore, by substituting $p = 3/7$ into Eq. (2.60),

$$\lambda^2 R_{(4)(4)} \approx \frac{18}{7} 2^{2/3} F_3^{5/3} (-F_5)^{-2/3} r^{2/3}. \tag{2.67}$$

On the other hand, in a spherically symmetric space-time,

$$C^{(m)}_{(4)(n)(4)} = 0 \tag{2.68}$$

holds, where $m, n = 1, 2$. Therefore, from Proposition 1.3.2, we conclude that SCC is not satisfied. Furthermore, from Eqs. (2.66) and (2.67), we obtain

$$R_{(4)(4)} \propto \lambda^{-12/7}. \tag{2.69}$$

Therefore, from Proposition 1.3.6, LFC is satisfied. This means that a congruence of light rays which hits the singularity is not crushed to zero area but is inevitably contracted. This result was first shown by Newman (1986).

Singh and Joshi (1996) and Jhingan, Joshi and Singh (1996) showed that, if we assume F and f are given in more general form (2.52) and (2.53), even SCC may be satisfied. For example, for $F_3 > 0$, $F_4 = F_5 = 0$ and $F_6 < -(26\sqrt{2} + 15\sqrt{6})F_3^{5/2}$ for marginally bound collapse, the singularity is naked and SCC is satisfied.

2.5 Divergent Behavior

Here we see divergent behavior of the central shell-focusing naked singularity in the marginally bound dust collapse, both on the synchronous comoving time slice at which the naked singularity occurs and on the earliest outgoing null geodesic which emanates from the central naked singularity. We assume smooth initial density profile. Then $F(r)$ is given in Eq. (2.47), where we take $F_3 > 0$ and $F_5 < 0$.

First we set $t = t_s(0) = \sqrt{2}/(3\sqrt{F_3})$. Then, from Eqs. (2.47) and (2.55), the following behavior is easily derived at $t = t_s(0)$ for sufficiently small r:

$$R \approx x_0 r^{7/3}, \tag{2.70}$$

$$R' \approx \frac{7}{3} x_0 r^{4/3}. \tag{2.71}$$

On the other hand,

$$F' \approx 3F_3 r^2 \tag{2.72}$$

holds. Then, from Eq. (2.21), we find

$$\epsilon \propto r^{-4}. \tag{2.73}$$

From Eqs. (2.20), (2.47) and (2.73), we conclude

$$\epsilon \propto R^{-12/7}, \tag{2.74}$$

$$\frac{m}{R} \propto R^{2/7} \tag{2.75}$$

on the spacelike hypersurface $t = t_s(0)$. This behavior around the naked singularity is the same for non-marginally bound collapse. The blow up of the central density is given from Eqs. (2.21), (2.47), (2.55) and (2.56) as

$$\epsilon(t, 0) \propto (t_s(0) - t)^{-2}, \tag{2.76}$$

while, for $r > 0$,

$$\epsilon(t, r) \propto (t_s(r) - t)^{-1}. \tag{2.77}$$

Next we examine divergent behavior on the earliest future-directed outgoing radial null geodesic from the central naked singularity which results from marginally bound collapse. From Eqs. (2.35), (2.38) and (2.59), the behavior of R and R' on this null geodesic around the center is given as,

$$R \approx x_0 r^{7/3}, \tag{2.78}$$

$$R' \approx \frac{3}{7} x_0 r^{4/3}. \tag{2.79}$$

Therefore, we conclude

$$\epsilon \propto R^{-12/7}, \tag{2.80}$$

$$\frac{m}{R} \propto R^{2/7}. \tag{2.81}$$

This behavior seen around the central naked singularity is also the same for non-marginally bound collapse.

Integrating the null condition (2.34) and using Eqs. (2.23), (2.54), (2.55) and (2.79), we obtain

$$t - t_s(0) \approx x_0 r^{7/3}, \tag{2.82}$$

along the outgoing null geodesic which emanates from the singularity. Hence, through Eqs. (2.66) and (2.78), it immediately leads to the following relation:

$$t - t_s(0) \approx x_0 r^{7/3} \approx R \propto \lambda, \tag{2.83}$$

around the center along the null geodesic, which means that the radial null ray is expressed by the straight line with the slope of 45° in the Rt-plane.

From the above discussions, the following proposition holds both on the spacelike hypersurface $t = t_s(0)$ and on the null hypersurface which originates from the singularity first: the naked shell-focusing singularity is massless ($m = 0$) but the attraction force m/R^2 and the tidal force m/R^3 diverge.

2.6 Summary

The collapse of an inhomogeneous dust ball, which is given by the LTB solution, results in shell-focusing naked singularity from generic initial data. The

collapse of a homogeneous dust ball, which is given by the Oppenheimer-Snyder solution, results in covered singularity. Though the Oppenheimer-Snyder solution has been believed to give a typical sample of complete gravitational collapse, the absence of naked singularity seen in this solution turns out to be not typical in general spherically symmetric dust collapse.

Note that the assumption of pressureless matter is no more a good approximation of real matter in any situation with blow up of energy density. The reason why the Oppenheimer-Snyder solution is considered to imitate the physical black hole formation is that the formation of event horizon associates with no divergence of energy density. In this sense, this model for the black hole formation is self-consistent.

The LTB solution is considered to be idealized too much to be realistic as physically realizable singularity formation in many respects, for example, zero-pressure, zero-temperature, no heat flow, no velocity dispersion, no rotation, spherical symmetry, no gravitational wave, and so on. It is very difficult to take all such effects into account, together. So, in the following, we will discuss separately some of such effects.

Chapter 3

Matter with Vanishing Radial Pressure

3.1 Metric Functions

3.1.1 Comoving Coordinates

The matter content in the LTB solution is a pressureless fluid. As an extension of the LTB solution, we consider a general description for spherically symmetric space-time with vanishing radial pressure. In the spherically symmetric space-time, the line element is written as Eq. (2.1) using the comoving coordinates. The field equations are given by Eq. (2.5)-(2.9). In the case where the matter has vanishing radial pressure, the field equations are given by substituting

$$\Sigma = 0, \tag{3.1}$$

into Eqs. (2.5)-(2.9). The results are

$$\begin{aligned} m' &= 4\pi\epsilon R^2 R', && (3.2)\\ \dot{m} &= 0, && (3.3)\\ \dot{R}' &= \dot{R}\nu' + R'\dot{\lambda}, && (3.4)\\ 0 &= -\epsilon\nu' + 2\Pi\frac{R'}{R}, && (3.5)\\ m &= \frac{R}{2}\left(1 - R'^2 e^{-2\lambda} + \dot{R}^2 e^{-2\nu}\right). && (3.6) \end{aligned}$$

We introduce a function $h(r, R)$ as

$$\Pi = -\frac{R}{2h} h_{,R} \epsilon, \tag{3.7}$$

where the comma denotes the partial derivative. For example, Singh and Witten (1997) considered an equation of state as $\Pi = k\epsilon$. Then Eqs. (3.2)-(3.6) are integrable to some extent as

$$\begin{aligned}
m &= F, && (3.8)\\
\epsilon &= \frac{F'}{4\pi R^2 R'}, && (3.9)\\
e^{2\lambda} &= \frac{R'^2 h^2}{1+f}, && (3.10)\\
\nu' &= -\frac{1}{h} h_{,R} R', && (3.11)\\
\dot{R}^2 e^{-2\nu} &= -1 + \frac{2F}{R} + \frac{1+f}{h^2}, \\
&= \frac{1}{h^2}\left[1 + f + \left(-1 + \frac{2F}{R}\right) h^2\right], && (3.12)
\end{aligned}$$

where arbitrary functions $F = F(r)$ and $1 + f = 1 + f(r) > 0$ are the conserved Misner-Sharp mass and the specific energy, respectively. The value of the function $h(r, R) > 0$ has a meaning of the internal elastic energy per volume and the dust limit is given by $h = 1$. The equation of state (3.7) is derivable from the Lagrangian density $\Lambda = -\sqrt{-g}\rho_0(t, r)h(r, R)$, where ρ_0 is the proper rest-mass density (Magli (1997)). Assuming that R is initially a monotonically increasing function of r and rescaling the radial coordinate r, we can identify r with the circumferential radius R on the initial spacelike hypersurface $t = 0$. If we take this radial coordinate r, regularity of the center requires

$$\begin{aligned}
f(0) &= h^2(0,0) - 1, && (3.13)\\
R(t,0) &= 0, && (3.14)\\
|\nu(t,0)| &< \infty, && (3.15)\\
\frac{F(r)}{r^3} &< \infty \quad \text{at} \quad r \to 0. && (3.16)
\end{aligned}$$

Note that we can set $f(0) = h^2(0,0) - 1 = 0$ because basic equations contain f and h only in the form of the ratio of h^2 to $(1 + f)$. Using the rescaling

freedom of the time coordinate, we can set $\nu(t,0) = 0$. The solution can be matched with the Schwarzschild space-time at an arbitrary radius $r = r_b$ if we identify the mass parameter with $F(r_b)$.

If the equation of state for the matter is independent of r, i.e.,

$$h = h(R), \tag{3.17}$$

then Eqs. (3.11) and (3.12) are decoupled and integrated as

$$e^{2\nu} = \frac{1}{h^2}, \tag{3.18}$$

$$t = \pm \int_{R^0(r)}^{R} h(x) \left[-1 + \frac{2F(r)}{x} + \frac{1+f(r)}{h(x)^2} \right]^{-1/2} dx, \tag{3.19}$$

where $R^0(r) \equiv R(0,r)$ is the initial circumferential radius of a mass shell r. However, since in general the $h(r,R)$ depends on r, Eqs. (3.11) and (3.12) are coupled and hence cannot be integrated explicitly.

3.1.2 Mass-Area Coordinates

We review the derivation of an exact solution with vanishing radial pressure in the mass-area coordinates by Magli (1998). The mass-area coordinate system was first introduced by Ori (1990). The line element is written in this coordinate system as

$$\begin{aligned} ds^2 = & -A(m,R)dm^2 - 2B(m,R)dmdR - C(m,R)dR^2 \\ & + R^2(d\theta^2 + \sin^2\theta d\phi^2). \end{aligned} \tag{3.20}$$

Since the Misner-Sharp mass m conserves with respect to each fluid element, the 4-velocity of the fluid element is written as

$$u^\mu = u\delta^\mu{}_R, \tag{3.21}$$

where u is defined as

$$u \equiv u^R = \frac{dR}{d\tau}, \tag{3.22}$$

and τ is the proper time of the fluid element. From the normalization condition $u^\mu u_\mu = -1$, we obtain

$$C = \frac{1}{u^2}. \tag{3.23}$$

Since the space-time can be matched with the Schwarzschild space-time at an arbitrary m, the component A of the metric tensor should be written in the form

$$A = H\left(1 - \frac{2m}{R}\right), \tag{3.24}$$

where H is defined by

$$H \equiv B^2 - AC. \tag{3.25}$$

The derivation of the relation (3.24) is as follows.

We use the fact that the space-time can be matched at an arbitrary comoving radius with the Schwarzschild space-time

$$ds^2 = -\left(1 - \frac{2m}{R}\right)dT^2 + \left(1 - \frac{2m}{R}\right)^{-1} dR^2 + R^2(d\theta^2 + \sin^2\theta d\phi^2). \tag{3.26}$$

Substituting

$$dT = T_{,m}dm + T_{,R}dR, \tag{3.27}$$

into Eq. (3.26), we obtain

$$\begin{aligned} ds^2 &= -\left(1 - \frac{2m}{R}\right)T_{,m}^2 dm^2 - 2\left(1 - \frac{2m}{R}\right)T_{,m}T_{,R}dmdR \\ &\quad - \left[\left(1 - \frac{2m}{R}\right)T_{,R}^2 - \left(1 - \frac{2m}{R}\right)^{-1}\right]dR^2 \\ &\quad + R^2(d\theta^2 + \sin^2\theta d\phi^2). \end{aligned} \tag{3.28}$$

Comparing with Eq. (3.20), we obtain

$$A = \left(1 - \frac{2m}{R}\right)T_{,m}^2, \tag{3.29}$$

$$B = \left(1 - \frac{2m}{R}\right)T_{,m}T_{,R}, \tag{3.30}$$

$$C = \left(1 - \frac{2m}{R}\right)T_{,R}^2 - \left(1 - \frac{2m}{R}\right)^{-1}. \tag{3.31}$$

From

$$H = B^2 - AC = T_{,m}^2, \tag{3.32}$$

we obtain the desired equation.

The energy density ϵ is expressed by the quantities in these coordinates as

$$\epsilon = \frac{h}{4\pi R^2|u|E\sqrt{H}}, \tag{3.33}$$

where $E(m)$ is defined by

$$E^2(m) \equiv 1 + f(F^{-1}(m)), \tag{3.34}$$

and F^{-1} is the inverse function of F. The derivation of Eq. (3.33) is as follows.

In the comoving coordinates, the line element in the radial direction on the spacelike hypersurface Σ_t which is orthogonal to the velocity field of every fluid element u^μ is written as

$$ds^2 = e^{2\lambda}dr^2 = \frac{R'^2h^2}{1+f}dr^2, \tag{3.35}$$

where we have used Eq. (3.10) for the second equality. In the mass-area coordinates, the 4-velocity of each fluid element is given by Eq. (3.21). Thereby, the radial curve on Σ_t is given by the following equation:

$$\frac{dR}{dm} = -\frac{B}{C}. \tag{3.36}$$

Hence, the line element in the radial direction on Σ_t is written as

$$ds^2 = \frac{H}{C}dm^2. \tag{3.37}$$

Then, the requirement of equivalence of these two expressions leads to

$$\frac{R'^2h^2}{1+f} = \frac{H}{C}\left.\frac{\partial m}{\partial r}\right|_t^2 = \frac{H}{C}F'^2. \tag{3.38}$$

Using Eqs. (3.9) and (3.23), and assuming that ϵ is nonnegative, we obtain the desired equation.

3.1.3 Field Equations

Since, in these coordinates, the stress-energy tensor with vanishing radial pressure is written as

$$T^\mu_{\ \nu} = \begin{array}{c} \\ \nu = m \\ R \\ \theta \\ \phi \end{array} \begin{array}{c} \begin{array}{cccc} \mu = m & R & \theta & \phi \end{array} \\ \begin{pmatrix} 0 & -Bu^2\epsilon & 0 & 0 \\ 0 & -\epsilon & 0 & 0 \\ 0 & 0 & \Pi & 0 \\ 0 & 0 & 0 & \Pi \end{pmatrix} \end{array}, \tag{3.39}$$

the Einstein equation is given as

$$G^m_{\ m} = \frac{1}{R^2}\left[1 - \frac{A}{H} - R\left(\frac{A}{H}\right)_{,R}\right] = 0, \tag{3.40}$$

$$G^R_{\ m} = -\frac{1}{R}\left(\frac{A}{H}\right)_{,m} = -8\pi B u^2 \epsilon, \tag{3.41}$$

$$G^m_{\ R} = -\frac{1}{RH}\left[\frac{BH_{,R}}{H} - C_{,m}\right] = 0. \tag{3.42}$$

The other components of the Einstein equation are not independent of the above three equations.

3.1.4 Integration

The above equations are easily integrated. Eq. (3.24) automatically satisfies Eq. (3.40). Substituting Eqs. (3.24) and (3.33) into Eq. (3.41), we obtain

$$B = -\frac{E\sqrt{H}}{h|u|}, \tag{3.43}$$

From Eqs. (3.23) and (3.43), we obtain

$$u = \pm\sqrt{-1 + \frac{2m}{R} + \frac{E^2}{h^2}}. \tag{3.44}$$

Substituting Eqs. (3.23) and (3.43) into Eq. (3.42), we obtain

$$(\sqrt{H})_{,R} = -\frac{h}{E}\left(\frac{1}{|u|}\right)_{,m}. \tag{3.45}$$

Integrating this equation, we finally obtain the explicit expression for $\sqrt{H}$ as

$$\sqrt{H} = g(m) + \int^R G(m,x)dx, \tag{3.46}$$

$$\begin{aligned} G(m,x) &\equiv -\frac{h}{E}\left(\frac{1}{|u|}\right)_{,m} \\ &= \frac{h}{xE}\left(1 + \frac{x}{2}\left(\frac{E^2}{h^2}\right)_{,m}\right)\left(-1 + \frac{2m}{x} + \frac{E^2}{h^2}\right)^{-3/2}, \end{aligned} \tag{3.47}$$

where $g(m)$ is an arbitrary function. $g(m)$ is determined by specifying the initial data as

$$g(m) = \sqrt{H(m, R^0(m))} - \int^{R^0} G(m, x)dx, \tag{3.48}$$

where R^0 is defined by

$$R^0(m) \equiv R(0, F^{-1}(m)). \tag{3.49}$$

3.1.5 Initial Data

From the two expressions for the energy density ϵ, (3.9) and (3.33), we obtain

$$\left.\frac{\partial R}{\partial m}\right|_t = \frac{R'}{F'} = \frac{E}{h}|u|\sqrt{H}. \tag{3.50}$$

Using this equation, we obtain the initial value for $\sqrt{H}$ as

$$\sqrt{H(m, R^0(m))} = \frac{R^0_{,m}(m)h(m, R^0(m))}{E(m)|u^0(m)|}, \tag{3.51}$$

where u^0 is defined by

$$u^0(m) \equiv \pm\sqrt{-1 + \frac{2m}{R^0(m)} + \frac{E^2(m)}{h^2(m, R^0(m))}}. \tag{3.52}$$

Then, Eq. (3.46) becomes

$$\sqrt{H} = \sqrt{H(m, R^0(m))} + \int_{R^0(m)}^{R} G(m, x)dx. \tag{3.53}$$

We summarize the obtained metric functions.

$$A = H\left(1 - \frac{2m}{R}\right), \tag{3.54}$$

$$B = -\frac{E\sqrt{H}}{h|u|}, \tag{3.55}$$

$$C = \frac{1}{u^2}, \tag{3.56}$$

$$u = \pm\sqrt{-1 + \frac{2m}{R} + \frac{E^2}{h^2}}, \tag{3.57}$$

$$\begin{aligned}
\sqrt{H} &= \frac{R^0_{,m} h(m, R^0)}{E|u^0|} \\
&\quad + \int_{R^0}^{R} \frac{h}{xE} \left(1 + \frac{x}{2} \left(\frac{E^2}{h^2} \right)_{,m} \right) \\
&\quad \times \left(-1 + \frac{2m}{x} + \frac{E^2}{h^2} \right)^{-3/2} dx, \qquad (3.58) \\
u^0(m) &\equiv \pm \sqrt{-1 + \frac{2m}{R^0(m)} + \frac{E^2(m)}{h^2(m, R^0(m))}}, \qquad (3.59) \\
\epsilon &= \frac{h}{4\pi R^2 |u| E \sqrt{H}}. \qquad (3.60)
\end{aligned}$$

Then, shell-crossing singularity occurs when $u\sqrt{H} = 0$ is satisfied. If shell-crossing occurs, the solution is no longer valid after that.

3.2 Existence of Central Naked Singularity

We will examine the nakedness and curvature strength of the central shell-focusing singularity, following Harada, Nakao and Iguchi (1998). If and only if the singularity is naked, there exists a future-directed outgoing null geodesic which emanates from the singularity. In the mass-area coordinates, we can derive the root equation which probes the existence of such geodesic as follows. The radial null geodesics are given as

$$\begin{aligned}
\frac{dR}{dm} &= \frac{-B \mp \sqrt{H}}{C} \\
&= \sqrt{H}|u| \left(\frac{E}{h} \mp |u| \right). \qquad (3.61)
\end{aligned}$$

Note that we will denote E/h as $1/h$ for the rest of this chapter as a matter of convenience. Of course, this change of notation does not imply any loss of generality. We should note that the upper sign refers to an outgoing null ray in a collapsing phase and an ingoing null ray in an expanding phase *at the same time*. Similarly, the lower sign refers to an ingoing null ray in a collapsing phase and an outgoing null ray in an expanding phase *at the same time*. Hereafter we mainly concentrate on a collapsing phase.

Here we define

$$y \equiv \frac{R}{2m^\beta}, \qquad (3.62)$$

where $\beta > 1/3$ is determined by requiring that y has a positive finite limit y_0. Note that we will only consider naked singularities with such β. The regular center corresponds to $\beta = 1/3$. Then, from the l'Hospital's rule, we obtain

$$\begin{aligned} y_0 &= \lim_{m\to 0} \frac{R}{2m^\beta}\Big| \\ &= \lim_{m\to 0} \frac{m^{1-\beta}}{2\beta}\frac{dR}{dm}\Big|_{R=2y_0m^\beta} \\ &= \lim_{m\to 0} \frac{m^{1-\beta}}{2\beta}|u|\sqrt{H}\left(\frac{1}{h} \mp |u|\right)\Big|_{R=2y_0m^\beta} . \end{aligned} \tag{3.63}$$

We will assume the existence of every limit in this chapter including $\pm\infty$. Therefore, we obtain the root equation

$$\begin{aligned} y_0 = \frac{1}{2\beta}\lim_{m\to 0}\Bigg[& m^{3(1-\beta)/2}\sqrt{H}\sqrt{\left(-1+\frac{1}{h^2}\right)m^{-(1-\beta)}+\frac{1}{y_0}} \\ & \times\left(\frac{1}{h} \mp \sqrt{\frac{m^{1-\beta}}{y_0}-1+\frac{1}{h^2}}\right)\Bigg]\Bigg|_{R=2y_0m^\beta} . \end{aligned} \tag{3.64}$$

In order for y_0 to be positive and finite, β must satisfy

$$\frac{1}{3} < \beta \leq 1. \tag{3.65}$$

From $u^2 \geq 0$ and $0 < y_0 < \infty$,

$$\lim_{m\to 0} h \leq \begin{cases} 1 & \text{for } \beta < 1 \\ (1-y_0^{-1})^{-1/2} & \text{for } \beta = 1 \end{cases} \tag{3.66}$$

holds along the null ray which emanates from the singularity. Here we should note that, if the singularity is *critically naked*, i.e.,

$$\lim_{m\to 0} \frac{2m}{R} = 1 \tag{3.67}$$

is satisfied along the null ray, higher order analysis is needed.

3.3 Curvature Strength of Naked Singularity

We consider a radial null geodesic which emanates from or terminates at the naked singularity. We prepare a parallely propagated tetrad $E^a_{(i)} : (i = 1, 2, 3, 4)$ with $E^a_{(1)}E_{(1)a} = E^a_{(2)}E_{(2)a} = -E^a_{(3)}E_{(4)a} = -E^a_{(4)}E_{(3)a} = 1$, all other products vanish and E^a_4 is equal to the tangent vector k^a of the null geodesic. In a spherically symmetric space-time,

$$C^{(m)}_{\ (4)(n)(4)} = 0 \tag{3.68}$$

is satisfied for $m, n = 1, 2$. Define

$$p \equiv \lim_{\lambda \to 0} \lambda^\alpha R_{(4)(4)}, \tag{3.69}$$

where $R_{(4)(4)}$ is given by

$$R_{(4)(4)} \equiv R_{ab}k^a k^b, \tag{3.70}$$

and λ is the affine parameter such that $\lambda \to +0$ corresponds to an approach to the singularity. Then, from Propositions 1.3.2, 1.3.3, 1.3.5 and 1.3.6, we obtain the following lemma:

Lemma 3.3.1 *For the radial null geodesic which emanates from or terminates at the singularity in the spherically symmetric space-time: SCC is satisfied if p is positive for $\alpha = 2$, and not satisfied if p is equal to 0 for $\alpha < 2$. LFC is satisfied if p is positive for $\alpha = 1$, and not satisfied if p is equal to 0 for $\alpha < 1$.*

Since the null geodesic is given as

$$k^R = \frac{-B \mp \sqrt{H}}{C} k^m, \tag{3.71}$$

we obtain, from the form of the stress-energy tensor (3.39),

$$R_{(4)(4)} = 8\pi\epsilon u^2 H (k^m)^2. \tag{3.72}$$

Then,

$$\begin{aligned} \lambda^2 R_{(4)(4)} &= \frac{1}{2}|u|h\sqrt{H}\left(\frac{2m}{R}\right)^2 \left(\frac{\lambda}{m}\frac{dm}{d\lambda}\right)^2 \\ &\approx \frac{\beta q^2}{y_0} m^{1-\beta} \frac{h^2}{1 \mp h|u|} \end{aligned} \tag{3.73}$$

holds, where q is defined by

$$q \equiv \lim_{m\to 0} \frac{d\ln m}{d\ln \lambda} \tag{3.74}$$

and we have used Eq. (3.63).

We should note that, for $(\beta, y_0) \neq (1,1)$,

$$0 < \lim_{m\to 0} \frac{h^2}{1-h|u|} < \infty, \tag{3.75}$$

$$0 \leq \lim_{m\to 0} \frac{h^2}{1+h|u|} < \infty \tag{3.76}$$

hold, where the equality holds only when

$$\lim_{m\to 0} h = 0 \tag{3.77}$$

is satisfied. Therefore, we obtain

$$R_{(4)(4)} \propto \lambda^{q(1-\beta)-2}, \tag{3.78}$$

for the outgoing null geodesic with $0 < q < \infty$ and $(\beta, y_0) \neq (1,1)$, and for the ingoing null geodesic with $0 < q < \infty$, $(\beta, y_0) \neq (1,1)$ and $\lim_{m\to 0} h > 0$. In summary, we present the following theorems:

Theorem 3.3.1 *For the outgoing radial null geodesic which emanates from the non-critically naked singularity with $0 < q < \infty$: if and only if $1/3 < \beta < 1$ and $1/(1-\beta) < q < \infty$ are satisfied, neither SCC nor LFC holds, if $1/3 < \beta < 1$ and $0 < q \leq 1/(1-\beta)$ are satisfied, not SCC but only LFC holds, and if and only if $\beta = 1$ is satisfied, both SCC and LFC hold.*

Theorem 3.3.2 *For the ingoing radial null geodesic which terminates at the non-critically naked singularity with $0 < q < \infty$ and $lim_{m\to 0} h \neq 0$: if and only if $1/3 < \beta < 1$ and $1/(1-\beta) < q < \infty$ are satisfied, neither SCC nor LFC holds, if and only if $1/3 < \beta < 1$ and $0 < q \leq 1/(1-\beta)$ are satisfied, not SCC but only LFC holds, and if and only if $\beta = 1$ is satisfied, both SCC and LFC hold.*

In order to estimate q, we must solve the null geodesic equation

$$\frac{d}{d\lambda}\left(\sqrt{H}k^m\right) \pm \frac{1}{2}\left[A_{,R} + 2B_{,R}|u|\sqrt{H}\left(\frac{1}{h} \mp |u|\right)\right.$$
$$\left. + C_{,R}u^2 H\left(\frac{1}{h} \mp |u|\right)^2\right](k^m)^2 = 0, \tag{3.79}$$

where we have used the null condition (3.71). From Eq. (3.45), we obtain

$$\sqrt{H}_{,R} = \frac{h}{2|u|^3}\left(\frac{2}{R} + \left(\frac{1}{h^2}\right)_{,m}\right). \tag{3.80}$$

Using this, the following expressions are derived:

$$A_{,R} = \frac{2m}{R^2}H + \frac{\sqrt{H}}{|u|^3}h\left(1-\frac{2m}{R}\right)\left(\frac{2}{R} + \left(\frac{1}{h^2}\right)_{,m}\right), \tag{3.81}$$

$$B_{,R} = -\frac{1}{2|u|^4}\left(\frac{2}{R} + \left(\frac{1}{h^2}\right)_{,m}\right) - \frac{\sqrt{H}}{|u|^3}\frac{1}{h}\left[\left(1-\frac{2m}{R}\right)\frac{h_{,R}}{h} + \frac{m}{R^2}\right], \tag{3.82}$$

$$C_{,R} = \frac{2}{u^4}\left(\frac{m}{R^2} + \frac{1}{h^2}\frac{h_{,R}}{h}\right). \tag{3.83}$$

Using these expressions, we finally obtain the radial null geodesic equation for $m \to 0$ in the explicit form

$$\frac{d^2m}{d\lambda^2} = \left[1-\beta-\frac{1}{2}\frac{h^2}{1\mp h|u|}\left(\frac{2m}{R} + \frac{d}{d\ln m}\frac{1}{h^2}\right)\right]\frac{1}{m}\left(\frac{dm}{d\lambda}\right)^2, \tag{3.84}$$

where the ordinary derivative is taken along $R = 2y_0 m^\beta$. On the other hand, if m is proportional to λ^q along the null geodesic, the following equation holds:

$$\frac{d^2m}{d\lambda^2} = \left(1-\frac{1}{q}\right)\frac{1}{m}\left(\frac{dm}{d\lambda}\right)^2. \tag{3.85}$$

Comparing Eqs. (3.84) and (3.85), we can determine q and therefore the curvature strength of the singularity only from β and $h(m, R = 2y_0 m^\beta)$. In evaluating the right hand side, we should note

$$R \approx 2y_0 m^\beta, \tag{3.86}$$

$$|u| \approx m^{(1-\beta)/2}\sqrt{\frac{1}{y_0} + m^{-(1-\beta)}\left(\frac{1}{h^2}-1\right)}, \tag{3.87}$$

$$\sqrt{H} \approx \beta\frac{R}{m}\frac{h}{|u|(1\mp h|u|)}. \tag{3.88}$$

3.4 Gravity-Dominated Singularity

Here we define the "gravity-dominated" singularity as follows:

Definition 3.4.1 *A central singularity is said to be gravity-dominated if and only if*

$$\lim_{m\to 0} \frac{R}{2m}\left(\frac{1}{h^2}-1\right)=0 \tag{3.89}$$

is satisfied along a radial null geodesic which emanates from or terminates at the singularity.

For the gravity-dominated singularity, the collapse is induced dominantly by the gravitational potential energy (see Eq. (3.12) or (3.44)) and the null geodesic equation is controlled only by the gravitational potential. The latter can be shown by the following proposition:

Proposition 3.4.1 *For the gravity-dominated singularity,*

$$\lim_{m\to 0} \frac{R}{2m}\frac{d}{d\ln m}\frac{1}{h^2}=0 \tag{3.90}$$

is satisfied.

Proof. We use $R \approx 2y_0 m^\beta$ along the null geodesic. Then, for $\beta < 1$, the l'Hospital's rule applies. For $\beta = 1$, we set $f \equiv h^{-2} - 1$. Then condition (3.89) implies $\lim_{x\to 0} f(x) = 0$. From the mean value theorem, there exists $c \in (0, x)$ for any $x > 0$ such that

$$|cf'(c)| = \left|c\frac{f(x)}{x}\right| \le |f(x)|.$$

From the existence of the limit, it must be zero. □

This class contains very wide range of naked singularities. Furthermore it might be thought that, if the gravitational collapse of physical matter from regular initial data results in the central naked singularity formation, the singularity would be gravity-dominated at least within our knowledge.

For the gravity-dominated singularity, Eqs. (3.87) and (3.88) become

$$|u| \approx y_0^{-1/2} m^{(1-\beta)/2} \tag{3.91}$$

and

$$\sqrt{H} \approx \begin{cases} 2\beta y_0^{3/2} m^{-3(1-\beta)/2}, & \text{for } \beta < 1 \\ \dfrac{2y_0^2}{y_0^{1/2} \mp 1}, & \text{for } \beta = 1 \text{ and } y_0 \neq 1 \end{cases}. \tag{3.92}$$

For $\beta < 1$, since Eq. (3.84) becomes

$$\frac{d^2m}{d\lambda^2} = (1-\beta)\frac{1}{m}\left(\frac{dm}{d\lambda}\right)^2, \tag{3.93}$$

we obtain

$$q = \frac{1}{\beta}. \tag{3.94}$$

Then, $1 < q < 3$ and $R \propto \lambda$ hold. Eq. (3.78) becomes

$$R_{(4)(4)} \propto \lambda^{-3+1/\beta}. \tag{3.95}$$

Therefore SCC is not satisfied. LFC is satisfied for $1/2 \leq \beta < 1$, while LFC is not satisfied for $1/3 < \beta < 1/2$.

For $\beta = 1$ and $y_0 \neq 1$, Eq. (3.84) becomes

$$\frac{d^2m}{d\lambda^2} = -\frac{1}{2(y_0^{1/2} \mp 1)y_0^{1/2}}\frac{1}{m}\left(\frac{dm}{d\lambda}\right)^2. \tag{3.96}$$

Therefore we obtain

$$q = \frac{2(y_0^{1/2} \mp 1)y_0^{1/2}}{2(y_0^{1/2} \mp 1)y_0^{1/2} + 1}, \tag{3.97}$$

Then, $0 < q < 1$ and $R \propto \lambda^q$ hold. Eq. (3.78) becomes

$$R_{(4)(4)} \propto \lambda^{-2}. \tag{3.98}$$

Therefore both SCC and LFC are satisfied.

In summary, we present the following theorems:

Theorem 3.4.1 *For the gravity-dominated non-critically naked singularity: if and only if $1/3 < \beta < 1/2$ is satisfied, neither SCC nor LFC holds, if and only if $1/2 \leq \beta < 1$ is satisfied, not SCC but only LFC holds, and if and only if $\beta = 1$ is satisfied, then both SCC and LFC hold, for the radial null geodesic which emanates from or terminates at the singularity.*

Theorem 3.4.2 *For the gravity-dominated non-critically naked singularity:*

$$\lim_{m\to 0}\frac{R}{\lambda}$$

along the radial null geodesic which emanates from or terminates at the singularity is nonzero finite value or infinity. If and only if the limit converges, SCC does not hold, and if and only if the limit diverges, both SCC and LFC hold, for the null geodesic.

3.5 LTB Solution in Mass-Area Coordinates

As an example, if we consider marginally bound dust collapse, i.e., $E = 1$ and $h = 1$, the integration can be executed by hand and we obtain the marginally bound LTB solution in the mass-area coordinates.

$$A = H\left(1 - \frac{2m}{R}\right), \tag{3.99}$$

$$B = -\frac{\sqrt{H}}{|u|}, \tag{3.100}$$

$$C = \frac{1}{u^2}, \tag{3.101}$$

$$u = \pm\sqrt{\frac{2m}{R}}, \tag{3.102}$$

$$\sqrt{H} = \sqrt{\frac{R^0}{2m}}m^{1/3}(m^{-1/3}R^0)_{,m} + \frac{2}{3}\left(\frac{R}{2m}\right)^{3/2}, \tag{3.103}$$

$$\epsilon = \frac{1}{4\pi R^2|u|\sqrt{H}}. \tag{3.104}$$

We restrict our attention to a collapsing phase. We set the initial spacelike hypersurface as

$$R^0(m) = F^{-1}(m), \tag{3.105}$$

which corresponds to the choice of the radial coordinate in the comoving coordinates as $R(0, r) = r$.

First we give the function $F(r)$ as

$$F(r) = F_3 r^3 + F_5 r^5 + \cdots, \tag{3.106}$$

which corresponds to generic smooth initial data. For $F_3 > 0$ and $F_5 < 0$, Eq. (3.64) has a finite positive root

$$y_0 = \left(\frac{-F_5}{4\sqrt{2}F_3^{13/6}}\right)^{2/3} \tag{3.107}$$

with $\beta = 7/9$. Then, from Theorem 3.4.1, not SCC but only LFC is satisfied for the radial null geodesic which emanates from the singularity.

Next, if we give $F(r)$ as

$$F(r) = F_3 r^3 + F_6 r^6 + \cdots, \tag{3.108}$$

which corresponds to non-generic regular initial data. For $F_3 > 0$ and $F_6 < -(26\sqrt{2} + 15\sqrt{6})F_3^{5/2}$, Eq. (3.64) has a finite positive root y_0 with $\beta = 1$, where $y_0 > 1$ is expressed using the root of some quartic equation. Then, from Theorem 3.4.1, both SCC and LFC are satisfied for the outgoing radial null geodesic which emanates from the singularity.

For the above two cases, the curvature strength is exactly the same for the ingoing radial null geodesic which terminates at the singularity.

Chapter 4

Counterrotating Particles

In Newton gravity, the final fate of the gravitational collapse of a cloud of collisionless particles crucially depends on whether or not it is initially rotating and whether or not its velocity dispersion vanishes. Hence, also in general relativity, it is expected that rotation and velocity dispersion would play a crucial role. In general case, the collapse of a rotating cloud will proceed in a very aspherical manner. It is, however, known that spherical symmetry is very helpful simplification in investigating the space-time. Here we introduce *counterrotation* of collisionless particles which is consistent with spherical symmetry in order to know the effect of rotation and velocity dispersion on the shell-focusing naked singularity formation.

A spherical cloud of counterrotating particles has been studied by several authors. The static case was first investigated by Einstein (1939). The static model is often referred to as an "Einstein cluster". Recently, Comer and Katz (1993) studied its mechanical stability. The dynamical model was investigated by Datta (1970), Bondi (1971) and Evans (1976). Evans (1976) also studied the infinitesimally thin case, i.e., a self-gravitating counterrotating shell. They obtained partially differential equations for the metric functions and had qualitative understanding, but could not obtain the metric functions in the explicit integral form. This system is described by a fluid with vanishing radial pressure as will be shown below. Here we will determine the metric functions in the explicit form and thereby see how the occurrence of the shell-focusing naked singularity in the LTB solution is altered, following Harada, Iguchi and Nakao (1998).

4.1 Construction

Suppose we are given a spherically symmetric space-time. In a spherically symmetric space-time, without loss of generality, the line element is written by Eq. (2.1). We assume that each particle has negligibly small mass m and that collisions of particles are negligible. If we put a particle with a certain velocity and a certain inclination α ($0 \leq \alpha < 2\pi$) with respect to the equatorial plane $\theta = \pi/2$ at a certain point, it begins to move along a timelike geodesic in the plane inclined by the angle α. We choose the radial coordinate r as the one which follows the radial motion of the particle.

The geodesic equation of the particle is integrable as

$$u^t = e^{-\nu}\sqrt{1 + \frac{L^2}{R^2}}, \tag{4.1}$$

$$u^r = 0, \tag{4.2}$$

$$(u^\theta)^2 + (u^\phi)^2 \sin^2\theta = \frac{L^2}{R^4}, \tag{4.3}$$

$$u^\phi = \frac{M}{R^2 \sin^2\theta}, \tag{4.4}$$

where $u^\mu \equiv dx^\mu/d\lambda$ is the 4-velocity of the particle, and λ is the proper time of the particle. L and M are constants of motion, which are the magnitude and z-component of the specific angular momentum of the particle, respectively. M satisfies

$$M = L\cos\alpha. \tag{4.5}$$

Moreover, from the condition for the radial coordinate

$$\frac{dr}{d\lambda} = \frac{d^2r}{d\lambda^2} = 0, \tag{4.6}$$

we obtain the condition for the lapse function,

$$\nu' = \left(1 + \frac{L^2}{R^2}\right)^{-1} \frac{R'}{R}. \tag{4.7}$$

We put another particle at the same point with the identical phase of the identical orbital motion except for the inclination. Repeating this many times, we can finally obtain the homogeneous distribution with respect to the inclination with common orbital motion at the point. We also obtain the homogeneous distribution with respect to the inclination at another point of

the same r. Repeating this many times, we can finally obtain a sufficiently homogeneous shell of collisionless particles at r with the common phase of the common orbital motion. We call this a thin shell. A thin shell is characterized by its energy density, specific energy and specific angular momentum. By constructing the thin shell, we recover spherical symmetry in the matter distribution. If we put together a lot of thin shells with smoothly distributed energy density, specific energy and specific angular momentum with respect to r, we can obtain a thick shell or a spherical cluster of counterrotating particles.

We regard this as a source of the spherically symmetric gravitational field which has been dealt with until now as if it was a given "background" space-time. Clearly, isotropic tangential velocity dispersion is introduced. Coherent local radial motion is allowed, while local radial velocity dispersion is not allowed.

4.2 Stress-Energy Tensor

By spherical symmetry, without loss of generality, we concentrate on a point p on the equatorial plane in estimating the averaged stress-energy tensor. From Eqs. (4.3), (4.4) and (4.5), we parametrize the tangential velocity by the inclination angle α as

$$u^\theta = \frac{L(r)}{R^2}\sin\alpha, \tag{4.8}$$

$$u^\phi = \frac{L(r)}{R^2}\cos\alpha \tag{4.9}$$

for each particle comprising the thin shell at r, where $L(r)$ is the common specific angular momentum of each particle on this thin shell. By construction, particles that pass through p are distributed homogeneously with respect to the inclination angle α. Therefore, if we average $u^\mu u_\nu$ with respect to the inclination angle α at p, we obtain, from Eqs. (4.1), (4.2), (4.8) and (4.9),

$$\begin{aligned} < u^\mu u_\nu >_\alpha &\equiv \frac{1}{2\pi}\int_0^{2\pi} d\alpha u^\mu u_\nu \\ &= \begin{pmatrix} -\left(1+\frac{L^2}{R^2}\right) & 0 & 0 & 0 \\ 0 & 0 & 0 & 0 \\ 0 & 0 & \frac{1}{2}\frac{L^2}{R^2} & 0 \\ 0 & 0 & 0 & \frac{1}{2}\frac{L^2}{R^2} \end{pmatrix}. \end{aligned} \tag{4.10}$$

Here, we note that the inclination-averaged stress-energy tensor $T^{\mu}_{\ \nu}$ is given as

$$T^{\mu}_{\ \nu} = mn < u^{\mu}u_{\nu} >_{\alpha}, \tag{4.11}$$

where $n = n(t, r)$ is the proper number density of particles. Then we finally obtain $T^{\mu}_{\ \nu}$ for the spherical cluster of counterrotating particles in the form of Eq. (2.2), where ϵ, Σ and Π are

$$\epsilon = mn\left(1 + \frac{L^2}{R^2}\right), \tag{4.12}$$

$$\Sigma = 0, \tag{4.13}$$

$$\Pi = \frac{mn}{2}\frac{L^2}{R^2}, \tag{4.14}$$

respectively. The "equation of state" for the cluster is given as

$$\Pi = \frac{1}{2}\frac{L^2}{R^2 + L^2}\epsilon. \tag{4.15}$$

This stress-energy tensor is consistent with spherical symmetry of the spacetime. Note again that the specific angular momentum may depend on the radial coordinate r.

4.3 Metric Functions

The derivation of an exact solution with general tangential pressure in the mass-area coordinates has been described in Chap. 3. From the equation of state for the cluster (4.15) and boundary condition $h(0, 0) = 1$, the function $h(r, R)$ is given as

$$h^2 = 1 + \frac{L^2}{R^2}, \tag{4.16}$$

where $L = L(r)$. We should note that, although the definition of $h(r, R)$ includes the ambiguity of factorizing by an arbitrary function of r, it can be placed on the function $f(r)$. Since, in this model, $h(r, R)$ depends on r, the coupled partially differential equations in the comoving coordinates cannot be decoupled. Adopting the results obtained in Chap. 3 to the present problem, we obtain the explicit form for the metric functions given in Eq. (3.20) as follows:

$$A = H\left(1 - \frac{2m}{R}\right), \tag{4.17}$$

$$B = -E\sqrt{H}\left[E^2 - 2V(R;m)\right]^{-1/2}, \tag{4.18}$$

$$C = \left(1+\frac{L^2}{R^2}\right)\left[E^2 - 2V(R;m)\right]^{-1}, \tag{4.19}$$

$$u = \pm\left(1+\frac{L^2}{R^2}\right)^{-1/2}\left[E^2 - 2V(R;m)\right]^{1/2}, \tag{4.20}$$

$$\begin{aligned}\sqrt{H(m,R)} &= \frac{(R^0)_{,m}}{E}\left(1+\frac{L^2}{(R^0)^2}\right)\left[E^2 - 2V(R^0;m)\right]^{-1/2} \\ &\quad + \int_{R^0}^{R}\frac{1}{E}\left[\left(1+\frac{L^2}{x^2}\right)^2 + \frac{1}{2}\left(1+\frac{L^2}{x^2}\right)xE_{,m}^2 - \frac{E^2}{2}\frac{L_{,m}^2}{x}\right] \\ &\quad \times\left[E^2 - 2V(x;m)\right]^{-3/2}\frac{dx}{x},\end{aligned} \tag{4.21}$$

$$\epsilon = \frac{1}{4\pi R^2 E\sqrt{H}}\left(1+\frac{L^2}{R^2}\right)\left[E^2 - 2V(R;m)\right]^{-1/2}, \tag{4.22}$$

where the effective potential $V(R;m)$ is defined as

$$\begin{aligned}V(R;m) &\equiv \frac{1}{2}\left(1-\frac{2m}{R}\right)\left(1+\frac{L^2}{R^2}\right) \\ &= \frac{1}{2} - \frac{m}{R} + \frac{L^2}{2R^2} - \frac{mL^2}{R^3}.\end{aligned} \tag{4.23}$$

The integral in the expression of $\sqrt{H}$ is reduced to

$$\begin{aligned}&\int_{R^0}^{R}\frac{2(x^2+L^2)^2 + x^3[(E^2)_{,m}(x^2+L^2) - (L^2)_{,m}E^2]}{2E[(E^2-1)x^3 + 2mx^2 - L^2x + 2mL^2]} \\ &\times\frac{1}{\sqrt{(E^2-1)x^4 + 2mx^3 - L^2x^2 + 2mL^2x}}\,dx.\end{aligned} \tag{4.24}$$

Therefore we find that the general solution is expressed by an elliptic integral.

If $L(m) = 0$, the solution is reduced to the LTB solution in the mass-area coordinates which is presented in Sec. 3.5. If $E(m) = 1$ and $L(m) = 4m$, the integral is expressed by elementary functions as follows:

$$A = H\left(1-\frac{2m}{R}\right), \tag{4.25}$$

$$B = -\frac{R}{|R-4m|}\sqrt{\frac{RH}{2m}}, \tag{4.26}$$

$$C = \frac{R(R^2+16m^2)}{2m(R-4m)^2}, \tag{4.27}$$

$$u = \pm|R-4m|\sqrt{\frac{2m}{R(R^2+16m^2)}}, \tag{4.28}$$

$$\begin{aligned}\sqrt{H} &= \frac{(R^0)_{,m}((R^0)^2+16m^2)}{|R^0-4m|\sqrt{2mR^0}} + \mathrm{sign}(R^0-4m) \\ &\times \left[\left(\frac{(R-8m)^2+80m^2}{3m(R-4m)}\sqrt{\frac{R}{2m}} + 4\sqrt{2}\ln\frac{\sqrt{R}+2\sqrt{m}}{|\sqrt{R}-2\sqrt{m}|}\right)\right. \\ &- \left.\left(\frac{(R^0-8m)^2+80m^2}{3m(R^0-4m)}\sqrt{\frac{R^0}{2m}} + 4\sqrt{2}\ln\frac{\sqrt{R^0}+2\sqrt{m}}{|\sqrt{R^0}-2\sqrt{m}|}\right)\right],\end{aligned} \tag{4.29}$$

$$\epsilon = \frac{R^2+16m^2}{4\pi R^2|R-4m|\sqrt{2mR}\sqrt{H}}. \tag{4.30}$$

4.4 Causal Structure

Now that we have obtained the explicit expression for the metric functions, we investigate singularities which may occur in the collapse of a spherical cloud of counterrotating particles. Since shell-crossing singularities are widely believed not to be true singularities, we concentrate on shell-focusing singularities. Furthermore, as in the dust case, no light ray can emanate from non-central shell-focusing singularities because $R = 0 < 2F$ for $r > 0$. Therefore it turns out to be sufficient to consider central shell-focusing singularity in order to discuss whether or not naked singularity exists.

4.4.1 General Case

The motion of each thin shell labeled by r is described by Eq. (3.12) or (4.20), which transforms as

$$\frac{1}{2}\left(1+\frac{L^2}{R^2}\right)\left(\frac{dR}{d\tau}\right)^2 + \frac{1}{2}\left(1-\frac{2F}{R}\right)\left(1+\frac{L^2}{R^2}\right) = \frac{1}{2}(1+f), \tag{4.31}$$

where τ is the proper time of the thin shell, i.e., $d\tau = e^{\nu}dt$. By investigating the shape of the effective potential $V(R;m)$, we obtain qualitative under-

standing about the motion of each shell. The motion of a mass shell labeled by r is the same as the radial motion of a test particle with the specific angular momentum $L(r)$ and specific energy $(1+f(r))$ in the Schwarzschild space-time of which mass parameter is $F(r)$. The factor $(1+L^2/R^2)$ in the first term in the left hand side of Eq. (4.31) is the Lorentz factor which originates from the difference between λ, the proper time of the particle which is orbiting the center, and τ, that of the shell-comoving observer which moves only in the radial direction.

In convenience for further discussions, we adopt here the radial coordinate r which agrees with the circumferential radius R on the initial spacelike hypersurface $t=0$. From this choice of the radial coordinate, the initial radius $R^0(m)$ is specified as

$$R^0(m) = F^{-1}(m). \tag{4.32}$$

We assume that not only regular but also smooth initial data. before the occurrence of the central singularity. From this assumption, the metric variables in the comoving coordinates can be expanded as

$$\begin{aligned} \nu(t,r) &= \nu_0(t) + \nu_2(t)r^2 + \cdots, & (4.33)\\ R(t,r) &= R_1(t)r + R_3(t)r^3 + \cdots, & (4.34) \end{aligned}$$

and we set $\nu_0(t)=0$ by using the rescaling freedom of the time coordinate. From the choice of r, we obtain

$$R_1(0) = 1,\ R_3(0) = \cdots = 0. \tag{4.35}$$

Then, from Eqs. (3.11) and (3.12), the arbitrary functions $F(r)$, $f(r)$ and $L^2(r)$ should be expanded as

$$\begin{aligned} F(r) &= F_3 r^3 + F_5 r^5 + \cdots, & (4.36)\\ f(r) &= f_2 r^2 + f_4 r^4 + \cdots, & (4.37)\\ L^2(r) &= L_4 r^4 + L_6 r^6 + \cdots. & (4.38) \end{aligned}$$

From Eq. (3.9), the energy density should be expanded as

$$\epsilon(t,r) = \epsilon_0(t) + \epsilon_2(t)r^2 + \cdots, \tag{4.39}$$

and then the energy density at the center is given by

$$\epsilon(t,0) = \epsilon_0(t) = \frac{3F_3}{4\pi R_1(t)^3}. \tag{4.40}$$

Observing the lowest order of Eq. (4.20) or (4.31), the time development of $R_1(t)$ is given by

$$\left(\frac{dR_1}{dt}\right)^2 = \frac{2F_3}{R_1} + f_2 - \frac{L_4}{R_1^2}. \tag{4.41}$$

From Eqs. (4.35) and (4.41), we obtain the condition for initial data

$$2F_3 + f_2 - L_4 \geq 0. \tag{4.42}$$

The equality holds only when $\dot{R}_1(0)$ vanishes.

First we consider the case of $L_4 > 0$. This condition corresponds to the generic initial data within this model. Then, from Eq. (4.41), we find that $R_1(t)$ cannot vanish. Therefore no central singularity occurs for $L_4 > 0$. This result was first shown by Evans (1976). Next we examine the motion of the shell $r > 0$. From Eq. (4.20) or (4.31), allowed regions for given r are obtained by

$$V(R;r) \leq \frac{1}{2}(1+f). \tag{4.43}$$

For sufficiently small r, we find

$$V(R;r) \rightarrow -\infty \quad \text{as} \quad R \rightarrow 0, \tag{4.44}$$

$$V(2F;r) = 0, \tag{4.45}$$

$$V(4F;r) \approx \frac{1}{64}\frac{L^2}{F^2} > \frac{1}{2}(1+f) \tag{4.46}$$

$$V(R;r) \rightarrow \frac{1}{2} \quad \text{as} \quad R \rightarrow \infty. \tag{4.47}$$

Considering that $V(R;r) - (1+f)/2$ for fixed r has at most three zeros and that $f(r) = O(r^2)$, the allowed regions are given as

$$0 \leq R \leq R_{\rm I}, \quad R_{\rm II} \leq R, \quad (\text{for} \quad f \geq 0), \tag{4.48}$$

$$0 \leq R \leq R_{\rm I}, \quad R_{\rm II} \leq R \leq R_{\rm III}, \quad (\text{for} \quad f < 0), \tag{4.49}$$

where $R_{\rm I} < R_{\rm II} < R_{\rm III}$ are positive zeros of $V(R;r) - (1+f)/2$. The following inequality is satisfied:

$$2F < R_{\rm I} < 4F < R_{\rm II}. \tag{4.50}$$

From $F = O(r^3)$ around $r = 0$, $R(0,r) = r$ cannot be in the inner allowed region $0 \leq R \leq R_{\rm I}$. This means that $R(t,r)$ must be in the outer allowed region at $t = 0$. Therefore we conclude that the region around $r = 0$, which was initially in a collapsing phase, necessarily experiences a bounce

and begins to expand. The motion after that is an eternal expansion for $f \geq 0$ or oscillations for $f < 0$. This implies that, due to the inequality $R > R_{\rm II} > 4F > 2F$, the region around $r = 0$ is untrapped. We summarize this case by no central singularity, no apparent horizon and a bounce of the region around the center.

We proceed to the case of $L_4 = 0$. Though this condition corresponds to zero-measure initial data within this model, we examine this case because some interesting facts are found. From Eq. (4.41), we find that the initially collapsing cloud inevitably form central shell-focusing singularity after a finite proper time. In order to see whether this central singularity is naked or covered, we examine the motion of the region around the center. Here we define

$$D \equiv \lim_{r \to 0} \frac{L}{F} = \frac{L_6^{1/2}}{F_3}. \tag{4.51}$$

For $D > 4$, for sufficiently small $r > 0$, we find

$$V(R; r) \rightarrow -\infty \quad \text{as} \quad R \rightarrow 0, \tag{4.52}$$

$$V(2F; r) = 0, \tag{4.53}$$

$$V\left(\frac{D^2}{4}F; r\right) \approx \frac{1}{2} + \frac{4(D^2 - 16)}{D^4} > \frac{1}{2}(1 + f), \tag{4.54}$$

$$V(R; r) \rightarrow \frac{1}{2} \quad \text{as} \quad R \rightarrow \infty. \tag{4.55}$$

Then, the allowed regions are given as

$$0 \leq R \leq R_{\rm I}, \quad R_{\rm II} \leq R \quad (\text{for} \quad f \geq 0), \tag{4.56}$$

$$0 \leq R \leq R_{\rm I}, \quad R_{\rm II} \leq R \leq R_{\rm III} \quad (\text{for} \quad f < 0), \tag{4.57}$$

where the following inequality is satisfied:

$$2F < R_{\rm I} < \frac{D^2}{4}F < R_{\rm II}. \tag{4.58}$$

In the same way as for the case of $L_4 > 0$, we conclude that the region around $r = 0$, which was initially in a collapsing phase, necessarily experiences a bounce and begins to expand. The motion after that is an eternal expansion for $f \geq 0$ or oscillations for $f < 0$. This implies that, due to $R > R_{\rm II} > 4F > 2F$, the region around $r = 0$ is untrapped. Therefore the central singularity is naked. Since the space-time can be matched to the Schwarzschild space-time at an arbitrary radius $r = r_b$, we can construct the space-time with a

globally naked singularity. The results given above do not depend on details of initial density distribution.

For $D = 4$, the behavior depends on the higher order terms. We will present the critical case in which $f(r) = 0$ and $L(r) = 4F(r)$ in the next subsection.

Then we proceed to the case $0 \leq D < 4$. Consider the sign of

$$\begin{aligned} g(R;r) &\equiv 2R(R^2+L^2)\left[V(R;r) - \frac{1}{2}(1+f)\right] \\ &= -fR^3 - 2FR^2 + L^2R - 2FL^2 \\ &\approx -fR^3 - 2FR^2 + D^2F^2R - 2D^2F^3, \end{aligned} \tag{4.59}$$

for sufficiently small $r > 0$. For $f \geq 0$, it is easily found that $g(R;r)$ is always negative. For $f < 0$, it is easily found that $g(R;r)$ takes the relative maximum and minimum at $R = R_{max}$ and R_{min} ($R_{max} < R_{min}$) respectively and that the relative maximum is negative. Therefore the allowed region is given as

$$0 \leq R \quad (\text{for} \quad f \geq 0), \tag{4.60}$$

$$0 \leq R \leq R_{\rm I} \quad (\text{for} \quad f < 0). \tag{4.61}$$

Therefore, the collapse continues to a covered singularity in the region around the center. An apparent horizon is formed in this case. In order to see whether the central singularity is naked or not, we have to examine the existence of future-directed outgoing null geodesic which emanates from the singularity. That can be done by the same scheme in Chap. 3 because we have now the explicit exact expression for the metric functions.

4.4.2 Special Case

Here we present the critical case in which $f(r) = 0$ and $L(r) = 4F(r)$. In this case, the metric functions are given explicitly only by elementary functions, and hence it is easy to examine the absence of shell-crossing singularity, the existence of future-directed outgoing null geodesic which emanates from the singularity and the curvature strength of the singularity.

Since $L_4 = 0$, the central singularity occurs. The effective potential for a mass shell is given in this case as

$$V(R;r) = \frac{1}{2} - \frac{F(R-4F)^2}{R^3}. \tag{4.62}$$

On the initial spacelike hypersurface, regularity requires $R(0,r) = r > 4F = O(r^3)$ in a sufficiently small but finite region around $r = 0$. Then each initially collapsing shell of $r > 0$ approaches $R = 4F$. From Eq. (4.31), the behavior of this approach is as

$$R - 4F \propto \exp\left(-\frac{\tau}{8F}\right). \tag{4.63}$$

This behavior means that R approaches $4F$ asymptotically. In the region around the center $r = 0$, the collapse becomes frozen to $R = 4F$ due to the angular momentum braking. Due to $R > 4F > 2F$, the region around the center is untrapped eternally. Therefore the central singularity is naked and can be globally naked.

Furthermore we can prove that no shell crossing occurs and the coordinate system is valid at least in the region around the center by directly showing $\sqrt{H} > 0$. Each term in the first couple of parentheses in the brackets on the right hand side of Eq. (4.29) is positive, because of $R > 4F$ in the region around the center. The contribution of the first term and the terms in the second couple of parentheses is expanded as

$$\frac{\sqrt{2}}{9}\frac{24F_3^2 - F_5}{F_3^{13/6}} m^{-1/3} + O(m^{1/3}), \tag{4.64}$$

where terms which is $O(m^{-1})$ cancel each other. Therefore, for $F_5 < 24F_3^2$, at least a sufficiently small region around the center is shell-crossing free, and we can construct a shell-crossing free solution by matching. This condition holds if the initial energy density profile $\epsilon(0,r)$ is a decreasing function of r around the center.

The central singularity is naked if and only if there exists a future-directed outgoing null geodesic which emanates from the singularity. For a spherically symmetric space-time with vanishing radial pressure, the nakedness of the central singularity is discussed in Sec. 3.2. The root equation which determines the tangent of the null geodesic which emanates from the singularity is obtained in Eq. (3.64). Considering the explicit metric functions, we obtain the positive finite root of the root equation with $\beta = 7/9$ as

$$y_0 = \left(\frac{24F_3^2 - F_5}{4\sqrt{2}F_3^{13/6}}\right)^{2/3} \tag{4.65}$$

for $F_5 < 24F_3^2$, i.e., when no shell-crossing singularity occurs. The above result implies that, along the future-directed outgoing radial null geodesic

which emanates from the naked singularity with the definite tangent

$$R \approx 2y_0 m^{7/9} \approx 2y_0 F_3^{7/9} r^{7/3}. \tag{4.66}$$

Therefore, unlike marginally bound dust collapse, the central shell-focusing singularity is naked even for initially homogeneous ball.

The curvature strength of the naked central singularity which appears in a spherically symmetric space-time with vanishing radial pressure is discussed in Chap. 3. From Eq. (3.89), $\beta = 7/9$ implies that the singularity is gravity-dominated. Then, from Theorem 3.4.1, not SCC but only LFC is satisfied for the null geodesic which emanates from or terminates at the singularity. This means that the cross section of any congruence of null geodesics which hit the singularity is not crushed to zero but is contracted.

4.5 Summary

In the realistic collapse from generic smooth initial data, net rotation will induce very large deformation from spherical symmetry. Nevertheless, this model will display us pure effect of counterrotation or tangential velocity dispersion on the formation of shell-focusing naked singularity. From this model we learn a lesson that generic counterrotation or tangential velocity dispersion will rub off the shell-focusing naked singularity which forms without it. This strongly suggests that the shell-focusing naked singularity cannot be a counterexample to CCH because the effect of counterrotation will be necessarily present in generic collapse of a cloud of collisionless particles which obey the Einstein-Vlasov equation.

The important corollary of the analysis in this chapter is that, if the generic spherical cluster of counterrotating particles collapses to singularity, then there necessarily exist shell-crossing singularities. This strongly suggests that the extension of the space-time beyond the shell-crossing singularities is an essential problem to overcome. It is expected that the extension beyond the shell-crossing singularity results in incorporating radial velocity dispersion. Therefore we must deal with radial velocity dispersion to obtain a picture of the formation of black holes and singularities from generic gravitational collapse of collisionless particles. Crossing of spherical timelike shells analyzed by Ida and Nakao (1998) and Nakao, Ida and Sugiura (1998) might contain some implications.

Chapter 5

Spherical Collapse of Perfect Fluid

In the previous section we have seen that the dust matter can be regarded as a cold limit of a system of collisionless particles. However it is also possible to regard the dust matter as a zero-pressure limit of a perfect fluid. In realistic situations it is expected that pressure is not negligible at all. In fact, in the blow up of energy density, it is expected that pressure would increase unboundedly and that its ratio to the energy density would not vanish observing the radiation fluid which is a good approximation of a system of highly relativistic particles in thermal equilibrium.

Ori and Piran (1987, 1988, 1990) investigated numerically the spherically symmetric collapse of a perfect fluid with a barotropic equation of state under the assumption of self-similarity. By this assumption the equation of state is restricted to the form $P = (\gamma - 1)\epsilon$. They showed that a central naked singularity forms in pure collapse for $\gamma \lesssim 1.0105$. They showed also that there are naked-singular solutions with oscillations in the velocity field for $1 < \gamma < 1.4$. Lake (1988) showed that the naked singularity satisfies SCC for the first null ray from the singularity. Indeed, Waugh and Lake (1989) showed that any central naked singularity which occurs in a spherically symmetric self-similar space-time satisfies SCC for the first null ray if the Cauchy horizon is generated by the homothetic Killing vector. Analytic discussions based on self-similarity followed it (Joshi and Dwivedi (1992b, 1993b)). However the whole of initial data from which a self-similar space-time develops occupies only zero measure in the space of spherically symmetric initial data. Thus, there have been discussions that the emergence of

the naked singularity may be an artifact of the assumption of self-similarity.

The effort of getting rid of the assumption of self-similarity was made by Onozawa, Siino and Watanabe (1994). They solved numerically the Misner-Sharp equations (Misner and Sharp (1964)) from smooth initial data and searched the formation of apparent horizon until the density blows up and the numerical scheme breaks down. In fact, their method is not sufficient to detect naked singularities because the combination of the blow up of curvature invariants and the absence of apparent horizon does not necessarily mean naked singularity.

Here, following Harada (1998), those difficulties in detection of naked singularities are avoided by constructing a null coordinate. Then, the causal structure of the space-time can be obtained automatically in solving the dynamics of the space-time and the matter. Furthermore, by using the "observer time coordinates", the coordinates never cross an event horizon and therefore the global nakedness is trivial.

5.1 Basic Equations

In the presence of the radial pressure it is impossible to solve the Einstein equation analytically for a general equation of state. Therefore we solve the Einstein equation numerically. The equations for relativistic hydrodynamics in spherical symmetry were first derived by Misner and Sharp (1964). In a spherically symmetric space-time, the line element is given by Eq. (2.1). The stress-energy tensor of a perfect fluid is given by Eq. (2.3). ϵ is written as

$$\epsilon = \rho_0(1+e), \tag{5.1}$$

where ρ_0 is the rest-mass density and e is the specific internal energy. The 4-velocity u^μ of a fluid element is written in the comoving coordinates as

$$u^\mu = (e^{-\nu}, 0, 0, 0). \tag{5.2}$$

The comoving radial coordinate r is chosen to be the rest mass A enclosed within R. Then, from the Einstein equation and the equation of motion for the fluid, we obtain the following Misner-Sharp equations:

$$\frac{\partial U}{\partial t} = -e^{\nu}\left[\frac{4\pi\Gamma R^2}{w}\frac{\partial P}{\partial A} + \frac{m+4\pi R^3 P}{R^2}\right], \tag{5.3}$$

$$\frac{\partial R}{\partial t} = e^{\nu}U, \tag{5.4}$$

$$\frac{\partial m}{\partial t} = -e^{\nu} 4\pi R^2 P U, \tag{5.5}$$

$$\Gamma = \left(1 + U^2 - \frac{2m}{R}\right)^{1/2}, \tag{5.6}$$

$$\rho_0 = \frac{\Gamma}{4\pi R^2 \left(\frac{\partial R}{\partial A}\right)}, \tag{5.7}$$

$$\frac{\partial e}{\partial t} = -P \frac{\partial}{\partial t}\left(\frac{1}{\rho_0}\right), \tag{5.8}$$

$$w = 1 + e + \frac{P}{\rho_0}, \tag{5.9}$$

$$\frac{\partial m}{\partial A} = (1+e)\Gamma, \tag{5.10}$$

$$\frac{\partial \nu}{\partial A} = -\frac{1}{\rho_0 w}\frac{\partial P}{\partial A}, \tag{5.11}$$

where U, m and w are the coordinate velocity, the Misner-Sharp mass and the specific enthalpy, respectively. Γ is the radial metric function defined as

$$\Gamma \equiv e^{-\lambda}\frac{\partial R}{\partial A}. \tag{5.12}$$

Then, from Eqs. (5.7) and (5.12), we obtain

$$e^{-\lambda} = 4\pi\rho_0 R^2. \tag{5.13}$$

The boundary conditions are given as

$$\begin{aligned} &R = 0, \quad U = 0, \quad \Gamma = 1, \quad m = 0, \quad \text{at the origin} \quad A = 0, \\ &P = 0, \quad e^{\nu} = 1, \quad \text{at the surface} \quad A = A_{total}. \end{aligned} \tag{5.14}$$

In fact, the boundary condition for e^{ν} is arbitrary. The above choice requires that t should agree with the proper time of the stellar surface.

Then we proceed to another formulation in the observer time coordinates given by Hernandez and Misner (1966). For a derivation, see also Baumgarte, Shapiro and Teukolsky (1995). We introduce the outgoing null coordinate u by

$$e^{\psi} du = e^{\nu} dt - e^{\lambda} dA, \tag{5.15}$$

so that the line element is given as

$$\begin{aligned} ds^2 = &-e^{2\psi(u,A)} du^2 - 2e^{\psi(u,A)} e^{\lambda(u,A)} du dA \\ &+ R^2(u,A)(d\theta^2 + \sin^2\theta d\phi^2). \end{aligned} \tag{5.16}$$

Transforming time coordinate from t to u, we obtain the following Hernandez-Misner equations:

$$\begin{aligned}
\frac{\partial U}{\partial u} &= -\frac{e^{\psi}}{1-v_s^2}\left[\frac{4\pi\Gamma R^2}{w}\frac{\partial P}{\partial A}+\frac{m+4\pi R^3 P}{R^2}\right] \\
&\quad -\frac{e^{\psi}v_s^2}{1-v_s^2}\left(4\pi\rho_0 R^2\frac{\partial U}{\partial A}+\frac{2U\Gamma}{R}\right), \qquad (5.17)\\
\frac{\partial R}{\partial u} &= e^{\psi}U, \qquad (5.18)\\
\frac{\partial m}{\partial u} &= -e^{\psi}4\pi R^2 PU, \qquad (5.19)\\
\Gamma &= \left(1+U^2-\frac{2m}{R}\right)^{1/2}, \qquad (5.20)\\
\rho_0 &= \frac{\Gamma+U}{4\pi R^2\left(\frac{\partial R}{\partial A}\right)}, \qquad (5.21)\\
\frac{\partial e}{\partial u} &= -P\frac{\partial}{\partial u}\left(\frac{1}{\rho_0}\right), \qquad (5.22)\\
w &= 1+e+\frac{P}{\rho_0}, \qquad (5.23)\\
\frac{\partial m}{\partial A} &= (1+e)\Gamma-\frac{PU}{\rho_0}, \qquad (5.24)\\
\frac{\partial \psi}{\partial A} &= \frac{1}{\Gamma}\frac{\partial U}{\partial A}+\frac{m}{4\pi\rho_0 R^4\Gamma}+\frac{P}{\rho_0\Gamma R}, \qquad (5.25)\\
v_s^2 &= \frac{1}{\rho_0^2 w}\left[P\left(\frac{\partial P}{\partial e}\right)_{\rho_0}+\rho_0^2\left(\frac{\partial P}{\partial \rho_0}\right)_e\right], \qquad (5.26)
\end{aligned}$$

where v_s is the sound speed. The boundary conditions are given as

$$\begin{aligned}
&R=0,\ \ U=0,\ \ \Gamma=1,\ \ m=0,\ \ \text{at the origin}\ \ A=0,\\
&P=0,\ \ e^{\psi}=\Gamma+U,\ \ \text{at the surface}\ \ A=A_{total}. \qquad (5.27)
\end{aligned}$$

The above boundary condition for e^{ψ} ensures that the coordinates are the outgoing Eddington-Finkelstein coordinates in the exterior of the star. Thereby the coordinate value u agrees with the proper time of a distant stationary observer, and hence that the time coordinate is called the observer time coordinate. Therefore, in approach to an event horizon, the lapse function e^{ψ} decreases to zero, and the coordinate system never crosses the event horizon. The limit curve of the time slices $u=$ const in the limit $u\to\infty$ is, if it exists,

an event horizon. If the observer time coordinates hit singularity, it turns out to be globally naked singularity. Note that u is not the characteristic coordinate because there is no gravitational radiation in a spherically symmetric space-time. Hence, for the Hernandez-Misner equations, a Cauchy problem for the fluid evolution is formulated in the same way as for the Misner-Sharp equations.

5.2 Method

Unfortunately, in general, we can analytically integrate neither the Misner-Sharp nor the Hernandez-Misner equations. Therefore we are forced to make numerical integration in order to obtain full general relativistic solutions. Both sets of the Misner-Sharp and the Hernandez-Misner equations are very similar to the Lagrangian formulation of spherical fluid dynamics in Newton gravity. Therefore we can use a code very similar to the spherical Newtonian Lagrangian hydrodynamical code. Compared with the Eulerian formulation, the relativistic Lagrangian formulation has the merits of the better accuracy and the save of exterior grids extending to a large distance in order to impose boundary conditions on the gravitational field. See Van Riper (1979), Baumgarte, Shapiro and Teukolsky (1995) for numerical schemes and difference equations.

The procedure to obtain a numerical solution for the space-time is as follows. First, we prepare initial data on a spacelike hypersurface $t = 0$. Then, we integrate the Misner-Sharp equations from the initial data $t = 0$ and store data on the first null ray which emanates from the center at $t = 0$. When this ray reaches the stellar surface, we begin to solve the Hernandez-Misner equations using the stored data on the first null ray as initial data $u = 0$.

The code was tested by the collapse of a homogeneous dust ball (the Oppenheimer-Snyder solution) and an inhomogeneous dust ball (the LTB solution). A supercritical neutron star collapsed while a subcritical neutron star did not collapse within many dynamical time scales. The code was also tested by the Riemann shock tube problem and point-source explosion described by the Sedov solution. The conservation of the total mass is a good indicator of numerical errors. In all calculations presented in Sec. 5.3, the total mass was conserved within the accuracy of 10^{-4}. We can add an artificial viscosity term to the pressure term in order to deal with possible shock waves. We use an empirical relativistic generalization of the Neumann

artificial viscosity, the expression of which is explicitly given in Baumgarte, Shapiro and Teukolsky (1995). The artificial viscosity term may play a rather subtle role in the formation of the central singularity. To avoid such additive difficulties, this term was not included basically. Absence of this term did not spoil the results for most calculations because shock waves did not occur for most cases. Only for the cases in which the central region expanded, shock waves occurred, and thereby the calculation suffered from serious numerical instabilities, the artificial viscosity was switched on. For those cases, the fluid did not collapse, and hence the center was regular. 2048 grid zones were prepared in most calculations.

Initial data are prepared on the spacelike hypersurface in order to obtain a clear relation with physical situations. The initial data are given by the following three arbitrary functions:

$$\rho_0 = \tilde{\rho}_0(R), \quad e = \tilde{e}(R), \quad U = \tilde{U}(R). \tag{5.28}$$

We choose the density distribution as

$$\tilde{\rho}_0(R) = \begin{cases} \tilde{\rho}_{0c}\left[1 - \left(\frac{R}{R_s}\right)^2\right] & (0 \le R \le R_s) \\ 0 & (R_s < R) \end{cases}. \tag{5.29}$$

The distribution of the specific internal energy and the velocity is set as

$$\tilde{e}(R) = \tilde{e}_c \left(\frac{\tilde{\rho}_0}{\tilde{\rho}_{0c}}\right)^{\gamma-1}, \tag{5.30}$$

$$\tilde{U}(R) = 0. \tag{5.31}$$

We use the following γ-law equation of state:

$$P = (\gamma - 1)e\rho_0. \tag{5.32}$$

For this equation of state, the sound velocity v_s is given as

$$v_s^2 = (\gamma - 1)\frac{w - 1}{w}. \tag{5.33}$$

The combination of the adiabatic condition (5.8) or (5.22), the initial data (5.30), and the equation of state (5.32) guarantees that the pressure is in proportional to ρ_0^γ, i.e.,

$$P = K\rho_0^\gamma, \tag{5.34}$$

where K is constant all over the star. In this case, the initial data are parametrized up to normalization only by $\tilde{e}_c$ and R_s/M, where M is the ADM mass. If we take the extremely relativistic limit ($e \gg 1$), the above equation of state becomes

$$P = (\gamma - 1)\epsilon, \tag{5.35}$$

which is the equation of state used by Ori and Piran (1987, 1988, 1990).

In determining the final fate of collapse, here we adopt the following criteria. If the ratio of the rest-mass density of the innermost grid zone to that of the next one excesses 2, we identify with central 'singularity' and stop the code. If the lapse function e^{ψ} in the Hernandez-Misner code decreases to less than 10^{-3}, we identify with an 'event horizon'. If singularity occurs before an event horizon is detected, we identify with 'naked singularity'. The result is not so sensitive to the choice of the thresholds.

5.3 Results

5.3.1 Naked Singularity

First we pay attention to the naked-singular case, the model with $\gamma - 1 = 10^{-4}$, $\tilde{e}_c = 10^2$ and $R_s = 100M$. Since the fluid is highly relativistic, the equation of state is approximately equivalent with the equation of state (5.35). Hence, it is expected that the feature of the collapse is not sensitive to the value of $\tilde{e}_c$ for $\tilde{e}_c \gg 1$. In this calculation, the artificial viscosity was switched off.

Fig. 5.1 shows time slicing by the Misner-Sharp and the Hernandez-Misner codes. The ordinate is the proper time τ of a comoving observer, and the abscissa is the circumferential radius. The Misner-Sharp slicing presented in Fig. 5.1 is a family of spacelike hypersurfaces, $t/M = 0$, 100, 200, 300, 400, 500, 600, 700, 707. On the last slice $t = 707M$, the Misner-Sharp code detected central singularity based on the criteria described above. The Hernandez-Misner slicing is a family of null hypersurfaces, $u/M = 0$, 100, 200, 300, 400, 500, 600, 700, 728. Also on the last slice $u = 728M$, a central singularity was detected. In this figure, locations of some fluid elements are marked.

Fig. 5.2 shows the Misner-Sharp time evolution of (a) the rest-mass density ρ_0, (b) the ratio m/R, and (c) $dR/dt = e^{\nu}(\Gamma + U)$ along outgoing null geodesics [which is hereafter denoted as $(dR/dt)_{\mathrm{ONG}}$]. As seen in Fig. 5.2(a), the time evolution of the density profile in this model looks like the Penston

(1969)'s dust collapse solution in Newton gravity and also the LTB solution in Einstein gravity. It is remarkable that the density distribution in the central region approaches a power-law profile. From Fig. 5.2(a), the divergent behavior of the density at the center with respect to R changes at the occurrence of the singularity as

$$\rho_0 \propto const \Longrightarrow \rho_0 \propto R^{-\alpha} \tag{5.36}$$

with $\alpha \simeq 1.7$. Penston (1969) showed that $\alpha = 12/7$ for the dust collapse in Newton gravity. In Sec. 2.5, it has been shown that $\alpha = 12/7$ is also valid for the LTB solution on the spacelike hypersurface $t = t_s(0)$ of the occurrence of the central singularity. As seen in Fig. 5.2(b), the ratio m/R is much less than unity. This suggests that this collapse is well approximated by Newton gravity. The behavior of the ratio changes at the occurrence of the singularity

$$\frac{m}{R} \propto R^2 \Longrightarrow \frac{m}{R} \propto R^{\beta} \tag{5.37}$$

with $\beta \simeq 0.3$. It should be noted that $\beta = 2/7$ in the Penston's dust collapse solution. In Sec. 2.5, it has been shown that $\beta = 2/7$ also for the LTB solution. Fig. 5.2(c) shows that the expansion of outgoing null geodesics are always positive until the central singularity is detected. In other words, the Misner-Sharp code does not find the apparent horizon before the occurrence of the singularity.

Fig. 5.3 shows the Hernandez-Misner time evolution of ρ_0, m/R and the lapse function e^{ψ}. From Figs. 5.2(a) and 5.3(a), it is found that there is little difference in the divergence property of the density profile in the central region in both codes. In Sec. 2.5, it has been shown that $\alpha = 12/7$ and $\beta = 2/7$ for the LTB solution also on the earliest null ray which emanates from the central naked singularity. Fig. 5.3(b) shows that the ratio m/R is much less than unity also on that null ray. In Fig. 5.3(c), it is found that e^{ψ} does not vanish but remains of the order of unity until the central singularity is detected. Since e^{ψ} does not converge to zero, an event horizon has not yet formed.

Fig. 5.4 shows growth of the central rest-mass density ρ_{0c} in this model. The simulation was repeated with various radial grid resolutions. Each curve is labeled by the number of spatial grid zones used. The value of the central rest-mass density grows unboundedly. The blow up of the central rest-mass density becomes more rapid and the maximum value of it that can be attained becomes larger as the resolution becomes higher. In summary, the collapse is well approximated by dust collapse both in Newton gravity

and in Einstein gravity, and central naked singularity forms in this model based on the present criteria.

5.3.2 Black Hole

Next we take the model with $\gamma - 1 = 10^{-4}$, $\tilde{e}_c = 10^2$ and $R_s = 10M$ as an example of the black hole formation. Also in this calculation, the artificial viscosity was switched off.

Fig. 5.5 shows time slicing by the Misner-Sharp and the Hernandez-Misner codes. The former slicing is $t/M = 0$, 10, 20, 22.3, and the latter is $u/M = 0$, 10, 20, 30, 40, 50, 60, 70, 72.3. The former code was stopped because of the steepness of the density profile around the center, while the latter code was stopped because e^{ψ} became less than 10^{-3} all over the star. The sequence of the outgoing null geodesics $u = \text{const}$ converges, and its limit curve is an event horizon.

Fig. 5.6 shows the Misner-Sharp time evolution of ρ_0, m/R and $(dR/dt)_{\rm ONG}$. The behavior of ρ_0 and m/R in the central region seen in Figs. 5.6(a) and 5.6(b) is quite similar to that in the naked-singular case. From Fig. 5.6(b), the ratio m/R is not so small although it remains less than $1/2$ which corresponds to the apparent horizon in the spherically symmetric space-time. Fig. 5.6(c) shows that the Misner-Sharp code does not detect the apparent horizon until the occurrence of the central singularity although the singularity is covered by the event horizon.

Fig. 5.7 shows the Hernandez-Misner time evolution of ρ_0, m/R and e^{ψ}. It is seen in Fig. 5.7(a) that the density profile around the center is not so steep even at the event horizon. The ratio m/R is increased and reaches $1/2$ at the surface. Therefore the Newtonian approximation is not valid. In Fig. 5.7(c), it is shown that e^{ψ} converges to zero as u increases, which indicates an approach to the event horizon.

Fig. 5.8 shows growth of the rest-mass density at the center for this case. The simulation was repeated with various radial grid resolutions. From this figure it would be sure that the resolution is sufficient for the following conclusion. Since the Hernandez-Misner code detects an event horizon before the occurrence of central singularity, the singularity is covered by the event horizon. Moreover, it can be expected that this collapse would result in locally naked singularity because the Misner-Sharp time evolution in the central region is very similar to that of the globally-naked-singular case.

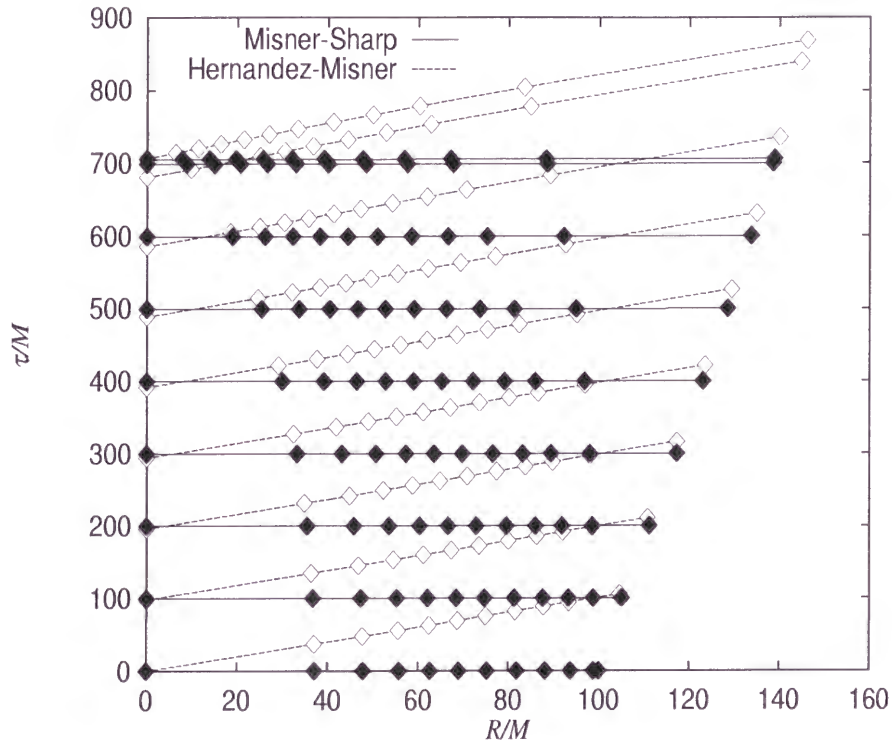

Figure 5.1: Naked-singular model with $\gamma - 1 = 10^{-4}$, $\tilde{e}_c = 10^2$ and $R_s = 100M$. Slicing by the Misner-Sharp and the Hernandez-Misner codes. The ordinate is the proper time of a comoving observer, and the abscissa is the circumferential radius. The Misner-Sharp slicing is $t/M = 0$, 100, 200, 300, 400, 500, 600, 700, 707, and the Hernandez-Misner slicing is $u/M = 0$, 100, 200, 300, 400, 500, 600, 700, 728. The Hernandez-Misner slicing is a set of outgoing null geodesics. We stopped the calculation in both codes when we detected central singularity. Locations of some fluid elements are marked.

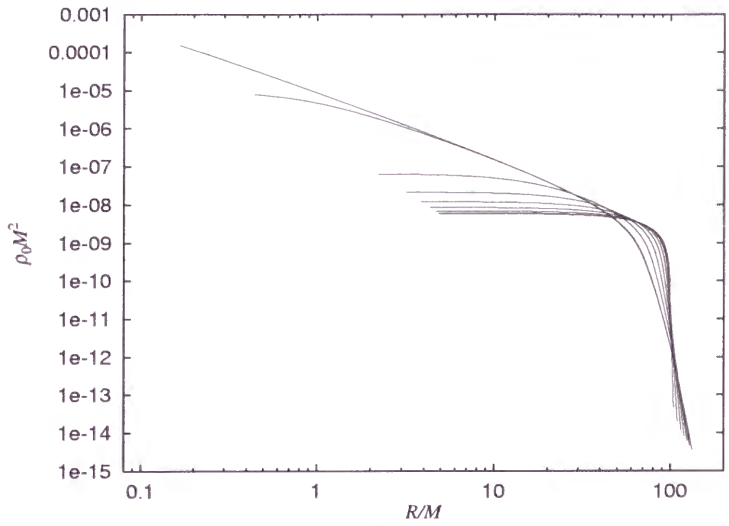
0.001
0.0001
1e-05
1e-06
1e-07
1e-08
1e-09
1e-10
1e-11
1e-12
1e-13
1e-14
1e-15
$\rho_0 M^2$
0.1
1
10
100
R/M

(a)

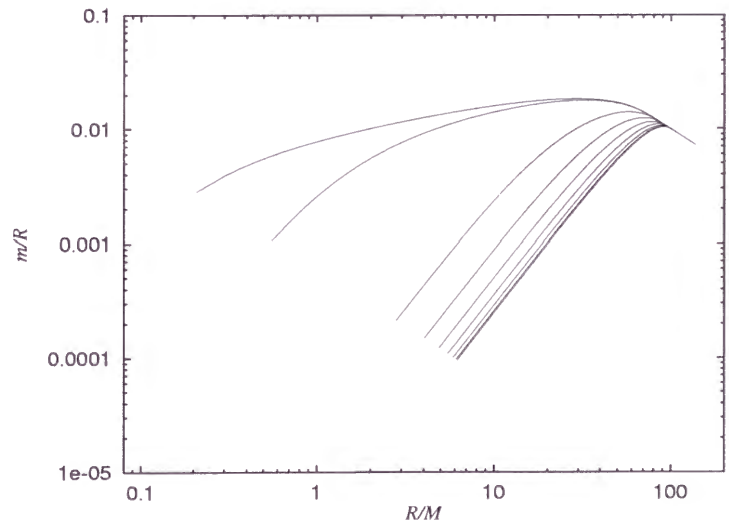
0.1
0.01
0.001
0.0001
1e-05
m/R
0.1
1
10
100
R/M

(b)

(c)

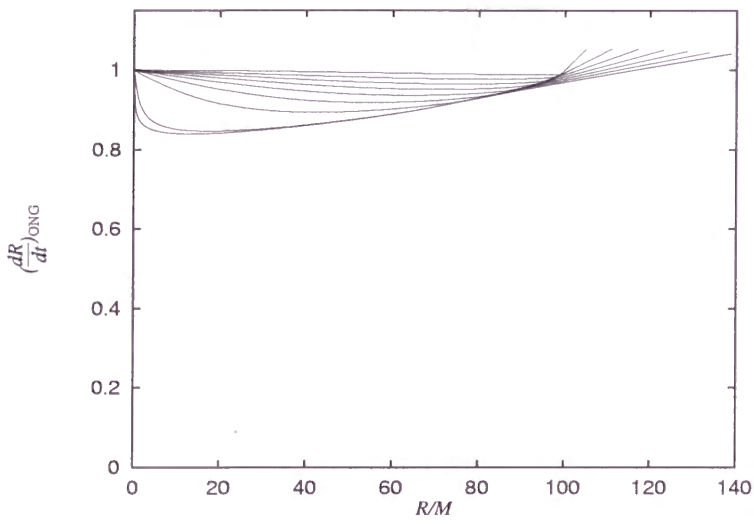

Figure 5.2: Evolution of (a) the rest-mass density ρ_0, (b) the ratio of the Misner-Sharp mass to the circumferential radius m/R and (c) dR/dt along outgoing null geodesics $(dR/dt)_{\rm ONG}$ in the Misner-Sharp code. The density distribution in the central region at $t = 707M$ becomes so steep that we identify with singularity.

(a)

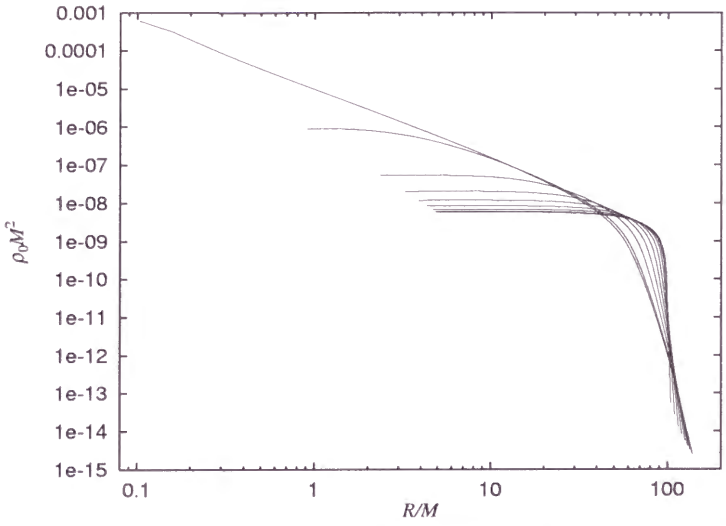
0.001
0.0001
1e-05
1e-06
1e-07
1e-08
1e-09
1e-10
1e-11
1e-12
1e-13
1e-14
1e-15
$\rho_0 M^2$
0.1
1
10
100
R/M

(b)

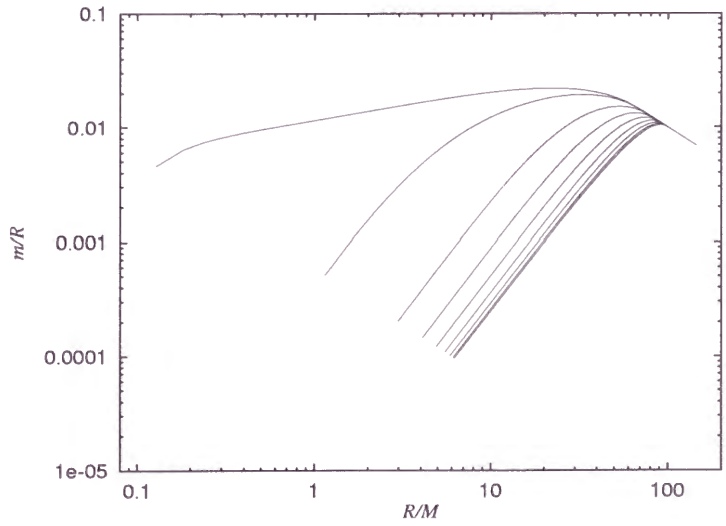
0.1
0.01
0.001
0.0001
1e-05
m/R
0.1
1
10
100
R/M

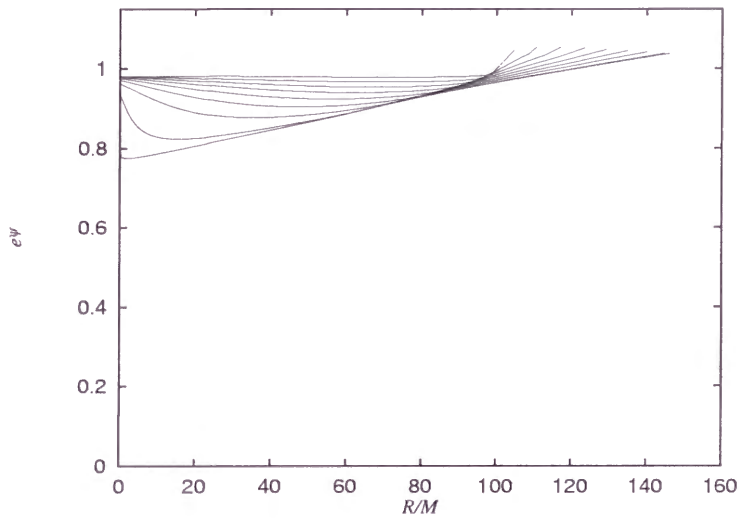

(c)

Figure 5.3: Evolution of (a) ρ_0, (b) m/R and (c) the lapse function e^{ψ} in the Hernandez-Misner code. The density distribution in the central region at $u = 728M$ becomes so steep that we identify with singularity.

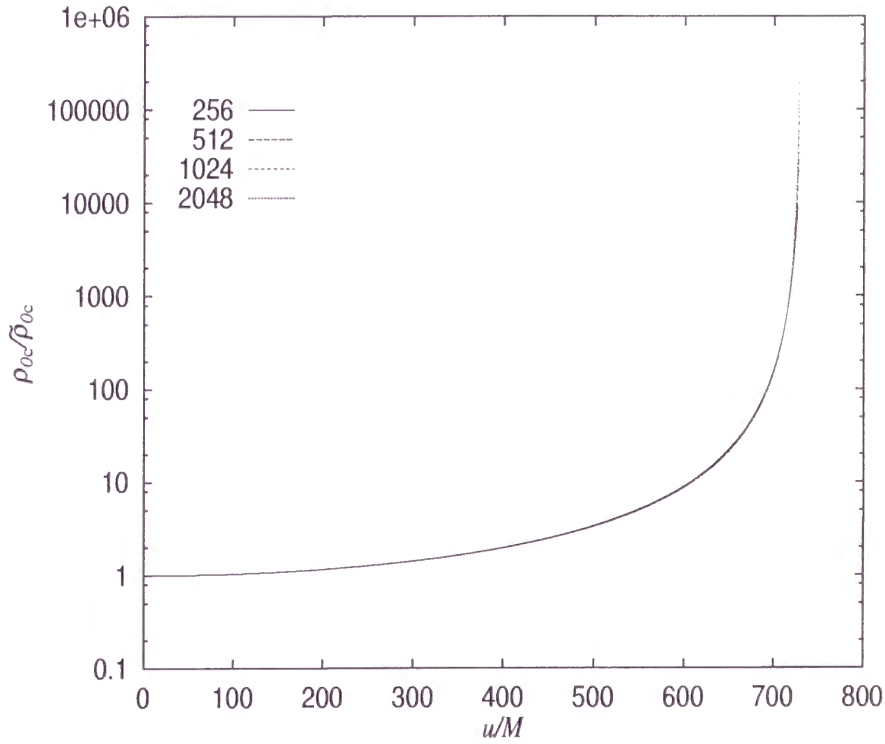

Figure 5.4: Blow up of the central rest-mass density ρ_{0c}. The simulation was repeated with various radial grid resolutions. Each curve is labeled by the number of spatial grid zones used.

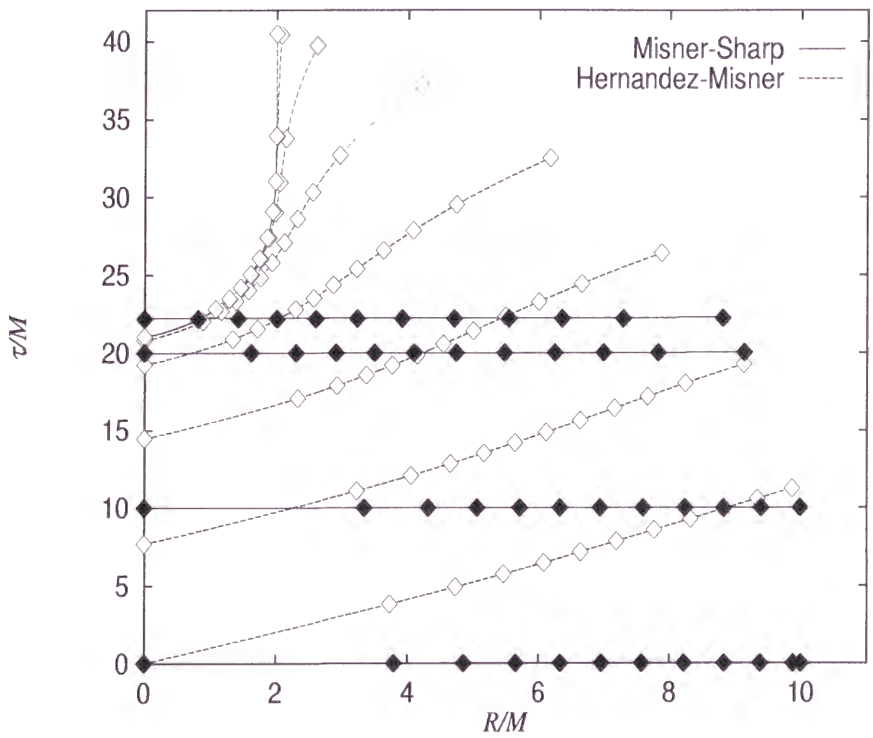

Figure 5.5: Black-hole model with $\gamma - 1 = 10^{-4}$, $\tilde{\epsilon}_c = 10^2$ and $R_s = 10M$. The Misner-Sharp slicing is $t/M = 0$, 10.0, 20.0, 22.3. On the last slice, a singularity was detected. The Hernandez-Misner slicing is $u/M = 0$, 10.0, 20.0, 30.0, 40.0, 50.0, 60.0, 70.0, 72.3. On the last slice, an event horizon was detected. The limit curve is the event horizon.

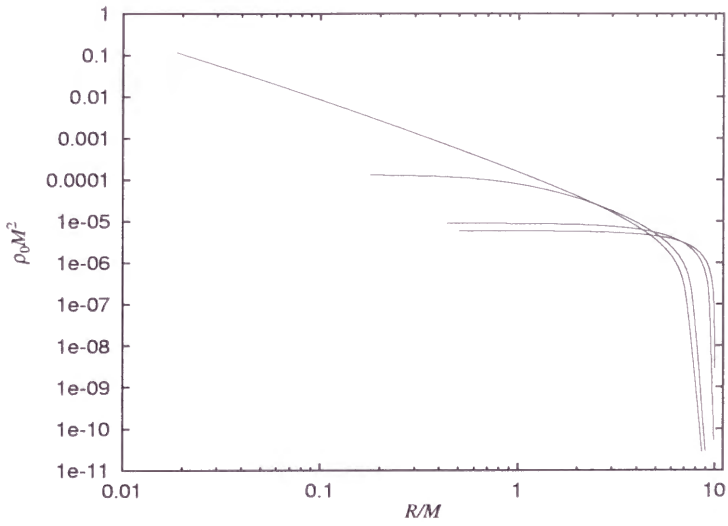
1
0.1
0.01
0.001
0.0001
1e-05
1e-06
1e-07
1e-08
1e-09
1e-10
1e-11
$\rho_0 M^2$
0.01
0.1
1
10
R/M

(a)

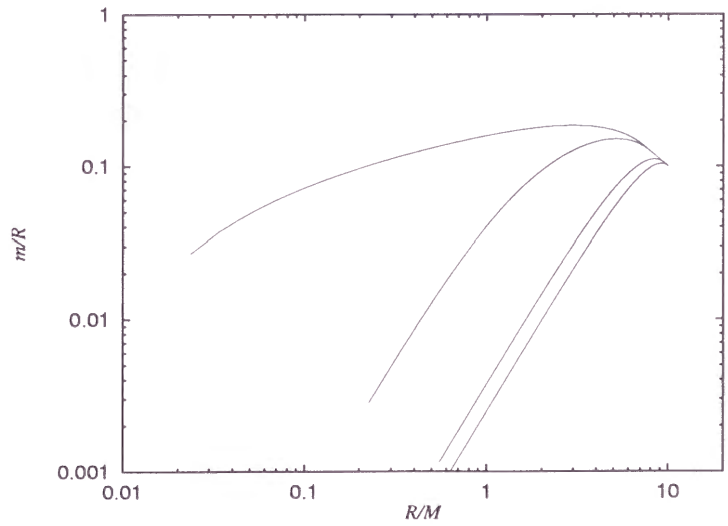
1
0.1
0.01
0.001
m/R
0.01
0.1
1
10
R/M

(b)

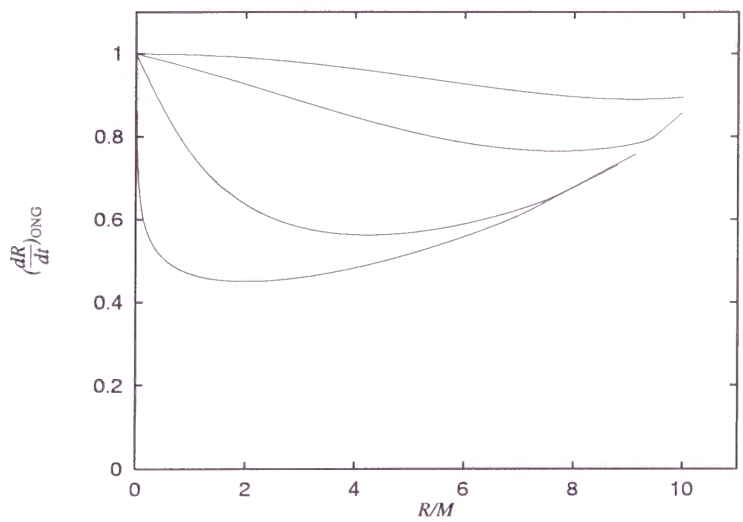

(c)

Figure 5.6: Evolution of (a) ρ_0, (b) m/R and (c) $(dR/dt)_{\rm ONG}$ in the Misner-Sharp code. The density distribution in the central region at $t = 22.3M$ becomes so steep that we identify with singularity.

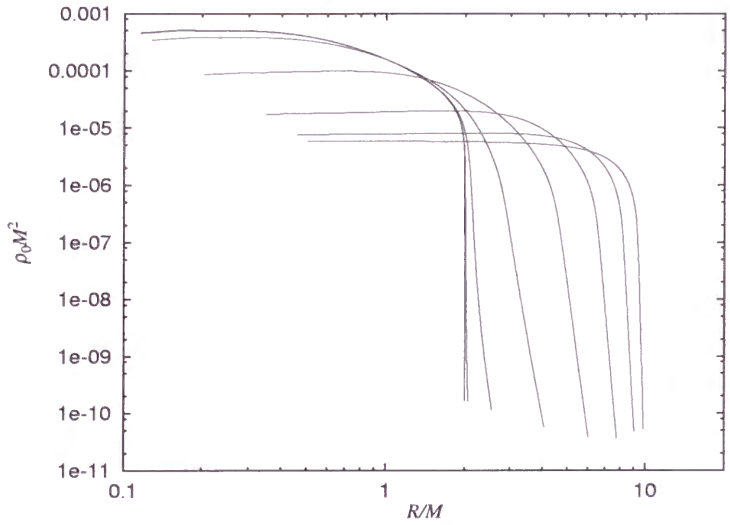
0.001
0.0001
1e-05
1e-06
1e-07
1e-08
1e-09
1e-10
1e-11
$\rho_0 M^2$
0.1
1
10
R/M

(a)

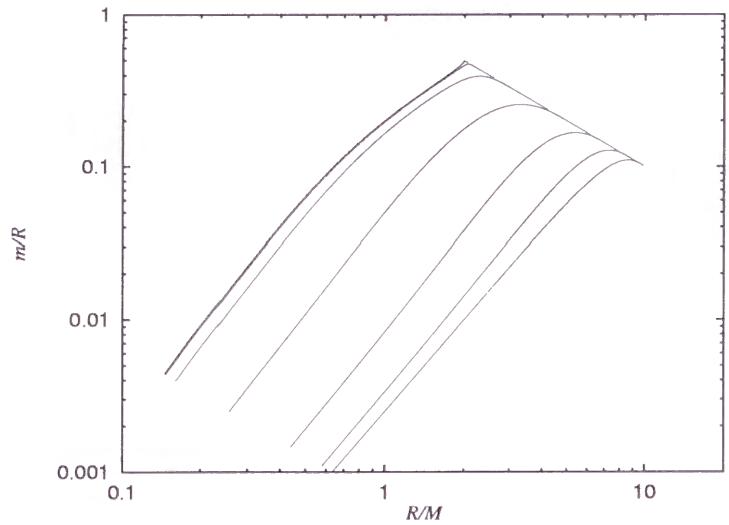
1
0.1
0.01
0.001
m/R
0.1
1
10
R/M

(b)

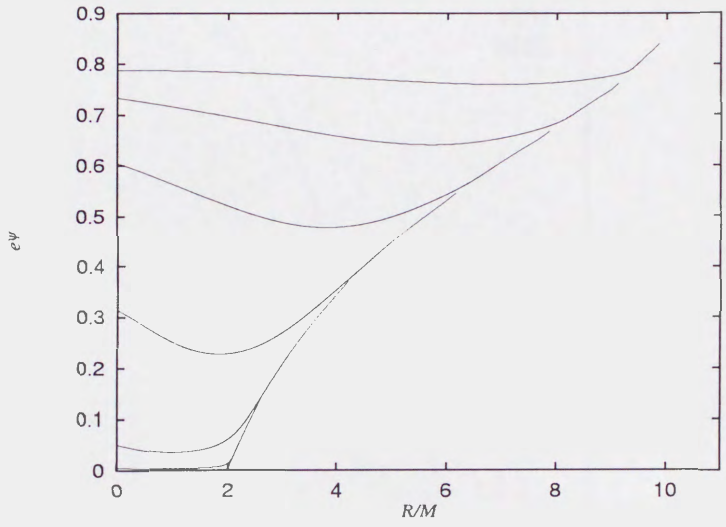

(c)

Figure 5.7: Evolution of (a) ρ_0, (b) m/R and (c) e^{ψ} in the Hernandez-Misner code. The density distribution in the central region remains not so steep even at the event horizon.

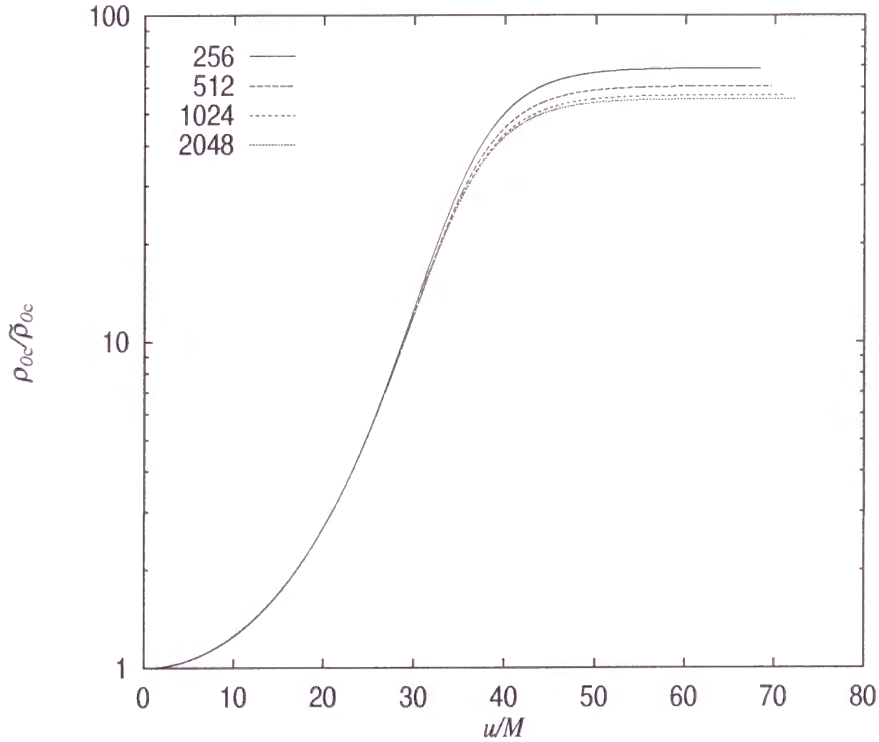

Figure 5.8: Evolution of ρ_{0c}. The simulation was repeated with various radial grid resolutions. Each curve is labeled by the number of spatial zones used.

5.3.3 Parameter Search

Tables 5.1-5.4 summarize the final fate of the collapse for $\tilde{e}_c = 10^2, 1, 10^{-2}$. Table 5.2 is the detailed search of the critical parameter region of Table 5.1. B, N, E, BE and SE denote a black hole, a naked singularity, an expansion, a black hole with an envelope and a star with an envelope, respectively. X and Y indicate some technical difficulties. X means that the present method does not work since a central singularity occurs before the first ray from the center reaches the stellar surface in the Misner-Sharp code. Y means that the stellar surface goes outward so rapidly that some numerical difficulty occurs.

From Tables 5.1 and 5.2, we find that the final fate of the collapse from diffuse ($R_s/M \gtrsim 20$) density distribution is, in general, not a black hole but a naked singularity if the fluid is highly relativistic and $\gamma \lesssim 1.01$ is satisfied. The final fate of the collapse from compact ($R_s/M \lesssim 10$) density distribution is a black hole even if the fluid is highly relativistic and $\gamma \lesssim 1.01$ is satisfied. If the fluid is highly relativistic and $\gamma \gtrsim 1.01$ is satisfied, the fluid begins to expand from diffuse density distribution. It was confirmed that the above statements do not depend on details of initial density profile. From Table 5.4, we find that, if the fluid is not relativistic and its profile is diffuse, the usual picture of collapse in Newton gravity is valid. For $\gamma < 4/3$, the pressure gradient cannot sustain the gravitational collapse. For $\gamma > 4/3$, the final fate of the collapse is a black hole, a naked singularity or a stable star depending on energetics, i.e., the total internal energy and the gravitational energy. It should be understood that, in Table 5.4, N, i.e., a naked singularity means not $e \gg 1$ but only the steep density profile at the center. In fact, in the present calculation, e did not become not so larger than the initial value until the central singularity breaks down our numerical code because of the finite resolution. It suggests that the dynamical range of the code used here is not sufficient to recognize N in Table 5.4 as a genuine naked singularity. From Tables 5.1-5.4, based on the criteria described above, naked singularity can occur from generic initial data for a relativistic perfect fluid with $\gamma \lesssim 1.01$.

5.4 Summary

As we have seen above, if $\gamma - 1$ is sufficiently small and the initial density distribution is diffuse, the spherically symmetric adiabatic collapse of a relativistic perfect fluid results in central naked singularity. The initial

data from which naked singularity occurs is generic as long as spherically symmetric initial data are considered. Here we compare the results obtained here about the highly relativistic fluid with the results under the assumption of self-similarity by Ori and Piran (1987, 1988, 1990). The equations of state in the both analyses are approximately common, and hence the difference will be only genericity of initial data. The value $\gamma_c \simeq 1.01$ which we have obtained here agrees with the value $\gamma_c \simeq 1.0105$ for pure collapse by Ori and Piran within a numerical accuracy.

Suppose the cosmic censorship must hold within classical theory of gravity. Then the results obtained here might suggest that a perfect fluid description would not be appropriate for high-density matter. If an asymptotic freedom of particles in high energy scale would be a universal nature, it could be a very reasonable approximation that the high density matter is described by a cluster of collisionless massive or massless particles. This picture is, in general, not contained in a perfect fluid description. Alternatively, it might be suggested that an extremely soft equation of state would be rather pathological in gravitational physics even though the matter satisfies energy conditions. The adiabatic index of a radiation fluid is 4/3 and hence quite larger than 1.01. For a highly relativistic gas in thermal equilibrium, a radiation fluid would be a good approximation. This fact might be a powerful evidence for CCH.

Table 5.1: Final fate of the collapse of a perfect fluid: $\tilde{e}_c = 10^2$

R_s/M	$\gamma - 1 = 0$	10^{-5}	10^{-4}	10^{-3}	10^{-2}	10^{-1}	1
10	B[1]	B	B	B	X[4]	Y	Y
50	N[2]	N	N	N	E[3]	Y	Y
100	N	N	N	N	E	Y[5]	Y
1000	N	N	N	E	E	Y	Y

[1] black hole

[2] naked singularity

[3] expansion

[4] numerical difficulty

[5] numerical difficulty

Table 5.2: Final fate of the collapse of a perfect fluid : $\tilde{e}_c = 10^2$

R_s/M	$\gamma - 1 = 2 \times 10^{-3}$	4×10^{-3}	6×10^{-3}	8×10^{-3}	10^{-2}	2×10^{-2}
10	B	B	BE[1]	X	X	X
20	N	N	N	N	N	BE
30	N	N	N	N	N	E
40	N	N	N	N	E	E
50	N	N	N	E	E	E
60	N	N	N	E	E	E
70	N	N	E	E	E	E
80	N	N	E	E	E	E
90	N	N	E	E	E	E
100	N	E	E	E	E	E

[1] black hole with expanding envelope

Table 5.3: Final fate of the collapse of a perfect fluid: $\tilde{e}_c = 1$

R_s/M	$\gamma - 1 = 0$	10^{-5}	10^{-4}	10^{-3}	10^{-2}	10^{-1}	1
10	B	B	B	B	BE	E	E
50	N	N	N	N	N	E	E
100	N	N	N	N	E	E	E
1000	N	N	N	E	E	E	E

Table 5.4: Final fate of the collapse of a perfect fluid: $\tilde{e}_c = 10^{-2}$

R_s/M	$\gamma - 1 = 0$	10^{-3}	10^{-2}	10^{-1}	1/3	2/3	1
10	B	B	B	B	B	B	B
50	N	N	N	N	B	SE[1]	SE
100	N	N	N	N	E	SE	SE
1000	N	N	N	E	E	E	E

[1] star with expanding envelope

Chapter 6

Gravitational Waves on LTB Space-Time

The LTB solution is spherically symmetric. If spherical symmetry is essential to the occurrence of shell-focusing naked singularity, the solution is not a genuine counterexample to CCH because the spherically symmetric space-time is not generic. If spherical symmetry is not essential, the shell-focusing naked singularity should be considered seriously. Szekeres (1975) found an exact solution of the space-time with non-spherical but quasi-spherical dust collapse. Joshi and Królak (1996) showed that central naked singularity occurs in the generic Szekeres solution from regular initial data and that it satisfies not SCC but only LFC. This work first examined the existence of shell-focusing naked singularity in the non-spherical extension of the LTB solution. However we must pay attention to the facts that the whole of quasi-spherical initial data occupies only zero-measure in generic initial data and that the quasi-spherical dust ball is irrotational and emits no gravitational wave.

In order to examine whether or not the assumption of no gravitational wave is essential to the occurrence of naked singularity, we should examine the behavior of general non-spherical perturbation of the LTB solution. A full order perturbation analysis is very difficult because it requires us to solve the full Einstein equation without any symmetry. Hence, we concentrate on the behavior of metric perturbations of the LTB solution up to linear order.

On the other hand, this study investigates the possibility that the naked singularity may be a strong source of gravitational waves. The gravitational wave detectors, such as, LIGO (Abramovici, et al. (1992)), VIRGO

(Bradaschia, et al. (1990)), TAMA (Kuroda, et al. (1997)) and GEO600 (Hough (1992)) are being constructed and will soon enter a stage of data taking. They will exploit a new regime of astronomy, i.e., the gravitational wave astronomy. Gravitational waves were predicted by general relativity, while the gravitational wave detection will give a strong impact on gravitational physics. The observations of gravitational waves might enable direct tests of general relativity (see Will (1992)). The possible sources of gravitational wave radiation are binary neutron stars, binary black holes, supernovae, rapidly rotating neutron stars, relic gravitational waves of early universe, stochastic gravitational waves from cosmic strings, and so on.

It has been suggested that the naked singularity may emit considerable gravitational wave radiation by Nakamura, Shibata and Nakao (1993). This suggestion was proposed from the estimate of gravitational radiation from spindle naked singularity. They modeled the spindle-like naked singularity formation in gravitational collapse by the Newtonian prolate dust collapse and the sequence of general relativistic momentarily static initial data. Here we tackle non-spherical full general relativistic dynamics using the linear perturbation theory. We perturb the generic LTB solution which results in a shell-focusing naked singularity from generic smooth initial data. For this motivation, the precise formulation of the cosmic censorship is not needed. We only consider the situation in which the extremely high-density region which results from the gravitational collapse can be seen by an observer. Such a situation can be regarded as naked singularity in a practical sense.

In this chapter, we mainly follow Iguchi, Nakao and Harada (1998) and Iguchi, Harada and Nakao (1998).

6.1 Basic Equations

Gauge-invariant formalism of linear perturbations of general spherically symmetric space-time was formulated by Gerlach and Sengupta (1979). A review of it will be described in Appendix A. Equations for linear perturbations are completely separated from each other to odd- and even-parity modes. For simplicity we concentrate on the odd-parity perturbations. For the odd-parity mode, the geometrical gauge-invariant perturbations are k^A, while the matter ones are L^A and L, where A refers to t and r. For notations, see Appendix A.

Then we take the LTB solution as the background space-time. We use the synchronous comoving coordinates introduced in Chap. 2. Because we

are considering the dust matter

$$T_{\mu\nu} = \epsilon u_\mu u_\nu, \tag{6.1}$$

there is no density perturbation and only the 4-velocity perturbation of the form

$$\delta u_\mu = (0, 0, U(t, r)S_a) \tag{6.2}$$

from observing the form of the odd-parity perturbations of the stress-energy tensor, Eq. (A.5) in Appendix A. Therefore the matter perturbations become

$$\begin{aligned} L_t &= \epsilon U, & (6.3)\\ L_r &= 0, & (6.4)\\ L &= 0. & (6.5) \end{aligned}$$

From Eqs. (A.23), (A.24) and (A.25) in Appendix A and the metric obtained in Chap. 2, we obtain equations for the metric perturbations,

$$\begin{aligned} \left(e^\lambda k_t\right)^{\cdot} - \left(e^{-\lambda} k_r\right)' &= 0, & (6.6)\\ \left(R^4 \psi_s\right)' + e^\lambda (l-1)(l+2) k_t &= 16\pi e^\lambda R^2 L_t, & (6.7)\\ \left(R^4 \psi_s\right)^{\cdot} + e^{-\lambda} (l-1)(l+2) k_r &= 0, & (6.8)\\ \left(e^\lambda R^2 L_t\right)^{\cdot} &= 0, & (6.9) \end{aligned}$$

where ψ_s is defined by

$$\psi_s \equiv e^{-\lambda} \left[\left(\frac{k_r}{R^2} \right)^{\cdot} - \left(\frac{k_t}{R^2} \right)' \right], \tag{6.10}$$

and e^λ is given by Eq. (2.22).

Eq. (6.9) is integrated as

$$e^\lambda R^2 L_t = J', \tag{6.11}$$

where $J(r)$ is an arbitrary function of r. From Eqs. (2.21), (2.22) (6.3) and (6.11), we obtain

$$U = \frac{4\pi \sqrt{1+f}\, J'}{F'}, \tag{6.12}$$

and hence $U(t,r) = U(r)$. $U(r)$ is interpreted as the conserved specific angular momentum.

From Eqs. (6.7), (6.8), (6.10) and (6.11), we obtain the following wave equation:

$$\left[\frac{e^{\lambda}}{R^2}\left(R^4\psi_s\right)^{\cdot}\right]^{\cdot} - \left[\frac{1}{e^{\lambda}R^2}\left(R^4\psi_s\right)'\right]' + (l-1)(l+2)e^{\lambda}\psi_s$$
$$= -16\pi\left(\frac{J'}{e^{\lambda}R^2}\right)'. \tag{6.13}$$

For the dipole ($l = 1$) mode, we find that Eqs. (6.7) and (6.8) are integrated as

$$\psi_s = \frac{16\pi}{R^4}J(r), \tag{6.14}$$

while a numerical integration is needed for the higher-multiple mode. For the axisymmetric mode of $l \geq 2$, from Eqs. (6.8), (6.10) and (B.24), we can evaluate the total power of radiated gravitational waves as

$$P = \frac{1}{16\pi}\frac{l(l+1)}{(l-1)(l+2)}r^6\dot{\psi}_s{}^2, \tag{6.15}$$

where ψ_s should be estimated at large distances.

6.2 Perturbation of Riemann Tensor

Here we derive the relation between the perturbations of Riemann tensor and the gauge-invariant quantity ψ_s around the center. We assume regularity on not only the background space-time but also the perturbed space-time before the occurrence of singularity. From regularity of the background space-time, we obtain

$$R = R_c(t)r + O(r^3), \tag{6.16}$$
$$e^{\lambda} = R_c(t) + O(r^2). \tag{6.17}$$

Hereafter we restrict ourselves to an axisymmetric mode, i.e., $m = 0$. It is noted that this restriction is by no means any loss of generality because equations of perturbations for each m are completely common for the same l. Following Bardeen and Piran (1983), regular axisymmetric perturbations

should satisfy the following regularity conditions:

$$L_t = L_c(t)r^{l+1} + O(r^{l+3}), \tag{6.18}$$
$$k_t = k_{tc}(t)r^{l+1} + O(r^{l+3}), \tag{6.19}$$
$$k_r = k_{rc}(t)r^{l+2} + O(r^{l+4}). \tag{6.20}$$

Then, from Eq. (6.3), we obtain

$$U(r) = U_c r^{l+1} + O(r^{l+3}). \tag{6.21}$$

On the other hand, from Eqs. (6.10), (6.17), (6.19) and (6.20), we obtain

$$\begin{aligned} \psi_s &= \psi_{sc}(t)r^{l-2} + O(r^l) \\ &= -(l-1)\frac{k_{tc}}{R_c^3(t)}r^{l-2} + O(r^l) \quad (l \geq 2), \end{aligned} \tag{6.22}$$
$$\psi_s = \psi_{sc}(t)r + O(r^3) \quad (l = 1). \tag{6.23}$$

Therefore, ψ_s does not vanish at the center $r = 0$ only for the quadrupole ($l = 2$) mode.

Next we will consider the behavior of perturbations of the Riemann tensor. The Riemann tensor $R_{\mu\nu\sigma\lambda}$ is decomposed into the Ricci tensor $R_{\mu\nu}$ and the Weyl tensor $C_{\mu\nu\sigma\lambda}$. Furthermore, the Weyl tensor $C_{\mu\nu\sigma\lambda}$ is decomposed into the electric part $E_{\alpha\beta}$ and the magnetic part $B_{\alpha\beta}$, which are defined as

$$E_{\alpha\beta} = C_{\alpha\mu\beta\nu}e^{\mu}_{(t)}e^{\nu}_{(t)}, \tag{6.24}$$
$$B_{\alpha\beta} = \frac{1}{2}\epsilon_{\alpha\sigma}{}^{\mu\nu}C_{\mu\nu\beta\lambda}e^{\sigma}_{(t)}e^{\lambda}_{(t)}, \tag{6.25}$$

where $\epsilon_{\mu\nu\alpha\beta}$ is the 4-dimensional skew tensor, and $e^{\mu}_{(t)}$ is a timelike basis vector of the following tetrad:

$$e^{\mu}_{(t)} = \left(1, 0, 0, -\frac{h_0 P_{l,\theta}}{R^2 \sin\theta}\right), \tag{6.26}$$
$$e^{\mu}_{(r)} = \left(0, e^{-\lambda}, 0, -\frac{h_1 P_{l,\theta}}{e^{\lambda} R^2 \sin^2\theta}\right), \tag{6.27}$$
$$e^{\mu}_{(\theta)} = \left(0, 0, \frac{1}{R}, -\frac{h_2}{R^3}\frac{\sin\theta P_{l,\theta,\theta} - \cos\theta P_{l,\theta}}{2\sin^2\theta}\right), \tag{6.28}$$
$$e^{\mu}_{(\phi)} = \left(0, 0, 0, \frac{1}{R\sin\theta}\right), \tag{6.29}$$

where P_l is the Legendre polynomial and its argument is $\cos\theta$. For the background LTB space-time, the Ricci tensor and the electric part of the Weyl tensor do not vanish, while the magnetic part of the Weyl tensor vanishes.

In the presence of perturbations the Riemann tensor is also perturbed. In particular, the magnetic part of the Weyl tensor has a nonzero value. The explicit form of perturbations of the Ricci and Weyl tensors is given in Iguchi, Nakao and Harada (1998) and we do not repeat. Here we note the behavior of nonvanishing tetrad components of perturbations of the Ricci and Weyl tensors around the center:

$$\delta(R_{(t)(\phi)}) \approx \frac{8\pi}{R_c} L_c P_{l,\theta} r^l \tag{6.30}$$

for all l,

$$\delta(E_{(r)(\phi)}) \approx \frac{(l-1)[(l+2)k_{rc} - R_c\dot{R}_c k_{tc}]}{2R_c^4} P_{l,\theta} r^{l-1}, \tag{6.31}$$

$$\delta(E_{(\theta)(\phi)}) \approx \frac{(l+2)k_{rc} - R_c\dot{R}_c k_{tc}}{2R_c^4} (P_{l,\theta,\theta} - \cot\theta P_{l,\theta}) r^{l-1}, \tag{6.32}$$

$$\delta(B_{(r)(r)}) \approx \frac{l(l+1)}{2} \psi_s P_{l,\theta}, \tag{6.33}$$

$$\delta(B_{(r)(\theta)}) \approx \frac{l+1}{2} \psi_s P_{l,\theta}, \tag{6.34}$$

$$\delta(B_{(\theta)(\theta)}) \approx \frac{1}{2}\frac{l+1}{l-1} \psi_s (P_{l,\theta,\theta} + l P_l), \tag{6.35}$$

$$\delta(B_{(\phi)(\phi)}) \approx \frac{1}{2}\frac{l+1}{l-1} \psi_s (\cot\theta P_{l,\theta} + l P_l) \tag{6.36}$$

for $l \geq 2$, and

$$\delta(E_{(r)(\phi)}) \approx \frac{1}{2}\dot{R}_c \psi_s \sin\theta r, \tag{6.37}$$

$$\delta(B_{(r)(r)}) \approx -\psi_s \cos\theta, \tag{6.38}$$

$$\delta(B_{(r)(\theta)}) \approx \frac{1}{4}\psi_s \sin\theta, \tag{6.39}$$

$$\delta(B_{(\theta)(\theta)}) \approx \frac{1}{2}\psi_s \cos\theta, \tag{6.40}$$

$$\delta(B_{(\phi)(\phi)}) \approx \frac{1}{2}\psi_s \cos\theta \tag{6.41}$$

for $l = 1$.

For the dipole mode, regularity condition (6.21) implies that the specific angular momentum is of the order of r^2. Then, it is inferred from the analysis on counterrotating particles in Chap. 4 that rotation may support the collapse and prevent the singularity formation by the centrifugal force which is a nonlinear effect. For the dipole mode, there is no degree of freedom for gravitational waves. Since we would like to examine the behavior of gravitational waves in the presence of shell-focusing naked singularity and its effect on the formation of the naked singularity, we concentrate on higher multiple mode, i.e., $l \geq 2$. Since the specific angular momentum $U(r)$ is of the order of r^3 or higher for $l \geq 2$, it is inferred that a central shell-focusing singularity may form from the analysis on counterrotating particles in Chap. 4.

From Eqs. (6.30) -(6.41), we find that the perturbations of the Riemann tensor at the center all vanish except for the quadrupole mode up to linear order. For the quadrupole mode, only the perturbations of the magnetic part of the Weyl tensor may not vanish at the center up to linear order. This fact implies that we should pay prior attention to the quadrupole mode in examining the effect of the presence of gravitational waves on the possible central naked singularity formation. Therefore hereafter we restrict ourselves to the quadrupole mode.

6.3 Method

The spacelike hypersurface of the occurrence of the central naked singularity, $t = t_s(0)$, is earlier than the Cauchy horizon and the $t = \text{const} > t_s(0)$ hypersurface encounters singularities. Therefore, the time slicing with $t =$ const hypersurfaces does not determine the maximal Cauchy development before the singularity is encountered. Here, instead of (t, r) coordinates, we introduce a single-null coordinates $(u, \tilde{r})$, where u is an outgoing null coordinate which agrees with t at the center and $\tilde{r} = r$. The transformation is expressed in the form

$$du = \dot{u}dt + u'dr, \tag{6.42}$$

$$d\tilde{r} = dr. \tag{6.43}$$

Since u is the outgoing null coordinate, we obtain

$$\frac{u'}{\dot{u}} = -e^{\lambda}. \tag{6.44}$$

Using this, we obtain the following expression of the line element:

$$ds^2 = -\alpha^2 du^2 - 2\alpha e^{\lambda} du d\tilde{r} + R^2(d\theta^2 + \sin^2\theta d\phi^2), \tag{6.45}$$

where α is given by

$$\alpha \equiv \frac{1}{\dot{u}}. \tag{6.46}$$

Then the transformation of partial derivatives is written as

$$\left(\frac{\partial}{\partial u}\right)_{\tilde{r}} = \alpha \left(\frac{\partial}{\partial t}\right)_r, \tag{6.47}$$

$$\left(\frac{\partial}{\partial \tilde{r}}\right)_u = e^{\lambda}\left(\frac{\partial}{\partial t}\right)_r + \left(\frac{\partial}{\partial r}\right)_t. \tag{6.48}$$

For simplicity, hereafter we restrict our attention to the marginally bound collapse which is given by Eqs. (2.54)-(2.56). Then, the wave equation (6.13) becomes

$$\begin{aligned} \ddot{\psi}_s - \frac{1}{R'^2}\psi'' &= \frac{1}{R'^2}\left(6\frac{R'}{R} - \frac{R''}{R'}\right)\psi_s' - \left(6\frac{R'}{R} + \frac{\dot{R}'}{R'}\right)\dot{\psi}_s \\ &\quad -4\left[\frac{\dot{R}'\dot{R}}{R'R} + \frac{1}{2}\left(\frac{\dot{R}}{R}\right)^2\right]\psi_s \\ &\quad -\frac{16\pi}{R'R^2}\left(\frac{r^2}{R'R^2}\epsilon^0(r)U(r)\right)', \end{aligned} \tag{6.49}$$

where $\epsilon^0(r) \equiv \epsilon(0,r)$ and we have made the choice of radial coordinate as $r = R(0,r)$. If no matter perturbation is included, the above wave equation becomes a homogeneous equation. Therefore, a general solution of the wave equation is decomposed into a general homogeneous solution and a particular solution which depends on the matter perturbation explicitly. Using the newly introduced single-null coordinate system, we obtain the following couple of first order differential equations:

$$\begin{aligned} \frac{d\phi_s}{du} &= -\frac{\alpha}{R}\left[3R' + \frac{1}{2}R\dot{R}\dot{R}' - \frac{5}{4}\dot{R}^2R'\right]\psi_s \\ &\quad -\frac{\alpha}{2}\left[\frac{R''}{R'^2} - \frac{2}{R}(1-\dot{R})\right]\phi_s \\ &\quad -\frac{8\pi\alpha}{R}\left(\frac{r^2}{R'R^2}\epsilon^0 U\right)' \end{aligned} \tag{6.50}$$

$$\left(\frac{\partial\psi_s}{\partial\tilde{r}}\right)_u = \frac{1}{R}\phi_s - 3\frac{R'}{R}(1+\dot{R})\psi_s, \tag{6.51}$$

where d/du is the ordinary derivative along the ingoing null direction which is written as

$$\begin{aligned} \frac{d}{du} &= \left(\frac{\partial}{\partial u}\right)_{\tilde{r}} + \frac{d\tilde{r}}{du}\left(\frac{\partial}{\partial \tilde{r}}\right)_{u} \\ &= \left(\frac{\partial}{\partial u}\right)_{\tilde{r}} - \frac{\alpha}{2R'}\left(\frac{\partial}{\partial \tilde{r}}\right)_{u}. \end{aligned} \tag{6.52}$$

The procedure of obtaining a numerical solution is as follows. First we prepare initial data for ψ_s on the initial null hypersurface $u = u_0$. Then, using Eq. (6.51), ϕ_s is obtained on the initial null hypersurface. Then, integrating Eq. (6.50), we obtain ϕ_s on the null hypersurface $u = u_0 + \Delta u$. Integrating Eq. (6.51), we obtain ψ_s on the null hypersurface $u = u_0 + \Delta u$. In this integration, we determine the central value of ψ_s by using the fact that ψ_s behaves as

$$\psi_s = -\frac{k_{tc}(t)}{R_c^3(t)} + O(r^2), \tag{6.53}$$

near the center. Then, we obtain ψ_s and ϕ_s on the null hypersurface $u = u_0 + \Delta u$. Repeating this process many times, we finally obtain the numerical solution up to the null hypersurface arbitrarily close to the Cauchy horizon associated with the central naked singularity.

The numerical code used here was checked in the Minkowski space-time. The obtained numerical solutions were compared with the analytic solutions which will be described in Sec. 6.4 and a good agreement was seen. We also confirmed that the numerical results shown here were almost independent of the number of grid points.

6.4 Results

6.4.1 Pure Gravitational Waves

For a while, we restrict our attention to perturbations with no matter perturbations, i.e., $U = 0$, in order to isolate the effect of pure gravitational waves. In other words, we restrict our attention to the behavior of a homogeneous solution of the wave equation given by Eqs. (6.50) and (6.51).

Before numerical integration, we must set the initial background density profile ϵ^0 and the initial configuration of the perturbation ψ_s. The initial

density profile at $t = 0$ was set as

$$\epsilon^0 = \begin{cases} \epsilon_c^0 \left[1 - \left(\frac{r}{r_b}\right)^2\right]^2 & \text{for } 0 \leq r \leq r_b, \\ 0 & \text{for } r > r_b. \end{cases} \tag{6.54}$$

The initial data for ψ_s on the initial null hypersurface $u = u_0$ were set to the following Gaussian-shaped wave packet:

$$\psi_s|_{u=u_0} = \psi_s^0 \exp\left[-\frac{(\tilde{r} - \tilde{r}_c)^2}{2\sigma^2}\right]. \tag{6.55}$$

The initial null hypersurface $u = u_0$ is chosen to a future-directed light cone the tip of which is at $(t, r) = (0, 0)$, except for the analysis on scattered waves which will be discussed later.

See Fig. 6.1, where the conformal diagram of the LTB space-time with globally naked shell-focusing singularity is depicted. We investigate three cases of initially incident wave packets: the one which reaches the symmetric center before the formation of the central naked singularity (case 1); the one which 'hits' the central naked singularity (case 2); and the one which reaches the Cauchy horizon associated with the central naked singularity (case 3).

The value of ψ_s at the center is plotted as a function of t for those three cases in Fig. 6.2 for the globally-naked-singular space-time and in Fig. 6.3 for the locally-naked-singular space-time. From these figures, we find that no violent growth is observed near the central naked singularity.

We also observe the time dependence of ψ_s along the trajectory of the constant circumferential radius outside the dust cloud. Since we would like to see the effect of the central naked singularity on ψ_s, we only consider the globally-naked-singular space-time. We set up an initial wave packet $\sigma = 0.05 r_b$ at $R = 100M$ on the initial null hypersurface which does not include $(t, r) = (0, 0)$ but is chosen so that the wave packet will reach the neighborhood of the central naked singularity. The results are shown in Fig. 6.4. Note that $R = 100M$ is located in the vacuum region which is the Schwarzschild space-time. Hence t along the timelike curve $R = 100M$ agrees with the time coordinate of the Schwarzschild coordinate system. In Fig. 6.4(a), the solid, broken and dotted curves denote cases 1, 2 and 3, respectively. In this figure, the initial peak corresponds to the initial incident wave, while the last oscillation corresponds to the scattered outgoing wave. Fig. 6.4(b) shows detailed behavior of the scattered ψ_s for case 2. It is the

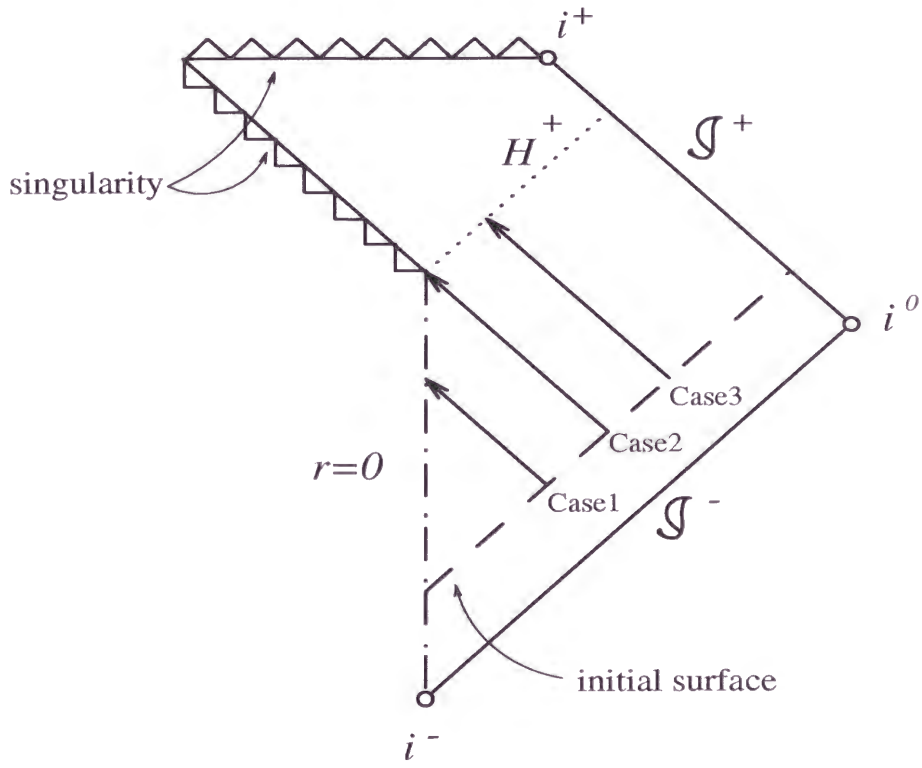

Figure 6.1: Conformal diagram of the LTB space-time with globally naked shell-focusing singularity. Three cases of incident wave packets are depicted.

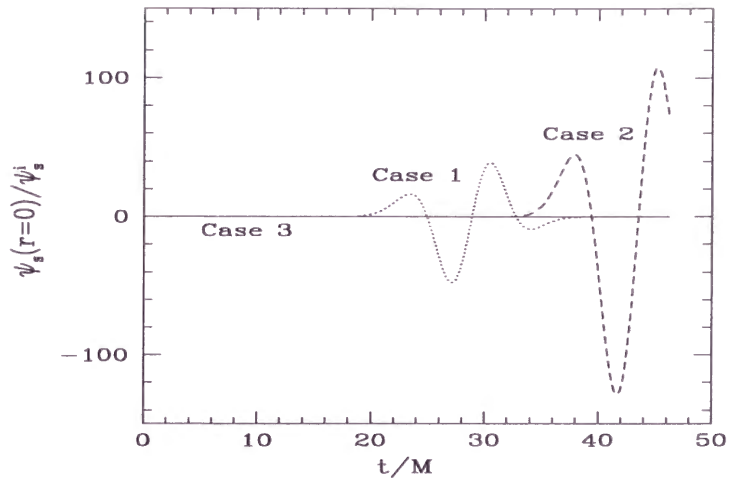

(a)

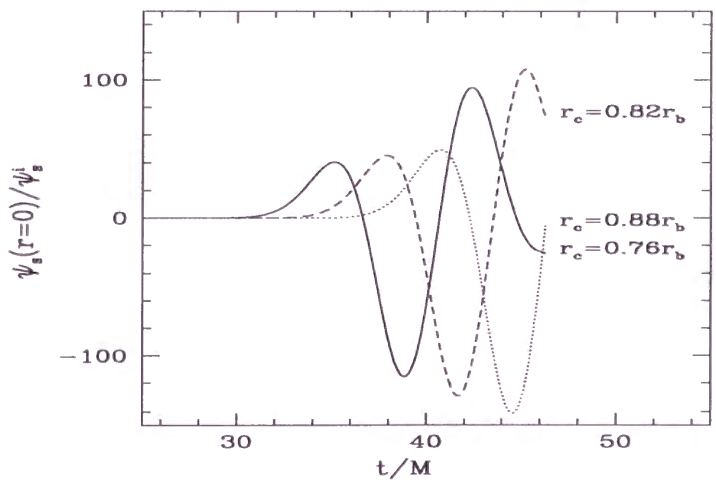

(b)

Figure 6.2: ψ_s at the center with an initial width $\sigma = 0.05r_b$ as a function of t for cases 1-3 for the globally-naked-singular space-time. In (a), the dotted, broken and solid lines denote cases 1 ($\tilde{r}_c = 0.5r_b$), 2 ($0.82r_b$) and 3 ($1.2r_b$), respectively. In (b), the results of case 2 are shown in more detail. The broken line in (b) is the same as the broken line in (a). The solid and dotted lines show the cases in which $\tilde{r}_c = 0.76r_c$ and $0.88r_b$, respectively.

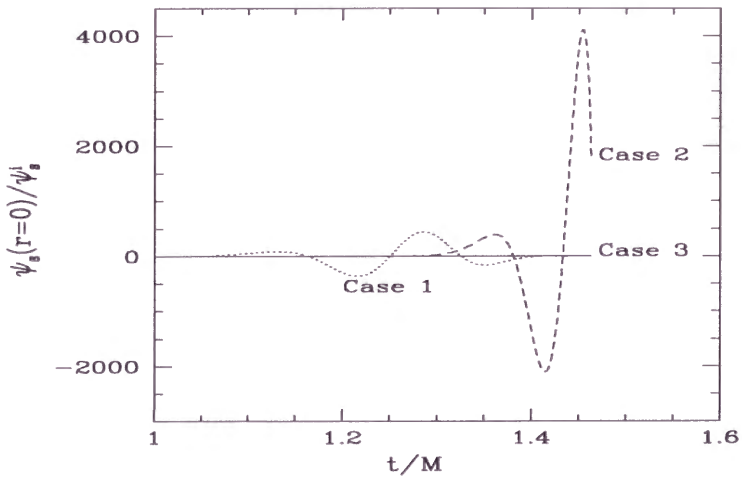

Figure 6.3: ψ_s at the center with an initial width $\sigma = 0.02r_b$ as a function of t for cases 1-3 for the locally-naked-singular space-time. The dotted, broken and solid lines denote cases 1 ($\tilde{r}_c = 0.28r_b$), 2 ($0.38r_b$) and 3 ($0.58r_b$), respectively.

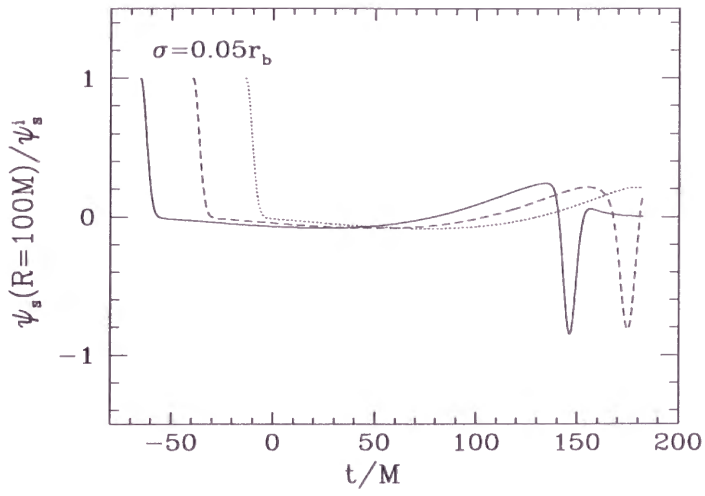

(a)

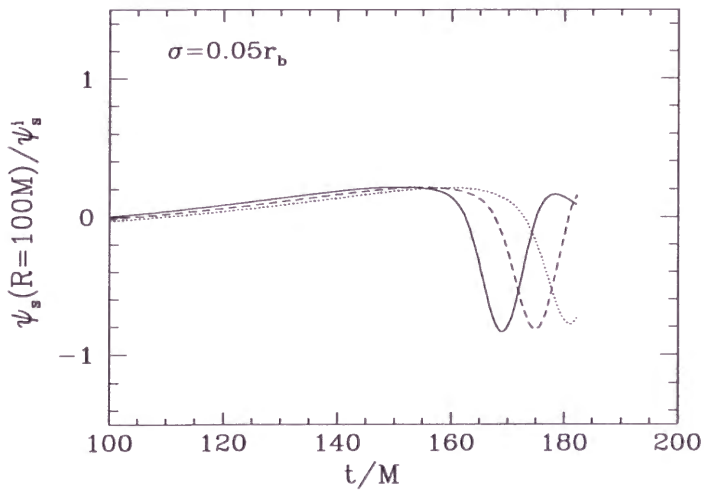

(b)

Figure 6.4: ψ_s with an initial width $\sigma = 0.05r_b$ at $R = 100M$ as a function of time t in the LTB space-time with globally naked singularity. In (a), the solid, broken and dotted lines denote cases 1 ($t_i/M = -65.310$), 2 (-38.529) and 3 (-13.610). In (b), we depict the details of case 2. The solid, broken and dotted lines denote the initial time $t_i/M = -34.336$, -38.529 and -44.677.

most important that the amplitude of the scattered wave is almost the same as that of the initial incident wave in cases 1 and 2.

Next, in order to isolate the effect of the space-time curvature on the propagation of gravitational waves, we compare the numerical results obtained in the LTB space-time with the analytic solution in the Minkowski space-time. In the Minkowski space-time, since $R(t,r)$ is equal to r, Eq. (6.49) becomes

$$\ddot{\psi}_s - \psi_s'' = \frac{6}{r}\psi_s'. \tag{6.56}$$

The solution which is regular at $r = 0$ is given as

$$\begin{aligned}\psi_s &= 3\frac{f(t-r)-f(t+r)}{r^5} + 3\frac{f^{(1)}(t-r)+f^{(1)}(t+r)}{r^4} \\ &\quad + \frac{f^{(2)}(t-r)-f^{(2)}(t+r)}{r^3},\end{aligned} \tag{6.57}$$

where f is an arbitrary function and $f^{(n)}$ denotes the n-th order derivative. We set the following initial wave packet on the initial null hypersurface $t = r$:

$$\psi_s = \exp\left[-\frac{(r-r_{cM})^2}{2\sigma_M^2}\right]. \tag{6.58}$$

Using the above solution, we compare the evolution of ψ_s in the globally-naked-singular LTB space-time with that in the Minkowski space-time. Since the circumferential radius R is closely connected with the behavior of ψ_s, we set the same initial data with respect to R for both space-times, adapting the parameters, r_{cM} and σ_M. The results for ψ_s at the center are given in Fig. 6.5. In Figs. 6.5(a) and (b), the results for cases 1 and 2 are shown, respectively. It should be noted that there is little difference between two curves for both cases. Next we compare the behavior of ψ_s at $R = 100M$ in the LTB space-time with that in the Minkowski space-time. The results are seen in Fig. 6.6. As seen in this figure, the behavior of ψ_s in the LTB space-time is basically the same as that in the Minkowski space-time, except for the time it costs in reflection. The effect of the space-time curvature and the naked singularity in this LTB space-time on the propagation of ψ_s would be rather small.

As a result, we conclude that even in the neighborhood of the central naked singularity and of the Cauchy horizon associated with it, the metric perturbation ψ_s shows no violent growth if no matter perturbation is included.

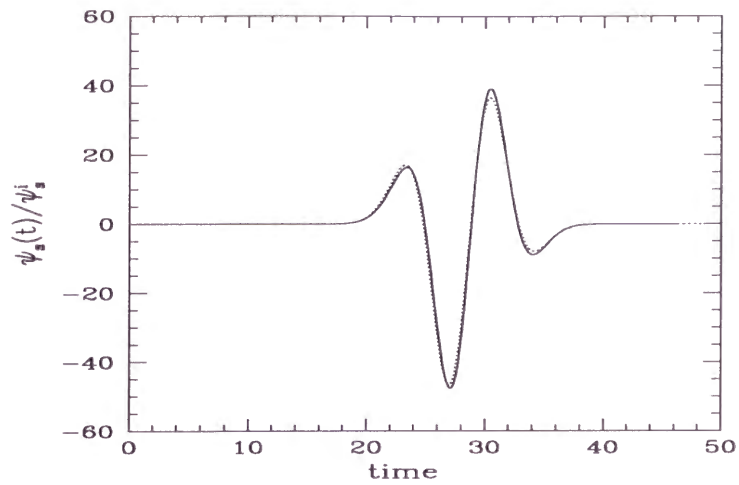

(a)

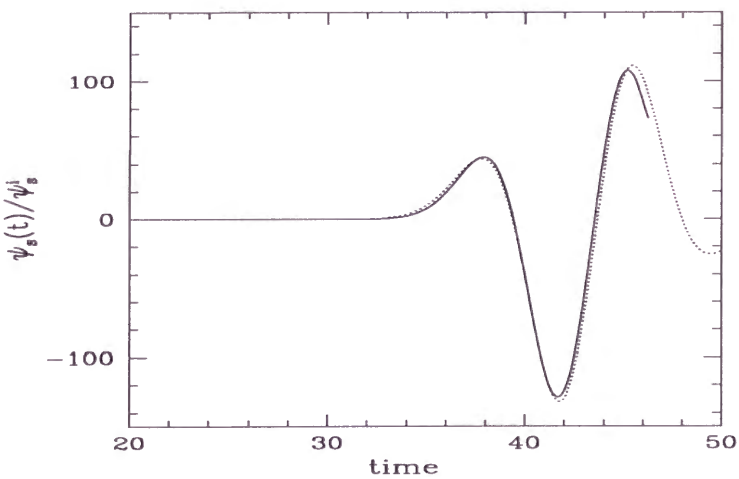

(b)

Figure 6.5: Comparison of wave forms at the center. The solid and dotted lines denote wave forms in the LTB space-time with globally naked singularity and in the Minkowski space-time, respectively. In (a), case 1 is plotted, while, in (b), case 2 is plotted.

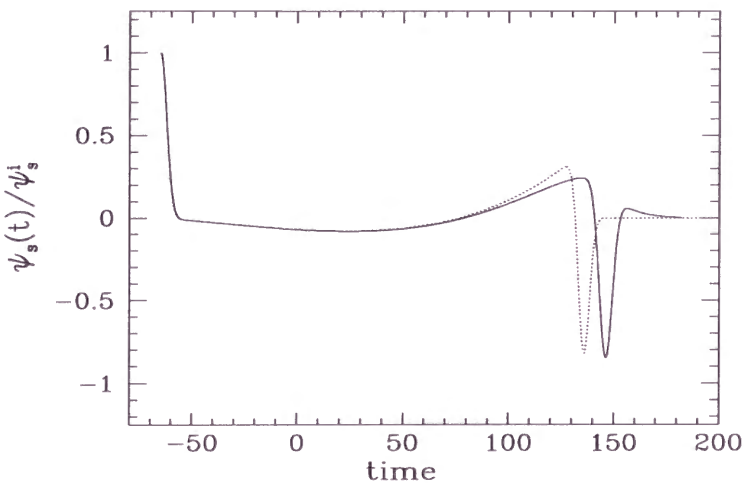

Figure 6.6: Comparison of wave forms at $R = 100M$. The solid and dotted lines denote case 1 in the LTB space-time with globally naked singularity and its counterpart in the Minkowski space-time, respectively.

6.4.2 Including Matter Perturbation

In the presence of matter perturbation, the source term in the wave equation (6.49) does not vanish. In the previous subsection, we have found that the homogeneous solution of the wave equation (6.49) does not show any violent behavior. Therefore, if the solution with nonvanishing source term shows divergent behavior, it does not depend on the choice of initial data for ψ_s on the initial null hypersurface because the divergent behavior is due to the particular solution part. So we choose the following initial data on the initial null hypersurface:

$$\psi_s = 0. \tag{6.59}$$

We adopt the following initial density profile:

$$\epsilon^0 = \epsilon_c^0 \frac{1 + \exp\left(-\frac{1}{2}\frac{r_1}{r_2}\right)}{1 + \exp\left(\frac{r^n - r_1^n}{2r_1^{n-1} r_2}\right)}, \tag{6.60}$$

where n is a positive even integer. It is noted that, although the above density profile spreads to infinity, almost all the mass of the dust cloud is contained within the following core radius:

$$r_{\rm core} = r_1 + \frac{1}{2} r_2. \tag{6.61}$$

If we set $n = 2$, there appears central naked singularity. Whether the singularity is locally or globally naked depends on the choice of the parameters ϵ_c^0, r_1 and r_2. On the other hand, for $n \geq 4$, no shell-focusing naked singularity forms. Then we consider three different types of density profiles which will result in (a) a globally naked singularity, (b) a locally naked singularity and (c) a spacelike singularity.

The specific angular momentum $U(r)$ should satisfy regularity condition (6.21). Then we set $U(r)$ as

$$r^2 \epsilon^0(r) U(r) = \begin{cases} U_0 \left(\frac{r}{r_b}\right)^5 \left[1 - \left(\frac{r}{r_b}\right)^2\right]^5 & \text{for } 0 \leq r \leq r_b, \\ 0 & \text{for } r > r_b. \end{cases} , \tag{6.62}$$

where we choose the parameter r_b as

$$r_b = \frac{1}{2} r_{core}. \tag{6.63}$$

First we observe the behavior of ψ_s at the center. The results are plotted in Fig. 6.7. As seen in this figure, ψ_s grows proportionally to $(t_0 - t)^{-\delta}$ for the naked-singular space-times, (a) and (b), near the formation epoch of the naked singularity, where $t_0 \equiv t_s(0)$. See Fig. 6.8, in which the local power-law index,

$$\delta^{\rm local} \equiv \frac{(t_0 - t)\dot{\psi}_s}{\psi_s} \tag{6.64}$$

is plotted for naked-singular space-times, (a) and (b). The numerical value of δ is about 1.67. For the spacelike-singular space-time, ψ_s shows the power-law growth in the earlier part while ψ_s does not show the power-law behavior in the later part. Anyway, ψ_s diverges at the central naked singularity. The divergence of ψ_s is completely controlled by the divergence of the source term which appears in the wave equation if we include matter perturbations. Since ψ_s is related to the perturbations of the Riemann tensor in a manner described in Sec. 6.2, the divergence of ψ_s implies the divergence of the magnetic part of the Weyl tensor in the neighborhood of the center. Nevertheless, it should be again emphasized that our perturbation analysis is restricted to linear order perturbations.

We also observe the wave form of ψ_s along the line of a constant circumferential radius outside the dust cloud. The results for globally-naked-singular, locally-naked-singular and spacelike-singular space-times are shown in Figs. 6.9, 6.10 and 6.11, respectively. For the locally-naked-singular and spacelike-singular space-times, damped oscillations dominate the wave form, the frequency of which agrees well with that of the fundamental quasi-normal ringing of the quadrupole mode of the Schwarzschild black hole (Chandrasekhar and Detweiler (1975)). In the globally-naked-singular space-time, we cannot observe the quasi-normal ringing because the Cauchy horizon exists earlier than the event horizon and the phenomena of quasi-normal ringing of a black hole associate with the event horizon. Anyway, the gravitational waves emitted from the dust cloud are at most weak quasi-normal ringing before the Cauchy horizon. Therefore the odd-parity perturbations behave in a regular manner and do not destroy the Cauchy horizon. It is noted that conclusions which will be obtained from the numerical results are not altered by the choice of r_b.

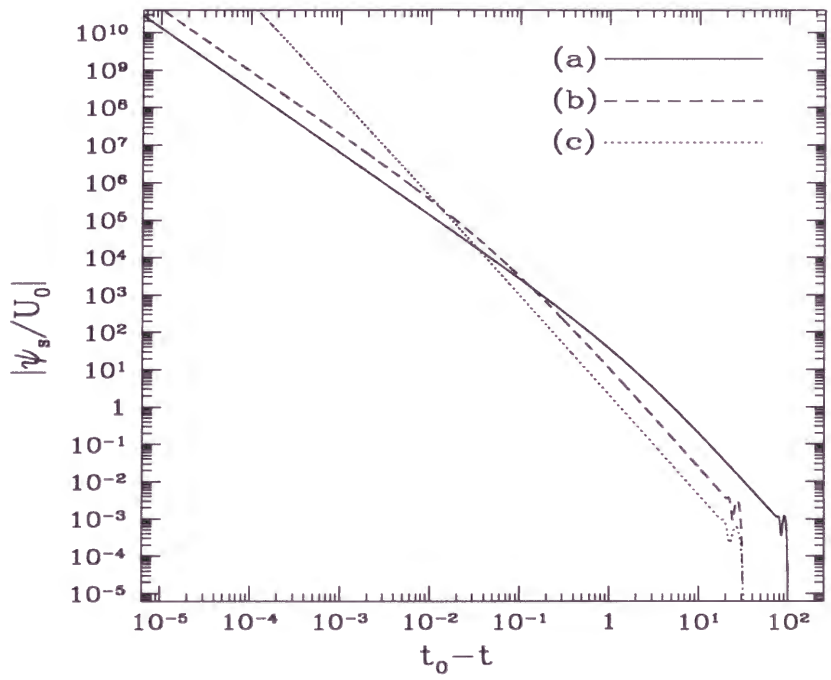

Figure 6.7: ψ_s at the center as a function of t. The solid, broken and dotted lines show (a) the globally-naked-singular, (b) the locally-naked-singular and (c) the spacelike-singular space-times, respectively.

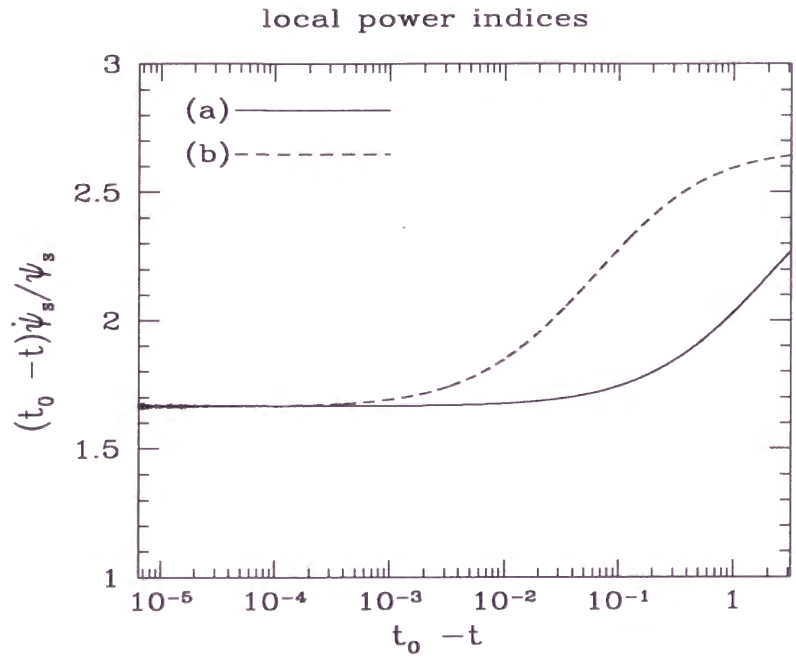

Figure 6.8: Local power index $\delta^{\rm local}$. The solid and broken lines denote (a) the globally-naked singular and (b) the locally-naked-singular space-times, respectively.

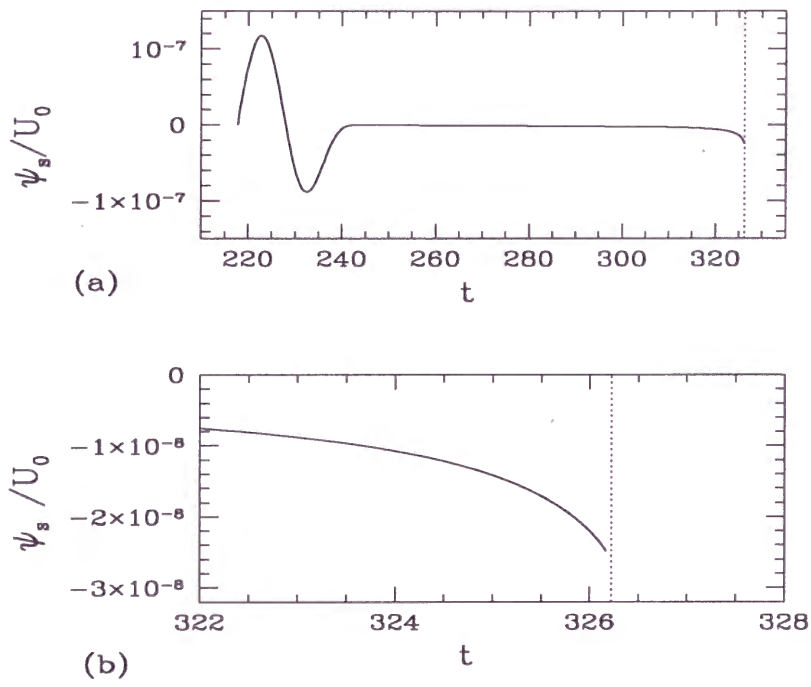

Figure 6.9: ψ_s for globally-naked-singular space-time at $R = 100M$. In (a) the initial oscillation is due to the choice of initial data. (b) is the magnification of (a). The dotted line denotes the Cauchy horizon.

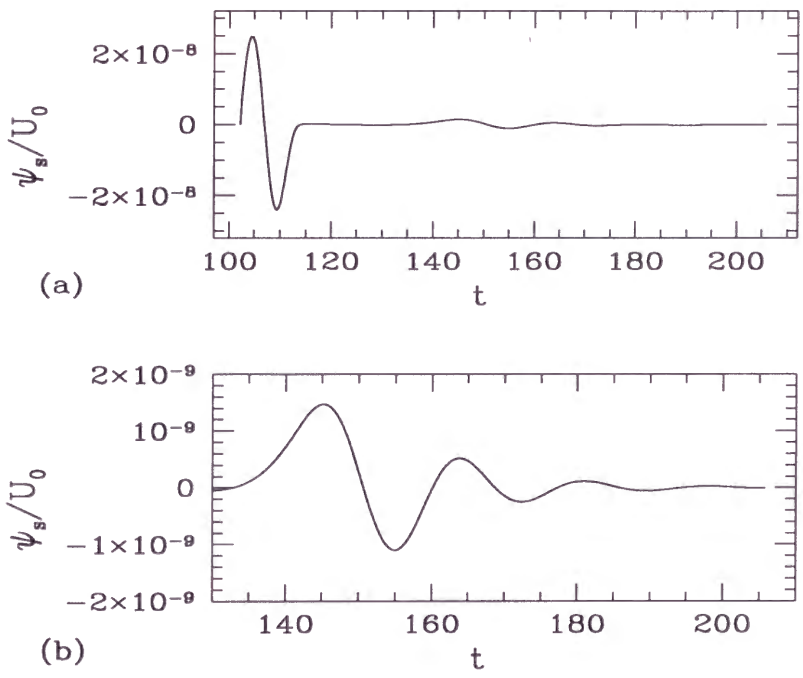

Figure 6.10: Same as Fig. 6.9, but for the locally-naked-singular space-time.

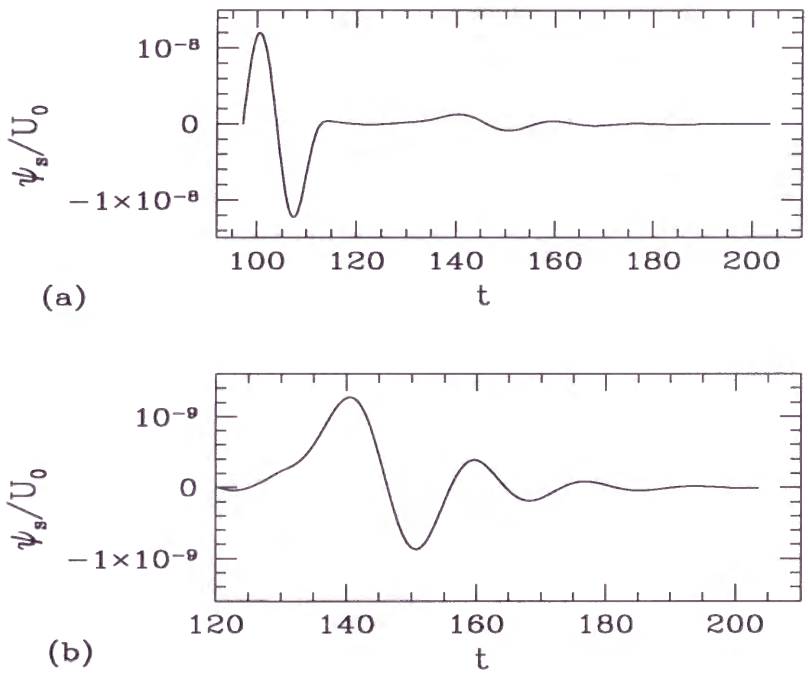

Figure 6.11: Same as Fig. 6.9, but for the spacelike-singular space-time.

6.5 Summary

Up to linear order, the odd-parity pure gravitational waves with no matter perturbation behave in a regular manner in the background of the LTB solution which has shell-focusing naked singularity. In contrast, in the presence of the odd-parity matter perturbation, the magnetic part of the Weyl tensor diverges near the central naked singularity. However the metric perturbation behaves in a regular manner even just before the Cauchy horizon. This implies that the space-time around the Cauchy horizon is altered only perturbatively while the space-time around the shell-focusing naked singularity altered nonlinearly. The stability of the Cauchy horizon is a highly nontrivial result because the divergence near the central naked singularity might be expected to propagate just before the Cauchy horizon and because the Cauchy horizon was proved to be unstable in the RNBH, (Chandrasekhar and Hartle (1982), Poisson and Israel (1990)) the RNdSBH (Brady and Poisson (1992), Brady, Moss and Myers (1998)) and the Kerr BH (Ori (1998)).

If the singularity formation cannot be prevented by rotation for $l \geq 2$ mode as inferred from the analysis in Chap. 4, another type of naked singularity than the shell-focusing singularity in the LTB space-time may emerge. Nevertheless it should be noted that whether or not rotation can prevent the shell-focusing singularity formation is an open problem because it will induce highly non-spherical situation that has not been dealt with in Chap. 4.

With respect to another important motivation of this study, that is, the possibility of the naked singularity being a strong source of gravitational radiation, unfortunately, the naked singularity is not a strong source of gravitational waves for the odd-parity mode.

At last, we must say that this approach is still not completed because the even-parity perturbation is not investigated. Only for the even-parity mode, metric and matter perturbations are essentially coupled. The density perturbation is also included in the even-parity mode, contrary to the odd-parity mode. Then, the naked singularity seems more likely to be a strong source of gravitational waves for the even-parity mode than for the odd-parity mode. If it is, the back reaction of the radiated energy flux from the naked singularity might destroy the regularity of the Cauchy horizon for this mode. The even-parity mode perturbation is being investigated now.

Chapter 7

Summary and Conclusions

7.1 Summary and Conclusions

In general relativity, the occurrence of singularity is a generic property of gravitational collapse. A naked singularity violates the future predictability of space-time within the framework of classical theory. Then, it has been conjectured that no naked singularity forms in physically realistic gravitational collapse. However, in the generic spherically symmetric dust collapse, which is described by the LTB solution, shell-focusing naked singularity forms. Then, it is our concern whether or not the naked singularity which appears in the LTB solution is physically realistic. The physical reasonableness could be separated into two concepts, sufficiently generic space-time and non-pathological matter content, although these two may be closely related with each other. The LTB solution seems to be unrealistic because it assumes exact spherical symmetry and because its matter content, the dust fluid, has exactly vanishing pressure. Then it is important whether or not the above unrealistic assumptions are essential to the shell-focusing naked singularity formation.

In this context, we have investigated the effects of violation of such apparently unrealistic assumptions on the shell-focusing naked singularity formation. First we have paid attention to the fact that the dust matter can be considered as a cold limit of collisionless gas. From this point of view, it is more generic for the gas to have nonvanishing velocity dispersion. In Chap. 3, we have developed a formulation on spherically symmetric space-time with only tangential pressure. Using this formulation, in Chap. 4, we have introduced counterrotation which is a kind of nonvanishing velocity dis-

persion in the tangential direction. We have succeeded to obtain the exact solution for the space-time. Then we have concluded that generic counter-rotation prevents the central shell-focusing singularity formation, although we have also found an example of the shell-focusing naked singularity formation with non-generic counterrotation. Moreover, we have shown that the generic continued collapse must result with shell-crossing singularities.

On the other hand, it is also possible to consider the dust matter as a soft limit of a perfect fluid with γ-law equation of state. Then, in Chap. 5, we have investigated the spherically symmetric collapse of a perfect fluid with γ-law equation of state. Since we have obtained the numerical solution by using an outgoing null coordinate, the causal structure has been obvious. Then we have concluded that the central globally naked singularity forms from generic initial data for sufficiently soft equation of state. This study has generalized the previous works under the self-similarity assumption.

Furthermore, in Chap. 6, we have proceeded to consideration of the violation of spherical symmetry, in particular, the existence of gravitational waves. From a linear perturbation analysis, we have obtained the conclusion that the odd-parity mode gravitational waves do not destroy the Cauchy horizon while the shell-focusing naked singularity may change its properties, for example, the divergence of the magnetic part of the Weyl tensor. We have also learn a lesson that nonlinear effect becomes very important on the formation of naked singularity.

Based on these results, we discuss the genericity of the shell-focusing naked singularity in the LTB solution. Consider a collisionless gas system, which will be a realistic matter model. Then, velocity dispersion would play an important role at the final stage of gravitational collapse with or without spherical symmetry. Generic velocity dispersion have a tendency of preventing the central shell-focusing singularity formation.

On the other hand, consider a perfect fluid with γ-law equation of state. Then its adiabatic, spherically symmetric collapse results in central naked singularity from generic initial data, if the equation of state is sufficiently soft. Provided that the cosmic censorship is to be true, this example calls another suspicion if the extremely soft equation of state for highly relativistic matter may be unphysical In fact, it is known that the highly relativistic collisionless gas in thermal equilibrium behaves as a radiation fluid. It should be also noted that the fluid picture is only an approximation for a group of particles which interact each other and that elementary particles would behave like free particles in high energy scales, that is, an asymptotic freedom would hold.

Without spherical symmetry, we must introduce gravitational waves in general. The odd-parity gravitational waves do not destroy the Cauchy horizon, contrary to the case of the inner horizon of the RNBH, RNdSBH and Kerr BH. The odd-parity gravitational waves cannot be radiated strongly from the naked singularity.

At last, although there remain open problems which deserve to be investigated in more detail, the shell-focusing naked singularity would not be generic and we cannot accept the shell-focusing naked singularity as a counterexample of CCH. Therefore, no serious counterexample of CCH has been discovered.

7.2 Future Prospects

There still remain a lot of open problems. In particular, the works in this thesis should be extended as follows.

Which is the naked singularity that appears in the collapse of counter-rotating particles, timelike or null ? The shell-focusing naked singularity which appears in the LTB space-time is ingoing null in this connection.

Our analysis strongly suggests that the shell-crossing singularities are very generic phenomena in gravitational collapse of collisionless particles. Hence it is very important to deal with the shell-crossing singularities in a distributional sense. The procedure for the crossing of shells may give a hint to the present problem. Alternatively, we should solve the Einstein-Vlasov equation with or without spherical symmetry. Anyway, we will be forced to have recourse to numerical techniques.

We should clarify the curvature strength of the naked singularity in the spherically symmetric collapse of a perfect fluid with very soft equation of state. Since the solution has been obtained numerically, the strength of the singularity must be examined by numerical techniques. Moreover, it should be clarified whether or not the collapse of a nonrelativistic fluid results in naked singularity. It needs very high resolution and it is expected that the adaptive mesh refinement code may reveal it. On the other hand, if the superstring theory or other Planck energy scale physics specifies a certain effective equation of state for the matter, what occurs in the complete spherically symmetric gravitational collapse ?

The behavior of the even-parity perturbations of the naked-singular LTB solution must be investigated. For the even-parity mode, the metric and matter perturbations are closely connected. In the presence of this mode,

does the Cauchy horizon remain stable ? Does the naked singularity emit gravitational waves for the even-parity mode? Are the gravitational waves observable ? This problem is very attractive in the present progress in the gravitational wave observation projects by laser interferometric detectors, such as, LIGO, VIRGO, TAMA and GEO.

Whether or not the naked singularity is inevitable in classical theory of gravity, singularities would result with divergence of curvature invariants. Then quantum effect which appears in curved space-time cannot be negligible. It is an open question how the singularity formation is altered.

ACKNOWLEDGEMENTS

I would like to thank H. Sato, T. Nakamura, N. Sugiyama, K. Nakao, M. Siino and H. Iguchi for helpful discussions and continuous encouragement. I would also like to thank all the members of theoretical astrophysics group at Kyoto University. This work was supported by Grant-in-Aid for Research Fellowships (No. 9204) of the Japan Society for the Promotion of Science for Young Scientists from the Japanese Ministry of Education, Science, Sports and Culture.

Appendix A

Gauge-Invariant Perturbations of Spherically Symmetric Space-Time

A.1 Perturbations of Spherically Symmetric Space-Time

Here we review gauge-invariant perturbation formalism on a general spherically symmetric space-time, following Gerlach and Sengupta (1979).

The perturbed metric tensor is written in the form

$$g_{\mu\nu} = \bar{g}_{\mu\nu} + h_{\mu\nu}, \tag{A.1}$$

where $\bar{g}_{\mu\nu}$ and $h_{\mu\nu}$ are the background metric tensor and the perturbation, respectively. The stress-energy tensor is written in the form

$$T_{\mu\nu} = \bar{T}_{\mu\nu} + t_{\mu\nu}, \tag{A.2}$$

where $\bar{T}_{\mu\nu}$ and $t_{\mu\nu}$ are the background stress-energy tensor and the perturbation, respectively. $\bar{T}_{\mu\nu}$ is expressed in the form

$$\bar{T}_{\mu\nu}dx^{\mu}dx^{\nu} = \bar{T}_{AB}dx^{A}dx^{B} + \frac{1}{2}\bar{T}_{a}{}^{a}R^{2}(t,r)(d\theta^{2} + \sin^{2}\theta d\phi^{2}), \tag{A.3}$$

where A, B, ... refer to the time and radial coordinates, while a, b, ... refer to θ and ϕ. Up to linear order, equations for perturbations are completely

separated from each other to odd- and even-parity modes. The odd-parity mode perturbations are written as

$$\begin{aligned} h_{\mu\nu}dx^\mu dx^\nu &= h_A(x^C)S_a(dx^A dx^a + dx^a dx^A) \\ &\quad +h(x^C)S_{(a;b)}dx^a dx^b, \qquad \text{(A.4)} \\ t_{\mu\nu}dx^\mu dx^\nu &= t_A(x^C)S_a(dx^A dx^a + dx^a dx^A) \\ &\quad +t(x^C)S_{(a;b)}dx^a dx^b, \qquad \text{(A.5)} \end{aligned}$$

where the semicolon denotes the covariant derivative on the two-sphere $x^A =$ const and S_a is the odd-parity vector harmonics ($S_a{}^{|a} = 0$). S_a is constructed as

$$S_a = \epsilon_a{}^b Y_{,b}, \qquad \text{(A.6)}$$

where $\epsilon_a{}^b$ and $Y(\theta, \phi)$ are the 2-dimensional skew tensor and the spherical harmonic function, respectively, and the comma denotes the partial derivative. $S_{(a;b)}$ is the odd-parity tensor harmonics. See also Regge and Wheeler (1957) for scalar, vector and tensor harmonics. The even-parity mode perturbations are written as

$$\begin{aligned} h_{\mu\nu}dx^\mu dx^\nu &= h_{AB}(x^C)Y dx^A dx^B + h_A Y_{,a}(dx^A dx^a + dx^a dx^A) \\ &\quad +R^2[K(x^C)Y\gamma_{ab} + G(x^C)Y_{,a;b}]dx^a dx^b, \qquad \text{(A.7)} \\ t_{\mu\nu}dx^\mu dx^\nu &= t_{AB}(x^C)Y dx^A dx^B + t_A Y_{,a}(dx^A dx^a + dx^a dx^A) \\ &\quad +R^2[t^1(x^C)Y\gamma_{ab} + t^2(x^C)Y_{,a;b}]dx^a dx^b, \qquad \text{(A.8)} \end{aligned}$$

where γ_{ab} is the metric tensor of the 2-sphere $x^A =$ const, i.e.,

$$\gamma_{ab}dx^a dx^b = d\theta^2 + \sin^2 d\phi^2. \qquad \text{(A.9)}$$

$Y_{,a}$ and $Y_{,a;b}$ are the even-parity vector harmonics and the even-parity tensor harmonics, respectively. Hereafter we suppress overbars in referring to the background quantities.

A.2 Gauge-Invariant Quantities

In order to isolate physical modes from gauge ones, we introduce gauge-invariant variables as follows. We abstract invariant quantities under the gauge transformation induced by the infinitesimal vector fields:

$$\xi_\mu dx^\mu = M(x^C)S_a dx^a \qquad \text{(A.10)}$$

for the odd-parity mode and

$$\xi_\mu dx^\mu = \xi_A(x^C) Y dx^A + \xi(x^C) Y_{,a} dx^a \tag{A.11}$$

for the even-parity mode. Then we obtain the following gauge-invariant quantities:

$$k_A = h_A - \frac{1}{2}R^2 \left(\frac{h}{R^2}\right)_{,A}, \tag{A.12}$$

$$L_A = t_A - \frac{1}{2}T_a{}^a h_A, \tag{A.13}$$

$$L = t - \frac{1}{2}T_a{}^a h \tag{A.14}$$

for the odd-parity perturbations, and

$$k_{AB} = h_{AB} - (p_{A|B} + p_{B|A}), \tag{A.15}$$

$$k = K - 2v^A p_A, \tag{A.16}$$

$$L_{AB} = t_{AB} - T_{AB}{}^{|C} p_C - 2(t_{CA} p^C{}_{|B} + t_{CB} p^C{}_{|A}), \tag{A.17}$$

$$L_A = t_A - T_A{}^C p_C - \frac{1}{4}R^2 G_{,A}, \tag{A.18}$$

$$L^1 = t^1 - \frac{1}{2}\frac{p^C}{R^2}(R^2 t_a{}^a)_{,C}, \tag{A.19}$$

$$L^2 = t^2 - \frac{1}{2}R^2 t_a{}^a G \tag{A.20}$$

for the even-parity perturbations, where

$$v_A \equiv \frac{R_{,A}}{R}, \tag{A.21}$$

$$p_A \equiv h_A - \frac{1}{2}R^2 G_{,A}, \tag{A.22}$$

and the vertical bar refers to the covariant derivative on the 2-dimensional submanifold M^2 spanned by x^A.

A.3 Field Equations

The linearized Einstein field equation ($\delta G_{\mu\nu} = 8\pi \delta T_{\mu\nu}$) for the odd-parity mode becomes

$$k^A{}_{|A} = 16\pi L \quad (l \geq 2), \tag{A.23}$$

$$
\begin{aligned}
&- \left[R^4 \left\{ \left(\frac{k^A}{R^2} \right)^{|C} - \left(\frac{k^C}{R^2} \right)^{|A} \right\} \right]_{|C} + (l-1)(l+2)k^A \\
&= 16\pi R^2 L^A \quad (l \geq 1). \qquad \text{(A.24)}
\end{aligned}
$$

The linearized conservation equation ($\delta(T_{\mu\nu}{}^{;\nu}) = 0$) for the odd-parity mode becomes

$$
(R^2 L^A)_{|A} = (l-1)(l+2)L \quad (l \geq 1). \qquad \text{(A.25)}
$$

On the other hand, the linearized Einstein equation for the even-parity mode becomes

$$
\begin{aligned}
&\frac{1}{R^2}[R^2(k_{AB|C} - k_{AC|B} - k_{BC|A})]^{|C} - \left[\frac{l(l+1)}{R^2} + G^C{}_C + G^a{}_a \right] k_{AB} \\
&+ g_{AB} \left[\frac{1}{R^2}(R^2 k_{CD})^{|C|D} - G^{CD} k_{CD} \right] + k^C{}_{C|A|B} \\
&- g_{AB} \left[\frac{1}{R^2}(R^2 k^C{}_{C|D})^{|D} - \frac{l(l+1)}{R^2} k^C{}_C - \frac{1}{2}(G^D{}_D + G^a{}_a) k_C{}^C \right] \\
&+ 2(v_A k_{,B} + v_B k_{,A} + k_{,A|B}) \\
&- g_{AB} \left[2k_{,C}{}^{|C} + 6v^C k_{,C} - \frac{(l-1)(l+2)}{R^2} k \right] \\
&= -16\pi L_{AB} \quad (l \geq 0), \qquad \text{(A.26)} \\
&k_{,A} - k_{AC}{}^{|C} + k^C{}_{C,A} - v_A k^C{}_C = -16\pi L_A \quad (l \geq 0), \qquad \text{(A.27)} \\
&-(k_{,C}{}^{|C} + 2v^C k_{,C} + G^a{}_a k) \\
&+ [k_{CD}{}^{|C|D} + 2v^C k_{CD}{}^{|D} + 2(v^{C|D} + v^C v^D) k_{CD}] \\
&- \left[k^C{}_{C|D}{}^{|D} + v^C k^D{}_{D|C} + \mathcal{R} k^C{}_C - \frac{l(l+1)}{R^2} k^C{}_C \right] \\
&= -16\pi L^1 \quad (l \geq 0), \qquad \text{(A.28)} \\
&k^C{}_C = -16\pi L^2 \quad (l \geq 0), \qquad \text{(A.29)}
\end{aligned}
$$

where $\mathcal{R}$ is the Gaussian curvature on the 2-dimensional submanifold M^2. The linearized conservation equation for the even-parity mode becomes

$$
\begin{aligned}
&\frac{1}{R^2}(R^2 L^A)_{|A} + L^1 + \frac{1 - l(l+1)}{R^2} L^2 \\
&= \frac{1}{2} T^a{}_a \left(k - \frac{1}{2} k^C{}_C \right) + \frac{1}{2} t^{AB} k_{AB} \quad (l \geq 0), \qquad \text{(A.30)} \\
&\frac{1}{R^2}(R^2 L_{AB})^{|B} - \frac{l(l+1)}{R^2} L_A - 2v_A L^1 + \frac{l(l+1)}{R^2} v_A L^2
\end{aligned}
$$

$$= \frac{1}{2}k_{BC|A}T^{BC} + k_{CB}{}^{|B}T^{C}{}_{A} - \frac{1}{2}k^{C}{}_{C|B}T^{B}{}_{A} - k_{,C}T^{C}{}_{A}$$
$$+ \left(\frac{1}{2}k_{,A} - kv_{A}\right)T^{a}{}_{a} + 2v^{B}k_{BC}t^{C}{}_{A} + k^{B}{}_{C}t^{C}{}_{A|B} \quad (l \geq 0). \quad (A.31)$$

Appendix B

Radiated Power of Gravitational Waves

Here we examine the asymptotic behavior of the gauge-invariant quantities defined in Appendix A in the asymptotically flat space-time with outgoing wave condition. Then we calculate the radiated power of gravitational waves and thereby we comprehend the physical meaning of the gauge-invariant quantities.

Note that, in vacuum at large distances, the spherically symmetric background metric is given by the Schwarzschild space-time, where hereafter we adopt the Schwarzschild coordinates:

$$ds^2 = -\left(1-\frac{2M}{r}\right)dt^2 + \left(1-\frac{2M}{r}\right)^{-1}dr^2 + r^2(d\theta^2+\sin^2\theta d\phi^2). \quad \text{(B.1)}$$

To relate the perturbation of the metric to the radiated gravitational wave power, it is useful to specialize to the radiation gauge, in which the tetrad components of the metric perturbations $h_{(\theta)(\theta)} - h_{(\phi)(\phi)}$ and $h_{(\theta)(\phi)}$ fall off as $O(1/r)$ at large distances, and all other tetrad components fall off as $O(1/r^2)$ with respect to the following background tetrad basis:

$$e^a_{(t)} = \left(1-\frac{2M}{r}\right)^{1/2}(dt)^a, \quad \text{(B.2)}$$

$$e^a_{(r)} = \left(1-\frac{2M}{r}\right)^{-1/2}(dr)^a, \quad \text{(B.3)}$$

$$e^a_{(\theta)} = r(d\theta)^a, \quad \text{(B.4)}$$

$$e^a_{(\phi)} = r\sin\theta(d\phi)^a. \quad \text{(B.5)}$$

In the radiation gauge, the metric perturbations in Eqs. (A.4) and (A.7) behave as

$$h_A = O\left(\frac{1}{r}\right), \tag{B.6}$$

$$h = f(t - r_*)r + O(1) \tag{B.7}$$

for the odd-parity mode, and

$$h_{AB} = O\left(\frac{1}{r^2}\right), \tag{B.8}$$

$$h_A = O\left(\frac{1}{r}\right), \tag{B.9}$$

$$K = O\left(\frac{1}{r^2}\right), \tag{B.10}$$

$$G = \frac{g(t - r_*)}{r} + O\left(\frac{1}{r^2}\right) \tag{B.11}$$

for the even-parity mode, where r_* is the tortoise coordinate defined as

$$r_* \equiv r + 2M \ln\left(\frac{r}{2M} - 1\right) + \text{const}, \tag{B.12}$$

and the outgoing wave condition is respected. Then, the gauge-invariant metric perturbations (A.12), (A.15) and (A.16) are calculated as

$$k_t = -\frac{1}{2}f'r + O(1), \tag{B.13}$$

$$k_r = \frac{1}{2}f'r + O(1) \tag{B.14}$$

for the odd-parity mode, and

$$k_{tt} = g''r + O(1), \tag{B.15}$$

$$k_{tr} = -g''r + O(1), \tag{B.16}$$

$$k_{rr} = g''r + O(1), \tag{B.17}$$

$$k = -g' + O\left(\frac{1}{r}\right) \tag{B.18}$$

for the even-parity mode, where the prime over f or g denotes the derivative with respect to its argument.

In this radiation gauge, the radiated power P per unit solid angle is given by the formula derived by Landau and Lifshitz (1975) from their stress-energy pseudo-tensor:

$$\frac{dP}{d\Omega} = \frac{r^2}{16\pi}\left[\left(\frac{\partial h_{\hat{\theta}\hat{\phi}}}{\partial t}\right)^2 + \frac{1}{4}\left(\frac{\partial h_{\hat{\theta}\hat{\theta}}}{\partial t} - \frac{\partial h_{\hat{\phi}\hat{\phi}}}{\partial t}\right)^2\right]. \tag{B.19}$$

For the axisymmetric mode, i.e., $m = 0$, the above formula is reduced as

$$\frac{dP}{d\Omega} = \frac{A_l(\theta)}{64\pi} f'^2 \tag{B.20}$$

for the odd-parity mode, and

$$\frac{dP}{d\Omega} = \frac{A_l(\theta)}{64\pi} g'^2 \tag{B.21}$$

for the even-parity mode, where $A_l(\theta)$ is given by

$$A_l(\theta) \equiv \frac{2l+1}{4\pi} \sin^4\theta P_l''(\cos\theta)^2. \tag{B.22}$$

It is found that, for the monopole and dipole modes, the radiated power exactly vanishes. Then, by using the gauge-invariant quantities and integrating over the whole solid angle, the formula for the power of gravitational radiation of $l \geq 2$ is obtained in the following form:

$$\frac{dP}{d\Omega} = \frac{A_l(\theta)}{16\pi r^2} k_t^2 = \frac{A_l(\theta)}{16\pi r^2} k_r^2, \tag{B.23}$$

$$P = \frac{B_l}{16\pi r^2} k_t^2 = \frac{B_l}{16\pi r^2} k_r^2 \tag{B.24}$$

for the odd-parity mode, and

$$\frac{dP}{d\Omega} = \frac{A_l(\theta)}{64\pi} k^2, \tag{B.25}$$

$$P = \frac{B_l}{64\pi} k^2 \tag{B.26}$$

for the even-parity mode, where B_l is given by

$$B_l \equiv (l-1)l(l+1)(l+2). \tag{B.27}$$

Bibliography

[1] A.M. Abrahams and C.R. Evans, Phys. Rev. Lett. **70**, 2980 (1993).

[2] A. Abramovici, et al., Science **256**, 325 (1992).

[3] J.M. Bardeen and T. Piran, Phys. Rep. **96**, 205 (1983).

[4] T.W. Baumgarte, S.L. Shapiro and S.A. Teukolsky, Astrophys. J. **443**, 717 (1995).

[5] H. Bondi, Mon. Not. R. astron. Soc. **107**, 410 (1947).

[6] H. Bondi, Gen. Relativ. Gravit. **2**, 321 (1971).

[7] C. Bradaschia, et al., Nucl. Instrum. and Methods **A289**, 518 (1990)

[8] P.R. Brady, I.G. Moss and R.C. Myers, Phys. Rev. Lett. **80**, 3432 (1998).

[9] P.R. Brady and E. Poisson, Class. Quantum Grav. **9**, 121 (1992).

[10] P.R. Brady and J.D. Smith, Phys. Rev. Lett. **75**, 1256 (1995).

[11] L.M. Burko, Phys. Rev. Lett. **79**, 4958 (1997).

[12] S. Chandrasekhar, Astrophys. J. **74**, 81 (1931).

[13] S. Chandrasekhar and S. Detweiler, Proc. R. Soc. Lond. A **344**, 441 (1975).

[14] S. Chandrasekhar and J.B. Hartle, Proc. R. Soc. Lond. A **384**, 301 (1982).

[15] M.W. Choptuik, Phys. Rev. Lett. **70**, 9 (1993).

[16] D. Christodoulou, Commun. Math. Phys. **93**, 171 (1984).

[17] D. Christodoulou, Ann. Math. **140**, 607 (1994).

[18] C.J.S. Clarke, *The Analysis of Space-Time Singularities*, (Cambridge University Press, Cambridge, England, 1993).

[19] C.J.S. Clarke and A. Królak, J. Geom. Phys. **24**, 127 (1985).

[20] C.L. Comer and J. Katz, Class. Quantum Grav. **10**, 1751 (1993).

[21] B.K. Datta, Gen. Relativ. Gravit. **1**, 19 (1970).

[22] D.M. Eardley and L. Smarr, Phys. Rev. D **19**, 2239 (1979).

[23] A. Einstein, Preuss. Akad. Wiss. Berlin, Sitzber., 844 (1915).

[24] A. Einstein, Annals of Mathematics **40**, 921 (1939).

[25] A.B. Evans, Gen. Relativ. Gravit. **8**, 155 (1976).

[26] C.R. Evans and J.S. Coleman, Phys. Rev. Lett. **72**, 1782 (1994).

[27] U.H. Gerlach and U.K. Sengupta, Phys. Rev. D **19**, 2268 (1979).

[28] T. Harada, Phys. Rev. D **58**, 104015 (1998).

[29] T. Harada, H. Iguchi and K. Nakao, Phys. Rev. D **58**, 041502 (1998).

[30] T. Harada, K. Nakao and H. Iguchi, Report No. KUNS-1551, submitted to Class. Quantum Grav. (1998).

[31] S.W. Hawking and G.F.R. Ellis, *The large scale structure of space-time*, (Cambridge University Press, Cambridge, England, 1973).

[32] S.W. Hawking and R. Penrose, Proc. R. Soc. Lond. A **314**, 529 (1970).

[33] W.C. Hernandez and C.W. Misner, Astrophys. J. **143**, 452 (1966).

[34] J. Hough, in *Proceedings of the Sixth Marcel Grossman Meeting*, ed. H. Sato and T. Nakamura (World Scientific, Singapore, Singapore, 1992), p.192.

[35] D. Ida and K. Nakao, Report No. KUNS-1524, submitted to Class. Quantum Grav (1998).

[36] H. Iguchi, T. Harada and K. Nakao, Report No. KUNS-1512, submitted to Phys. Rev. D (1998).

[37] H. Iguchi, K. Nakao and T. Harada, Phys. Rev. D **57**, 7262 (1998).

[38] S. Jhingan, P.S. Joshi and T.P. Singh, Class. Quantum Grav. **13**, 3057 (1996).

[39] P.S. Joshi and I.H. Dwivedi, Phys. Rev. D **45**, 2147 (1992a).

[40] P.S. Joshi and I.H. Dwivedi, Commun. Math. Phys. **146**, 333 (1992b).

[41] P.S. Joshi and I.H. Dwivedi, Phys. Rev. D **47**, 5357 (1993a).

[42] P.S. Joshi and I.H. Dwivedi, Lett. Math. Phys. **27**, 235 (1993b).

[43] P.S. Joshi and A. Królak, Class. Quantum Grav. **13**, 3069 (1996).

[44] R.P. Kerr, Phys. Rev. Lett. **11**, 237 (1963).

[45] A. Królak, Gen. Relativ. Gravit. **15**, 99 (1983).

[46] A. Królak, J. Math. Phys. **28**, 138 (1987).

[47] K. Kuroda, et al., in *Proceedings of International Conference on Gravitational Waves: Sources and Detectors*, ed. I. Ciufolini and F. Fidecaro (World Scientific, Singapore, Singapore, 1997), p.100.

[48] K. Lake, Phys. Rev. D **60**, 241 (1988).

[49] L.D. Landau, Phys. Z. Sowjetunion **1**, 285 (1932).

[50] L.D. Landau and E.M. Lifshitz, *The Classical Theory of Fields*, 4th ed., (Pergamon, London, England, 1975).

[51] P.S. Laplace, *Le Système du Monde*, Vol. II, (Paris, France, 1795); English edition: *The System of the World*, W. Flint, (London, England, 1809).

[52] G. Magli, Class. Quantum Grav. **14**, 1937 (1997).

[53] G. Magli, Class. Quantum Grav. **15**, 3215 (1998).

[54] C.W. Misner and D.H. Sharp, Phys. Rev. B **136**, 571 (1964).

[55] C.W. Misner, K.S. Thorne and J.A. Wheeler, *Gravitation*, (Freeman, San Francisco, USA, 1973).

[56] H. Müller zum Hagen, P. Yodzis and H.-J. Seifert, Commun. Math. Phys. **37**, 29 (1974).

[57] T. Nakamura, M. Shibata and K. Nakao, Prog. Theor. Phys. **89**, 821 (1993).

[58] K. Nakao, D. Ida and N. Sugiura, Report No. KUNS-1525, submitted to Prog. Theor. Phys. (1998).

[59] R.P.A.C. Newman, Class. Quantum Grav. **3**, 527 (1986).

[60] H. Onozawa, M. Siino and K. Watanabe, Report No. TIT/HEP-226/COSMO-34, unpublished (1994).

[61] J.R. Oppenheimer and H. Snyder, Phys. Rev. **56**, 455 (1939).

[62] A. Ori, Class. Quantum Grav. **7**, 985 (1990).

[63] A. Ori, Phys. Rev. D **58**, 084016 (1998).

[64] A. Ori and T. Piran, Phys. Rev. Lett. **59**, 2137 (1987).

[65] A. Ori and T. Piran, Gen. Relativ. Gravit. **20**, 7 (1988).

[66] A. Ori and T. Piran, Phys. Rev. D **42**, 1068 (1990).

[67] R. Penrose, Riv. del Nuovo Cimento **I**, 252 (1969).

[68] R. Penrose, in *General Relativity, an Einstein Centenary Survey*, ed. S.W. Hawking and W. Israel, (Cambridge University Press, Cambridge, England, 1979), p.581.

[69] M.V. Penston, Mon. Not. R. astr. Soc. **144**, 425 (1969).

[70] K. Pfaffelmoser, J. Diff. Eq. **95**, 281 (1992).

[71] E. Poisson and W. Israel, Phys. Rev. D **41**, 1796 (1990).

[72] T. Regge and J.A. Wheeler, Phys. Rev. **108**, 1063 (1957).

[73] A.D. Rendal, in *Approaches to Numerical Relativity*, ed. R.A. d'Inverno, (Cambridge University Press, Cambridge, England, 1992), p.94.

[74] R. Schoen and S.T. Yau, Commun. Math. Phys. **90**, 575 (1983).

[75] K. Schwarzschild, Sitzungsber. Dtsch. Akad. Wiss. Berlin., Kl. Math.-Phys. Tech., 189 (1916).

[76] S.L. Shapiro and S.A. Teukolsky, Phys. Rev. Lett. **66**, 994 (1991).

[77] S.L. Shapiro and S.A. Teukolsky, Phys. Rev. D **45**, 2006 (1992).

[78] M. Shibata, K. Nakao and T. Nakamura, Phys. Rev. D **50**, 7304 (1994).

[79] T.P. Singh and P.S. Joshi, Class. Quantum Grav. **13**, 559 (1996).

[80] T.P. Singh and L. Witten, Class. Quantum Grav. **14**, 3489 (1997).

[81] P. Szekeres, Phys. Rev. D **12**, 2941 (1975).

[82] K.S. Thorne, in *Magic Without Magic: John Archibold Wheeler*, edited by J. Klauder, (Freeman, San Francisco, USA, 1972).

[83] F.J. Tipler, Phys. Lett. A **64**, 8 (1977).

[84] R.C. Tolman, Proc. Nat. Acad. Sci. **20**, 169 (1934).

[85] P.C. Vaidya, Current Science **13**, 183 (1943).

[86] P.C. Vaidya, Phys. Rev. **47**, 10 (1951a).

[87] P.C. Vaidya, Proc. Indian Acad. Sci. A **33**, 264 (1951b).

[88] K.A. Van Riper, Astrophys. J. **232**, 558 (1979).

[89] R. Wald, *General Relativity*, (The University of Chicago Press, Chicago, USA, 1984).

[90] B. Waugh and K. Lake, Phys. Rev. D **40**, 2137 (1989).

[91] J.A. Wheeler, American Scientist **56**, 1 (1968).

[92] C.M. Will, *Theory and Experiment in Gravitational Physics*, revised ed., (Cambridge University Press, Cambridge, England, 1992).

[93] P. Yodzis, H.-J. Seifert and H. Müller zum Hagen, Commun. Math. Phys. **34**, 135 (1973).